UNIVERSITY OF SOUTHAMPTON

FACULTY OF ENGINEERING AND THE ENVIRONMENT
AERONAUTICS, ASTRONAUTICS AND COMPUTATIONAL ENGINEERING

STOCHASTIC ENGINEERING SIMULATIONS USING SPARSE GRID COLLOCATION METHOD AND KRIGING BASED APPROACHES.

by

D. Chandra Sekhar

Thesis submitted for Postgraduate Research Degree

November 2017

UNIVERSITY OF SOUTHAMPTON

ABSTRACT

FACULTY OF ENGINEERING AND THE ENVIRONMENT
AERONAUTICS, ASTRONAUTICS AND COMPUTATIONAL ENGINEERING

STOCHASTIC ENGINEERING SIMULATIONS USING SPARSE GRID COLLOCATION METHOD AND KRIGING BASED APPROACHES.

by D. Chandra Sekhar

The estimation of probabilistic moments is central to robust design process. Typically one would like to estimate the mean and variance of some performance critical metric such as stress, life, etc., of a component in any engineering system, aiming a robustly optimized design that is less sensitive to the input variations/uncertainties. For complex aerospace engineering systems such as aero-engine, a single numerical simulation of any component can often take a substantial amount of time and few samples can be afforded at which the deterministic simulations can be carried out. Considering the variations in the parameters and performing a large number of simulations on such problems is unrealistic and necessitate the improvement of existing UQ approaches.

In this study, we present the significance of probabilistic moment estimation approaches for uncertainty quantification and its importance in robust design optimization studies. The background for few popular approaches is provided, where emphasis is put on sparse grid collocation method, adaptive sparse grid collocation approach and Kriging based Bayesian approaches.

A non-intrusive multi-point adaptive strategy using sparse grid based collocation design and Kriging based approaches is proposed to reduce the problems arising in high dimensional probabilistic moment estimation studies. The comparison of multi-point adaptive approach with other existing approaches for probabilistic moment estimation in terms of efficiency and accuracy is provided. Further on, the effectiveness of the proposed approach is demonstrated for few mathematical test functions and stochastic structural problems with varying dimensionality and strong interaction among the random variables.

Contents

List of Figures

List of Tables

Declaration of Authorship

I, D. Chandra Sekhar , declare that the thesis entitled *Stochastic Engineering Simulations using Sparse Grid Collocation method and Kriging based approaches.* and the work presented in the thesis are both my own, and have been generated by me as the result of my own original research. I confirm that:

- this work was done wholly or mainly while in candidature for a research degree at this University;
- where any part of this thesis has previously been submitted for a degree or any other qualification at this University or any other institution, this has been clearly stated;
- where I have consulted the published work of others, this is always clearly attributed;
- where I have quoted from the work of others, the source is always given. With the exception of such quotations, this thesis is entirely my own work;
- I have acknowledged all main sources of help;
- where the thesis is based on work done by myself jointly with others, I have made clear exactly what was done by others and what I have contributed myself;
- one of this work has been published before submission.
- parts of this work have been published as [70].

Signed:.....

Date:.....

Acknowledgements

I would like to thank Dr Kamal Djidjeli and Dr Alex Forrester for their helpful advice and support during my studies. I would like to thank Professor Andy Keane for giving an oppurtunity to work on the project and for his advice and help through out my studies.

The financial support from Rolls-Royce Plc., is very much appreciated and was helpful in attending conference. Thanks goes to Dr Ron Bates and Tamsyn Thorpe of Rolls-Royce Plc., for their help and support over the course of study. Also I would like to thank University and graduate school for the help in difficult times and ensuring things move forward.

List of acronyms

UQ	Uncertainty Quantification
PDF	Probability Density Function
FEA	Finite Element Analysis
CFD	Computational Fluid Dynamics
PC	Polynomial Chaos
gPC	generalized Polynomial Chaos
MCS	Monte-Carlo Simulation
SPDE	Stochastic Partial Differential Equation
LHS	Latin Hypercube Sampling
SGCM	Sparse Grid Collocation Method
SG	Sparse Grid
ANOVA	Analysis Of Variance
MARS	Multivariate Regression Splines
DOE	Design Of Experiments
FFD	Full Factorial Design
CCD	Central Composite Design
SQP	Sequential Quadratic Programming
MSE	Mean Squared Error

Nomenclature

Y	System output response
ξ^i	Random variable
Ω	Event space
F	$\sigma-$algebra associated with the support space
E	Expectation
Γ	Support space
d	dimension
θ_h	Hyperparameter governing rate of correlation
p_h	Hyperparameter governing degree of smoothness
f_h	Regression functions
β	Regression parameters
ϵ	Error in approximation
μ	Mean
$\hat{\mu}$	Kriging mean
σ^2	Variance
$\hat{\sigma^2}$	Kriging variance
$\hat{s}(x)$	Estimated error in Kriging prediction at x
$\mathbf{R}$	Kriging correlation matrix
Φ	Variance
ϵ_m	Relative percentage error in estimation of mean
ϵ_v	Relative percentage error in estimation of standard deviation
ϵ_{ms}	Relative percentage error in estimation of mean stresses
ϵ_{vs}	Relative percentage error in estimation of standard deviation in stresses
n	Number of points
w	Weight
$\vec{U_d}$	d-dimensional collocation points
k	Level or order of integration.
i	Sparse grid index
P_s	Number of all possible combinations

$N(a\ b)$	Gaussian distribution with $\mu = a$ and $\sigma^2 = b$
$U[a\ b]$	Uniform distribution with bounds [a b]
D	Dimension
$\in$	Belongs to
C	Rectifiable boundary
R	Real line
P_n	Orthogonal polynomial
L_n	Legendre polynomial
T_n	Tschebycheff polynomial
H_n	Hermite polynomial
G_n	Laguerre polynomial
δ	Kronecker delta
$\varphi(x)$	Gaussian probability measure
$< fg >$	Inner product or expectation of f,g
$()'$	Spatial derivative wrt. x
t	Time
u	Space
p	Probability measure
ε	Error using MSE criteria

Chapter 1

Introduction

Modelling and simulation of complex systems has become a reality with the significant growth in modern day computing power. Numerical simulations are performed in order to understand the underlying physics and behaviour of engineering systems. The primary goal of numerical analysis is to provide accurate solutions to real-world problems. To this end, effective algorithms are developed to evaluate the systems, and this is still an active research field. However, understanding the impact of uncertainties in the physical and numerical parameters involved in such fields is less advanced.

Uncertainties are of two types, the first one, aleatoric uncertainty is due to inherent randomness in the behaviour of the system; it is irreducible because of the variability in the physical or environmental aspects of the system being analysed. The second one, epistemic uncertainty is due to lack of knowledge of the operating system. This can be due to the simplified assumptions in the description of the mathematical model or neglecting the significance of correlation between various physical processes involved in the system. It can be reduced through better understanding and thorough modelling of the system. Probabilistic approaches can be used to represent both aleatory and epistemic uncertainties. In addition Helton et al. [1] illustrated the use of interval analysis, possibility theory and evidence theory as alternatives to probability theory in representation of epistemic uncertainties in the system.

The uncertainties in input parameters of the engineering systems (such as aero-engine, Fig 1.1.), can be due to :

- deviation of manufactured geometry from design,

Figure 1.1: Rolls-Royce Trent 1000 engine on Boeing 787.

- inaccuracies in measurement of manufactured geometry,
- variation in material properties and residual stresses,
- in-service degradation of a component, and
- boundary conditions such as temperatures, flow rates, and leakages.

The response quantities of interest can be:

- displacements, equivalent stresses, stress intensity factors, etc., in case of finite element analysis.
- temperatures and pressures in the context of thermo-mechanical analysis.

1.1 Motivation

In deterministic design processes, the uncertainties or variabilities are disregarded and nominal (or idealized) values of parameters such as for loads, boundary conditions, geometry, working conditions etc., are often considered in modeling and simulation. The system is often be over designed with an appropriate safety criteria or failure criteria selected, to account for the expected variations in the input parameters [2]. The design optimum attained signifies the best performance in theory, but in practical implementation such a design may not be feasible due

to the uncertainties in the design parameters. Such variations about the nominal values of design variables result in scatter of system performance as shown in Fig. 1.2. The ideal determinitic design structure may perform far worse than an alternative robust design model which is less sensitive to parameter variations.

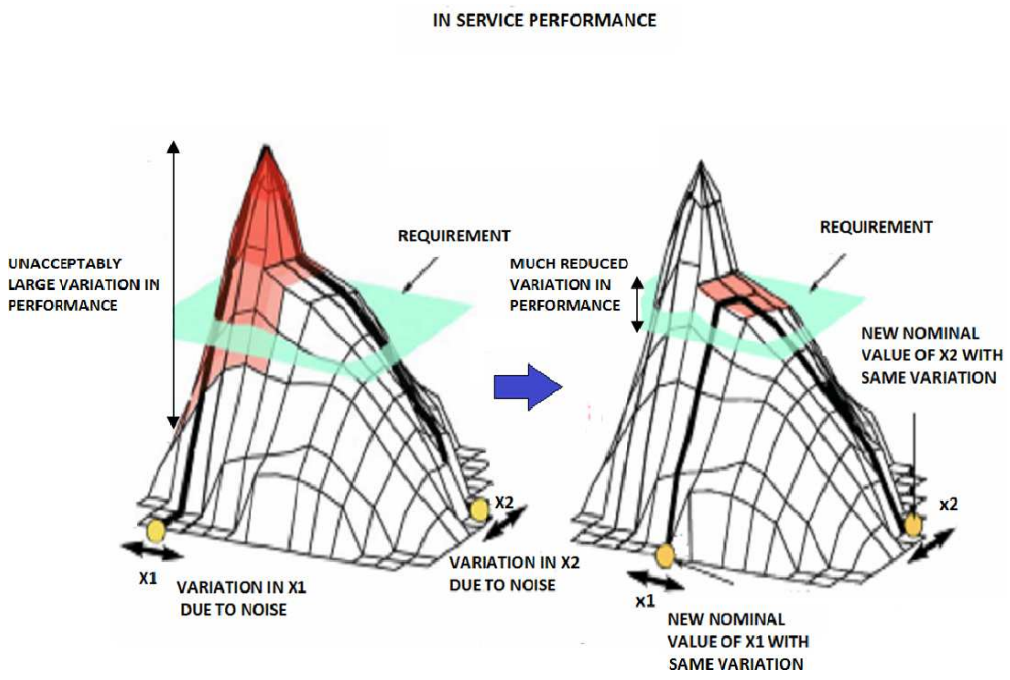

Figure 1.2: Deterministic Design Vs Robust Design [3].

To design systems which can perform their intended function with desired confidence, the uncertainties involved should be considered in the initial stage of design process. A probabilistic framework in quantifying uncertainties for safe assessment of technological systems such as nuclear power plants etc., was provided by Apostolakis et al. [4]. In that paper the role of expert opinions along with experimental results and statistical observations, to quantitatively assess the risks involved in the systems were also discussed.

Complex multi-physics engineering problems like fluid-structure interaction problems, routinely involve tens of physical and numerical parameters. The numerical solution of such deterministic problems is often a computationally demanding task. Considering the variations in the parameters and performing a large number of simulations on such problems is unrealistic. From a design perspective, and for reliable prediction of system response, uncertainties should be systematically identified and classified. The uncertainties should be described by accurate approaches and be propagated through the system in an acknowledged systematic way as shown in literature [5,6].

This has motivated the development of efficient uncertainty quantification (UQ) methods to assess the system output response statistics, by propagating the input uncertainties through the governing system. Such approaches would further help in reducing the time involved in experimental validation procedures.

A physical system can be modeled as a general function $\boldsymbol{Y} = \mathrm{M}(\boldsymbol{\xi})$, where $\boldsymbol{\xi}$ is the vector of input parameters, $\boldsymbol{Y}$ is the system response. The model M can be a simple mathematical function or "black box" function such as computer program (FEA, CFD). The focus of the thesis is to study the probabilistic content (or joint probability density function) of a typical response $\boldsymbol{Y}$. However each input parameter ($\boldsymbol{\xi_i}$) has a set of realizations in one-dimensional space based on the probabilistic distribution of the variable. The problem becomes multidimensional because of the many parameters involved. The solution of such problems is analytically intractable: they suffer from "the curse of dimensionality", a term used to describe the computational difficulties that arise in high-dimensional spaces.

Uncertainty quantification techniques can be broadly classified into two types, intrusive or non-intrusive, based on their implementation and usage. In intrusive approaches, the existing code (FEA, CFD) needs to be modified to a large extent to incorporate the variation in the input parameters. Non-intrusive approaches use the computational model as a black box within uncertainty quantification studies and the cost of implementation is less, although system run time can be longer in these approaches.

A schematic view of the typical working procedure of non-intrusive[1] UQ approaches is shown in Fig. 1.3. The following steps may be identified in these approaches :

1. Identifying the input parameters ($\boldsymbol{\xi_i}$) of the stochastic simulation model and prescribing them in a probabilistic context. The parameters can be uniform, normal or exponentially distributed, etc. The randomness in the variables can involve non-uniform PDF's with cross correlations, taken from industrial measurements [7].

2. The random variables are incorporated into the simulation model, which is defined using appropriate criteria (safety, risk, etc).

3. After performing deterministic analysis on the model considering all the realizations of the random variables ($\boldsymbol{\xi_i}$), one collects an ensemble of solutions, i.e.,

[1] non-intrusive approaches rely exclusively on deterministic analysis methods.

realizations of the random solutions $\boldsymbol{Y}(\boldsymbol{\xi_i})$. Various methods exist (also called *uncertainty propagation methods*) to estimate the response of the system (mean, variance, and other higher order moments).

4. In the last and final step a sensitivity analysis is done. This study helps in quantifying the different random variables in the system based on their respective influence on the system output [8]. The random variables/inputs of the system are not independent in their effects, hence this study helps in understanding the correlation between random outputs.

Thus UQ approaches help to design systems, whose performance is not compromised by variations in parameters (aleatory and epistemic) and ensures designs which are least sensitive to local variations.

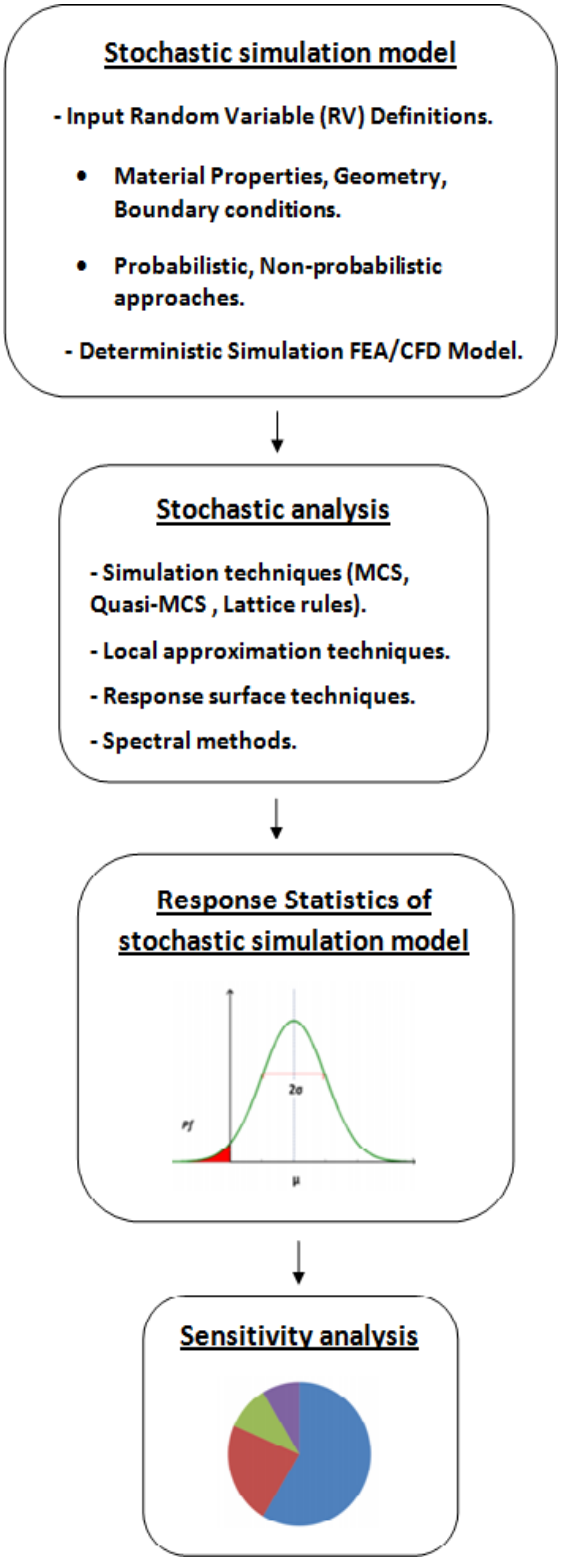

Figure 1.3: General sketch for uncertainty quantification approaches.

1.2 Background

Many existing techniques can be adopted for *uncertainty propagation* to estimate the statistical quantities of system output response. These include simulation techniques, local approximation methods, spectral stochastic projection schemes and response surface techniques, to name a few.

Monte Carlo sampling (MCS) based techniques are widely used simulation methods and find their application in many fields of engineering and science. In the field of mathematics, MCS are used to obtain numerical solution to complex problems which are analytically intractable; numerical integration in high dimensions is one of those complicated problems. The general procedure in MCS is to generate random sample points of input parameters based on their probability distribution and then perform the deterministic solution of the problem considering each input sample. The problem is deterministic, since the points are fixed in each input sample. All such deterministic evaluations are collected, from which statistical information on the outputs can be extracted eg., mean, variance, etc. It has been shown that in accordance to the "*Law of large numbers*" the expected value of MCS method have convergence $O(1/\sqrt{N})$, where N is the number of random sample points [9]. For example, as the number of sample points is quadrupled, the error in estimation can be halved. Thus the number of sample points required can be quite high, in order to attain sufficient accuracy.

Several variants of MCS have been developed to accelerate the convergence of the traditional MCS. The quasi Monte-Carlo sampling technique improves the covergence in the order of $O(1/N)$, by choosing the sample points with minimum discrepancy [10]. Latin hypercube sampling (or LHS) based MCS methods choose the sample points based on a technique called "*stratified sampling without replacement*" as shown in literature (e.g. [11]). Though these methods have slightly better accuracy than MCS, their applicability can be limited for high-dimensional integrals.

More efficient alternatives based on sparse quadrature rules are developed, enabling us to use the existing simulation model similar to MCS. In this approach one uses collocation points and then performs the deterministic simulations at these points to evaluate the response of the system. Sparse quadrature based on Smolyak's formula is developed in the context of stochastic collocation schemes. The selection of the type of orthogonal polynomials depend on the probabilistic density functions of the random variables. It was first proposed by Tatang et

al. [12] and because of its non-intrusive nature, holds an advantage over classical polynomial chaos approaches. Xiu et al. [13] suggested a class of high-order collocation methods and different choices of collocation nodal sets have been investigated. Acharjee et al. [14] implemented this approach for stochastic deformation processes depicting the ease and effectiveness of this approach over MCS.

Among the local approximation techniques, perturbation methods and stochastic operator based methods offer effective ways to estimate the first two statistical moments of the response. Perturbation methods are popular non-sampling techniques and their application is quite wide spread in many fields [15,16]. The physical parameters are continuous in space and because of inherent randomness in them, we have random variable/fields. The random fields of the parameters are incorporated into the governing equations via second order Taylor series, expanded around their mean where higher orders are neglected because of the complexity in the solution of governing equations. The limitation of this approach is that the deviations or magnitude of uncertainty in the physical parameters should be less than 10% else they do not perform well. In Operator-Based methods, the stochastic operators in the governing equations are manipulated using the Neumann expansion technique. In the stochastic finite element method, inverse stochastic stiffness parameters (in the equilibrium equation) are deduced using the Neumann expansion [17,18]. This approach is better compared to MCS in characterizing the uncertainty and reducing the computational time for some linear static problems. But similar to perturbation approach it is restricted to small uncertainties in the physical parameters. The two methods were developed in the context of static problems. The number of stochastic variables involved in these problems is less compared to any comprehensive design model of engine, rotorcraft etc.

Spectral stochastic projection schemes enable to represent the randomness in the output response using functional approximations and have gained a lot of interest over the past 10-20 years because of their mathematical rigour and effective representation of stochastic processes (or stochastic field if time is invariant). Stochastic projection schemes based on polynomial chaos (PC) expansions are intrusive, in which the stochastic process is represented by a Wiener expansion similar to Fourier series expansion. It was initially developed by Norbert Weiner [19], where multidimensional Hermite polynomials (also known as the PC basis) are used as basis functions to represent the stochastic process. Further details about the theory and its implementation for discrete mathematical models of random systems is given by Ghanem et al. [20]. Debusschere et al. [21] developed a non-intrusive type polynomial chaos approaches, also termed as generalized polynomial chaos (gPC),

where non-Hermite polynomials were used to represent the stochastic process encompassing various problems with non-Gaussian random variables. In recent years, it is being studied by many researchers in the context of building efficient numerical methods for solving stochastic partial differential equations (SPDE's), in fields like elasticity and fluid flow problems. Recent works by Eldred et al. [22], show that these approaches are efficient for low to moderate dimensional problems.

The uncertainty quantification techniques developed for stochastic systems should be efficient in their implementation and execution. Response surface methods are another class of approximation techniques that are used to represent the stochastic system under consideration. In classical response surface methodology [23], an approximate polynomial such as linear, quadratic or higher order polynomial is built that can optimally characterize the output response by conducting a series of experiments or runs of the simulation model of the system. Uncertainty propagation methods can be applied on the response surface, rather than performing deterministic simulations on the actual system, further reducing the computational time involved in UQ studies.

The objectives of the presented research are two-fold; firstly to investigate the complexities incurred in applying the high-dimensional numerical integration schemes for stochastic propagation and uncertainty quantification. Secondly, try enhance the performance by reducing the simulations required for uncertainty quantification at higher dimensions, for a stochastic system.

1.3 Layout of thesis

The thesis begins by introducing important concepts and emphasises the need for better methods in performing uncertainty quantification studies. The main focus of this work is to develop efficient probabilistic moment estimation methods for complex, nonlinear functions in high-dimensional stochastic space.

The presentation of the current work is made in six chapters :

The first chapter deals with the motivation for the current work. A brief literature survey is presented and a review of important published literature in relation to the present work is done. The chapter ends with a short note on the present work and layout of the thesis.

Chapter 2, describes various aspects pertaining to the mathematical modeling of uncertainty. An overview of different approaches for the propagation of stochastic responses are described. Further the theoretical and computational aspects of various structural optimisation methods in presence of uncertainties is presented. For the sake of completeness the topic is extended to multi-criteria optimisation and the emphasis is put on structural robustness, taking into account the intrinsic variabilities involved in the system.

Chapter 3, presents an overview of stochastic collocation approach and the construction of sparse grid method using a one-dimensional Clenshaw-Curtis rule. The advantage and limitations of the sparse grid collocation method over conventional approaches is shown for few mathematical test functions.

Chapter 4, presents the use of surrogate modeling in UQ studies. A brief review of surrogate modeling approaches such as radial basis functions and Kriging approach is provided. A novel adaptive approach is proposed and compared with other existing approaches for few test problems. The adaptive approach proves to be superior to other conventional approaches used in probabilistic moment estimation.

Chapter 5, covers the implementation of methods for stochastic structural problems that are discussed in the earlier chapters. The description and implementation of proposed adaptive approach is also provided for the structural problems.

Chapter 6, presents a summary and the conclusions of this thesis. The conclusions reveals the extension of the proposed method to high-dimensional engineering application oriented problems.

Chapter 2

Formulation of stochastic systems

This chapter presents various aspects pertaining to the mathematical modeling of uncertainty. The first section of this chapter provides insight into the mathematical modeling of uncertainty in stochastic systems. The concept of random field and its discretization are discussed in the probabilistic approaches, for representing uncertainty.

In the second section a detailed review of various approaches for the propagation of uncertainty are described. The probabilistic representation of uncertainties using sampling based techniques such as Monte Carlo simulation, Quasi-Monte Carlo, lattice rules are presented.

In the third section an overview of existing formulations for structural optimization methods considering uncertainty is presented. The emphasis is put on structural robustness, taking into account the uncertainties involved in the system.

2.1 Mathematical models of Uncertainty

Accurate representation of uncertainty in the input random parameters is crucial and first step in the formulation of stochastic systems. The stochastic response output has no significance without the appropriate description of uncertainties. Typically there exist many methods and techniques to represent randomness in stochastic system but most often these approaches rely on the information of the marginal distributions and co-variance of the uncertainties in a system. The lack of sufficient information and experimental data usually forces one to assume quantitatively and qualitatively the stochastic information in the underlying parameters

of the stochastic system. The lack of available data is due to few reasons such as lack of well-defined measurement techniques, necessity for large amount of measurements for defining the statistical data, cost of measurement procedures. Very few studies are reported in the literature, where analysis of stochastic systems is performed based on actual measurements (see for example, Bendat et al. [7]) The modeling of stochastic input parameters using limited data is still an ongoing research.

Aleatory uncertainties characterised by inherent randomness and which cannot be reduced using further data are typically represented with probability distributions. Epistemic uncertainties are prevalent in the system due to the lack of knowledge about the nominal values of parametric uncertainties and are modeled using limited data. Regulatory bodies, design certification authorities are increasingly pressing towards charaterising and quantifying the aleatory, epistemic uncertainties individually and separate the effects that usually arise in an engineering system (e.g [24,25]).

There exist many approaches to represent uncertainty of the random parameters in dealing with the structural design problems. Some of the mathematical theories adopted to model uncertainties are probability theory, possibility theory, Dempster-Shafer evidence theory, fuzzy set theory, etc. However the need for data remains great, since the spatial or temporal variation charateristics of input parameters is necessary to improve the reliability of stochastic parameters in the framework of stochastic formulations.

2.1.1 Probability theory

To circumvent the above difficulties, a general and popular approach is to make assumptions for the parametric uncertanties using probabilistic approach. The statistical nature and physical selection criteria may lead to using appropriate distribution type for probabilistic description of uncertain parameters.

For example in a probabilistic approach, a Gaussian distribution is usually preferred to model the uncertainties arising in manufacturing tolerances. The use of Gaussian distribution based on data/experience from previous studies may be viewed as the sum of many individual effects according to central limit theorem.

A log-normal or uniform distribution is preferred if the parameter to be modeled is always positive such as Young's modulus. If the uncertain parameter depicts

external conditions of some physical phenomena, an extremum value distribution is used. For example, a Gumbel type distribution is often used to model the loads (such as Gust loads) due to its capabilities to capture the maximum values. On the other hand, Weibull distribution is often used to model parameters with low values which are important in such situation. The validity of the distibution type can be verified by means of Goodness-of-fit tests (eg., Chi-square, Kolmogrov-Smirnov tests). The decision making involves engineering experience and expert opinion to further mitigate any undesirable situations.

Probabilistic approach suggests the use of random variables in order to model uncertainities. A single random variable is inadequate to represent the spatial or temporal variation in the uncertain parameters. For example, the thickness/stiffness/strength of fuselage structure can vary spatially along its length but the gound acceleration at any point can be random with respect to time. Such phenomena have the characterisitcs of random function rather than a random variable. Stochastic processes are needed to take into account such variablities. Before any further discussion on this aspect, the definition of event and the mathematical representation of algebra of events is discussed in next section.

2.1.2 Algebra of events and stochastic processes

The set Ω is a sample space or sure event and is collection of all possible outcomes in an experiment. In general, individual outcomes are not preferred but collection of outcomes called events are of importance. If Ω is uncountable, then some of the subsets would be extremely difficult to work and a need for suitable collection of sets is required also termed as σ- algebras.

Let (Ω,F,P) be a complete probability space, where Ω is the event space, $F \subset 2^{\Omega}$ the σ- algebra and P is the probability measure of F. The random variable X is a mapping from Ω to real line R denoted as X: $\Omega \rightarrow R$. The random variable X is continuous rather than discrete and admits a probability density function $f_X(x)$ or cumulative distribution function $F_X(x)$ and defined by,

$$F_X(x) = P(X \leq x),$$

the following relation holds between the two,

$P(a \leq X \leq b) = \int_a^b f_X(x)dx, \quad f_X(x) = \frac{dF_X(x)}{dx}$

Instead of dealing with the PDF's, a finite dimensional stochastic space is defined and is given by ξ=[ξ^1,ξ^2,ξ^3,...ξ^N] : $\Omega \rightarrow R^N$, where ξ^i represents marginally distributed random variables N in the stochastic space. Let f be any real valued function having dependence on space (u), time (t) and random variable ξ with a known PDF, the stochastic process can be written as $g(u, t : \xi)$. As mentioned earlier if the spatial or temporal variations of uncertain parameters are considered they are represented by the above mentioned stochastic processes. The term random field stands for the stochastic processes which have an index in space, $g(u : \xi)$.

A random field H(u : ξ) is a collection of random variables defined on (Ω, F, P), where (Ω, F, P) is the Hilbert space of real random variables with finite variance. Here u represent the spatial coordinates and ξ is the realization in the sample space Ω. For example H($u^i : \xi$) is the random variable for given spatial coordinate u^i, conversely for a given realization of ξ_{u^i}, H(u : ξ_{u^i}) is a sample of the random field. The modeling of parametric uncertainties relies heavily on the ingredients of random field such as probability distribution and correlation structure. Loads, material or geommetrical properties of a stochastic system can be modeled using random fields.

2.2 Non-probabilistic approaches

As mention earlier in section 2.1, the possibility theory, evidence theory, interval theory are few approaches used to take into account uncertainty with incomplete information in random variables. The foregoing sections discuss the various aspects of uncertainty and decision making about systems that contain non-random uncertainty.

2.2.1 Interval analysis

In interval analysis, a set X comprising of input parameters ξ_i are simply defined within intervals as shown in Fig 2.1., and it is assumed that no prior information about the uncertain input varibles is known other than that it is contained within set X and defined as,

$$X = \{\xi_i : a_i \leq \xi_i \leq b_i\}$$

where $[a_i\ b_i]$ is an interval that contains possible values for ξ_i.

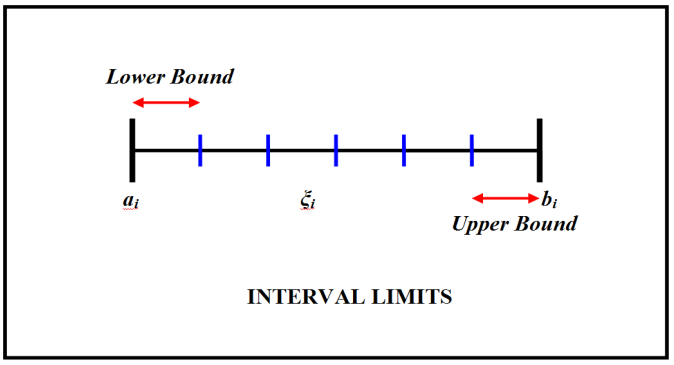

Figure 2.1: Interval Analysis.

For a vector $\xi = [\xi_1, \xi_2, ..., \xi_n]$ of uncertain variables contained in the sets $X_1, X_2, ...X_n$, the set of possible values is given by,

$$X = X_1 \times X_2 \times ..... \times X_n.$$

From above representation it is assumed that no restrictions in choice of specific combinations for the variables in ξ. The representation of uncertainty in variable y defined as,

$$y = M(\xi), \xi = [\xi_1, \xi_2, ...\xi_{\mathbf{n}}],$$

where M is a function of the vector ξ. Propagation of uncertain input values contained in X through function M results in set,

$Y = \{y : \xi \in \mathbf{X}\}$ for possible values for y.

Since there is know uncertain structure for the set X, there is no uncertain structure for set Y. Although conceptually simple it is very difficult to determine the bounds on the output or corresponding interval on the outputs.

A general approach to determine output in interval analysis is to take samples from the uncertain interval inputs and then consider the maximum and minimum output values based on sampling process as upper/lower bounds of the output. Few other approaches are presented in literature such as Moore et al. [26], Khodaparast et al. [27] and Walter et al. [28], where optimization methods are used to evaluate the max/min values of ouptut measure of interest corresponding to upper and lower bounds on the output, respectively. It may require prohibitively large number of simulations to determine the output bounds.

To circumvent the above difficulties one can make use of a surrogate model (eg: a regression model, adaptive spline model, nueral net, Kriging; etc) created with few samples from the interval bounds. The surrogate model can be sampled extensively to estimate upper/lower bounds of the output. Surrogate model based optimization methods are used to obtain upper/lower bounds. The feasibility and accuracy of surrogate model approaches for calculation of margins in epistemic uncertainties depends on the goodness of surrogate with repect to sampling points upon which it was built.

2.2.2 Possibility theory

Possibility theory assumes more structure to represent uncertain information compared to interval analysis. It is based on theory of possibility space for the variable ξ defined by specification of pair (X, r_i) for uncertain variable ξ, where X is the set of possible values for ξ and r_i is defined as function on X such that $0 \leq r_i(\xi_i) \leq 1$ for $\xi \in X$ and $\sup\{r(\xi_i) : \xi_i \in X\} = 1$. The function r_i also referrerd as possibility function for ξ and provides a measure of "confidence" that is assigned to each element of X. If the value of $r(\xi_i) = 1$ it implies there is no available information that refutes the occurence of specic value for ξ and a value $r(\xi_i) = 0$ suggests that there is no known information which refutes the occurence of ξ contained in X [29]. Hence as the value of possibility function $r(\xi)$ varies from 0 to 1 it suggests the absence of infomation that refutes the occurence of ξ.

Possibility theory provides two measures of likelihood: possibility and necessity respectively for the subsets of set X. The possibility and necessity for subset υ of X are defined by,

$$Pos_i(\upsilon) = \sup\{r_i(\xi_i) : \xi_i \in \upsilon\}$$

and

$$Nec_i(\upsilon) = 1 - Pos_i(\upsilon^c) = 1 - \sup\{r_i(\xi_i) : \xi_i \in \upsilon^c\},$$

respectively. From the consistency in properties of possibility distribution function r_i, $Pos_i(\upsilon)$ implies the measure of amount of information that does not refute the proposition that subset υ contains the value for ξ. Similarly $Nec_i(\upsilon)$ provides a measure of the uncontradicted information supporting the notion that υ contains the value for ξ_i.

The following relations holds for possibility and necessity for the possibility space(X, ξ_i) for the subsets υ of X,

$$1 = Nec_i(\upsilon) + Pos_i(\upsilon^c), \quad Nec_i(\upsilon) \leq Pos_i(\upsilon)$$

$$1 \leq Pos_i(\upsilon) + Pos_i(\upsilon^c), \quad Nec_i(\upsilon) + Nec_i(\upsilon^c) \leq 1$$

$$1 = max\{Pos_i(\upsilon), Pos_i(\upsilon^c), \quad 0 = min\{Nec_i(\upsilon), Nec_i(\upsilon^c)\}$$

$$Pos_i(\upsilon) \leq 1 \Rightarrow Nec_i(\upsilon) = 0, Nec_i(\upsilon) \geq 0 \Rightarrow Pos_i(\upsilon) = 1$$

Similar to the properties of probability space, the graphical representation of possibility space are provied by cumulative necessity function (CNF), cumulative possibility function (CPF), complimentary cumulative necessity function (CCNF), complimentary cumulative possibility function (CCPF). For further exposition of these aspects please refer deCooman et al. [29].

The variables $\xi_1, \xi_2, ..., \xi_n$ have associated probability spaces (X_1, r_1), (X_2, r_2),...., (X_n, r_n) and vector $\xi = [\xi_1, \xi_2, ..., \xi_n]$ also has associated possibility space (X, r_X), and

$$r_X(\xi) = \textbf{min}\ \{r_1(\xi_1), r_2(\xi_2), ..., r_n(\xi_n)\}$$

It is assumed that the possible combinations for values of $\xi's$ exist and no further restrictions are imposed in defining the set X and r_X respectively. The possibility and necesstiy functions for subsets υ of X are defined once the possibility space (X, r_X) for ξ are known from earlier derived equations.

The uncertainty propagation of elements of ξ contained in X through funtion M, results in set Y of possible values for y. The resultant possibility space (Y, r_y) also exists for values of y. The resultant possibility distribution function r_y defined by,

$r_Y(y) = sup\{r_x(\xi) : \xi \in \mathbf{X}$ and $y = M(\xi)\} = Pos_X\{M^{-1}(y)\}$ for $y \in Y$, where $M^{-1}(y)$ represents the set $M^{-1}(y) = \{\xi : \xi \in \mathbf{X}$ and $y = F(\xi)\}$. The terms $Pos_Y(\upsilon)$ and $Nec_Y(\upsilon)$ for subsets υ of Y can be determined using the above derived equations.

The plots for CNF, CCNF, CPF, CCPF can be produced and provide a graphical representation of uncertainty for y in terms of necessity and possibility.

2.2.3 Dempster-shafter Evidence theory

Evidence theory is based upon the representation of uncertainty through specification of triple (X, Ξ, m_i) for variable ξ_i and assumes more structure than possibility theory [30-32].

Here X is the set of possible values for varaible ξ_i, Ξ_i is a countable collection of subsets of X and m_i is a function defined on subsets ν of X such that,

1. $m_i(\nu) > 0$ if $\nu \in \Xi_i$

2. $m_i(\nu) = 0$ if $\nu \notin \Xi_i$ and

3. $\Sigma_{\nu \in \Xi_i} m_i(\nu) = 1$

In the mathematical description of the evidence theory using triple (X, Ξ, m_i), the terms X is the sample space or universal set, Ξ_i is the set of focal elements for X and $m_i(\nu)$, termed as basic probabitiy assignment (BPA) associated with subset ν of Ξ_i. In general the basic probability assignment provides a measure of information associated with subset ν of X.

Evidence theory gives two measures of likelihood namely, plausibility and belief for subsets of X. Typically the pausibility and belief for subset ν of X are defined respectively as,

$$Pl_i(\nu) = \sum_{\upsilon \cap \nu \neq \emptyset} m_i(\upsilon) \tag{2.1}$$

$$Bel_i(\nu) = \sum_{\upsilon \subset \nu} m_i(\upsilon) \tag{2.2}$$

Here $Pl_i(\nu)$ provides a measure of amount of information possibly associated with ν satisfying the requirement i.e., $\upsilon \cap \nu \neq \emptyset$ in Eq 2.1 and similarly $Bel_i(\nu)$ provides a measure of information known to be associated with ν as a result of requirement $\upsilon \subset \nu$ in Eq 2.2.

For evidence space (X, Ξ, m_i), the following relationships hold for plausibility and belief for subsets ν of X.

$$Bel_i(\nu) + Pl_i(\nu^c) = 1, \tag{2.3}$$

$$Bel_i(\nu) + Bel_i(\nu^c) \leq 1, \tag{2.4}$$

and

$$Pl_i(\nu) + Pl_i(\nu^c) \geq 1. \tag{2.5}$$

.

The graphical representation of evidence space are provided by cumulative belief functions (CBF's), complementary cumulative belief functions (CCBF's), cumulative pausibility functions (CPF's) and complementary cumulative pausibility functions (CCPF's). Typically for the evidence space (X, Ξ, m_i), the CBF, CCBF, CPF and CCPF are defined by sets,

$$CBF_i = \{[\xi, Bel_i(\nu_\xi)] : \xi \in X\}, \quad CCBF_i = \{[\xi, Bel_i(\nu_\xi^c)] : \xi \in X\} \tag{2.6}$$

.

$$CPF_i = \{[\xi, Pl_i(\nu_\xi)] : \xi \in X\}, \quad CCPF_i = \{[\xi, Pl_i(\nu_\xi^c)] : \xi \in X\} \tag{2.7}$$

.

where ν_ξ is defined same as in Eq 2.3-2.4. The plots for $CBF, CCBF, CPF$ and $CCPF$ for the evidence space (X, Ξ, m_i) can be produced and provide a graphical representation of uncertainty for y in terms of plausibility and belief for subsets of X.

2.2.4 Fuzzy set & Membership

The fuzzy approach for uncertainty quantification is based upon the idea of modeling the random parameters as fuzzy quantities. In conventional approaches of set theory an element either belongs or not belongs to a set defined by probability, possibity or evidence spaces. But fuzzy sets have a membership function that allows for partial membership in the set. The idea of set membership proposed by

Zadeh [33], holds key to decision making when facing the uncertainty. Zadeh in his seminal paper presents the notion of fuzzyset and its capability in providing a conceptual framework construction similar to ordinary set theory. Such framework facilitates one to deal with uncertainties where the source of imprecision is due to lack of well defined criteria for imprecision, and thus helps in restricting the usage of random variables.

The notion of set membership is central to representation of objects within a universe by sets defined in the universe also termed universal set. Hence classical sets contain objects that satisfy precise properties of membership and on the other hand fuzzy set contain objects that satisfy imprecise properties of membership where the membership of object in a fuzzyset can be approximate.

Let X be an exhaustive collection of individual elements x making a universal set. Further various combination of these individual elements make up sets A on the universal set. For crisp set, an elemet x in the universe X is either a member of some crisp set A or not. This binary set of information can be represented mathematically with an indicator function,

$\chi_A = \{^1_0 x \in A \notin A$

where the symbol χ gives the indication of unambigious membership of element x in set A.

Zadeh extended the concept of binary membership to accomodate various "degrees of membership" on the real continuous interval [0 1], where end points of 0 and 1 confirm to no membership or full membership just as indicator function does for crisp sets, where infinite number of values in between end points can represent various degrees of membership for element x in some set on the universe. The sets on the universal set X that can accomodate degrees of membership are termed as fuzzy sets. The key difference between crisp and fuzzy set is their membership function where the former has unique membership function and the latter have infinite number of membership functions.

The membership function as shown in Fig 2.2., represents the mathematical representation of membership in a set and a fuzzy set is denoted by $\tilde{A}$ where the functional mapping is given as,

$\mu_A(x) \in [0, 1]$

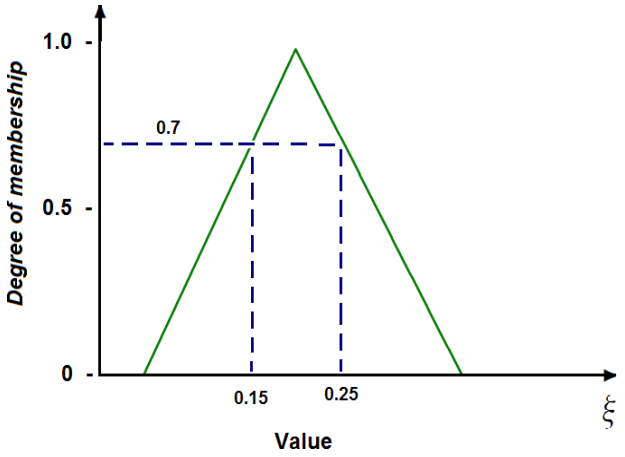

Figure 2.2: Membership Function.

and the $\mu_A(x)$ is the degree of membership of element x in fuzzy set A. Therefore $\mu_A(x)$ is a value on the unit interval that measures the degree to which element x belongs to fuzzy set A; equivalently $\mu_A(x)$ is the degree to which x $\in \tilde{A}$.

2.3 Propagation of stochastic responses

After the description of different aspects regarding to the modeling of uncertainties, the next step in the stochastic structural system would be the assessment of probabilistic content of output response, i.e to propagate the randomness through the stochastic model. Although different approaches to propagate the uncertainty are briefly mentioned in the first chapter, in the corresponding sections we set stage for a detailed discussion of such approaches.

An appreciation of the merits of uncertainty propagation methods is impossible without rudimentary understanding of simulation based techniques such as Monte Carlo, Quasi-Monte Carlo, Lattice rules etc., used in the numerical evaluation of integrands in high-dimensional probabilistic weighted design space. The essence of such approaches consists of three main steps : i) generation of samples for parametric uncertainty according to probabilistic description of the variable, ii) to perform the simulations corresponding to each input sample, iii) to calculate the response statistics of the output quantity of interest from the deterministic responses.

2.3.1 Monte Carlo Simulation

In simple terms, Monte Carlo method (MCS) is described as a numerical method based on random sampling and has a strong statistical significance. Developed in 1940's to reduce the complexities arising in high-dimensional spaces, MCS finds its applications in many fields without restricting itself to numerical integration [9]. A crucial step in the application of MCS is the generation of appropriate random samples. In computational application of MCS the random samples are generated using a deterministic code and the numbers or vectors are termed "psuedo random numbers" and "psuedo random vectors" respectively.

Considering random variable represented by the vector ξ=[ξ^1, ξ^2, ξ^3, ...ξ^k], the input distribution $p(\xi^1, \xi^2, \xi^3, ...\xi^k)$ can be obtained by a finite number N of independent samples $\{\xi^m\}_{m=1}^N$. The individual vector ξ^m specifies deterministic value for uncertain parameter, for which the response $f^m = f(\xi^m)$ is obtained from deterministic analysis. Here the mean and variance of response quantity f can be obtained as,

$$\mu_i =< f_i > \approx \frac{1}{N}\sum_{m=1}^{N} f(\xi^m). \tag{2.8}$$

$$\sigma^2 =< (f_i - \mu_i)^2 > \approx \frac{1}{N-1}\sum_{m=1}^{N} (f(\xi^m) - \mu_i)^2. \tag{2.9}$$

According to the strong law of large numbers given in Niederreter [9], the above equation guarantees that fluctuation in the statistical estimates that are random reduces, as the number of sample size N increases.

$$\mathrm{Lim}_{N\to\infty}\frac{1}{N}\sum_{n=1}^{N}(f) = E(f) \tag{2.10}$$

In the above equation, $E(f)$ is the expected value. For the probabilistic error estimate, the variance is given by,

$$\sigma^2(f) = \int_B (f - E(f))^2 df. \tag{2.11}$$

which is finite for $f \in L^2$.

On the basis of the central limit theorem, the MCS for numerical integration yields a probabilistic error bound of the form $O(N^{(-1/2)})$ in terms of number of samples N. As mentioned earlier MCS offers a way of overcoming "curse of dimensionality" where the probabilistic error bound doesn't depend on the dimension d but requires the samples to be regularised and independent.

2.3.2 Quasi-Monte Carlo approach

Quasi-Monte Carlo simulation is the traditional Monte Carlo simulation but using quasi-random sequences or low discrepancy sequences such as Halton, Faure, Sobol sequence instead of pseudo random numbers as shown in Fig 2.3.

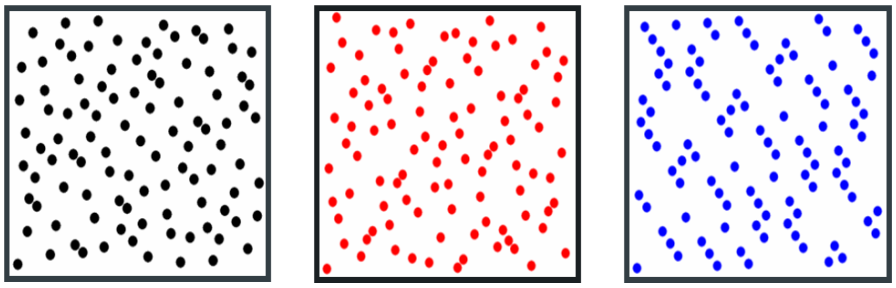

Figure 2.3: Low Discrepency Sequence Points (Sobol, Halton, Faure Sequences).

Some of the advantages and disadvantages of QMC techniques are as follows,

Advantages:

- totally deterministic,
- low-discrepancy sequences permit to improve the performance of Monte Carlo simulations, offering shorter computational times and/or higher accuracy,
- The evaluation of an integral is the strongest application of quasi-random sequences.

Disadvantages:

- quasi-Monte Carlo methods are valid for integration problems, but may not be directly applicable to simulations due to the correlations between the points of a quasi-random sequence which can be solved using lattice rules as given by Morokoff [10].

- for high dimensional problems, the use of low discrepancy sequences should adequately sample the d-dimensional hypercube.

- An inspection of appropriate error bounds for Quasi Monte Carlo methods reveals a feature that is a draw back for these methods. Typically if the integrand is sufficiently regular, then any additional regularity of the integrand is not affected in the order of the magnitude of the error bound. This is in contrast to one dimensional numerical schemes such as Gauss formulas and Newton Cotes rules which can be tailored for the regularity class of the integrand so that they become efficient for more regular integrands.

For quasi-Monte Carlo methods discussed in this section, the degree of regularity of integrand is not reflected in the order of magnitude of error bound and to achieve this, one must consider the integrand to be periodic with an interval P so that the underlying Fourier analysis make sense but is no serious issue since the non periodic integrand can always be periodized. The integration rules for such periodic integrands can be viewed as multi-dimensional analogues of one dimensional trapezoidal rule. These integration rules arose as special form of good lattice points introduced by Korobov [34] in 1959.

2.3.3 Lattice rules

As discussed earlier, these integration rules were first introduced by Korbov as good lattice points but a general class of lattice rules or methods was defined and analyzed recently. In last few years, much research work is devoted to these type of numerical integration schemes.

Here the d dimensional cube comprises of points generated using lattice rules. The points are deterministic but differs to quasi-MonteCarlo methods, where the points are generated using low-discrepancy sequences. The points are constructed using rank-1 lattice (as shown in Figure 2.4), or rank-2 lattice, Fibonacci lattice etc. There are different lattice structures provided in the literature [34]. They are a generalisations of one-dimensional rectangle rule. Kuo et al. [35], further developed a component-by-component algorithm to rapidly generate lattice points in the high dimensional integral domain using order-weighted lattice rules. But many challenges lie ahead in the implementation of the algorithm for varied class of integral functions.

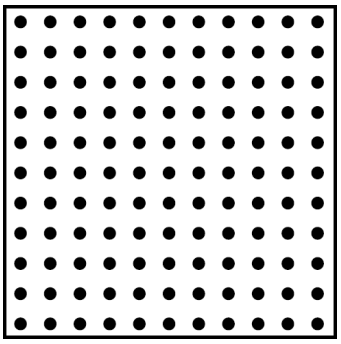

Figure 2.4: Lattice Points

The lattice points are regularised in the integral domain and deterministic simulations can be performed similar to MCS, SGM. Using lattice rules the probabilistic moments can be calculated, when apriori moment estimates of the objective function are not attainable using conventional approaches.

2.4 Structural optimization under uncertainty

The methods for structural optimization are widely used for the improvement of performance and reduce the costs incurred in the design of engineering structures. Over the past few decades, the complexity of systems need to be studied has grown in accordance with the computational abilities associated with design optimization. Considerable progress has been achieved in the field of design optimization and is still an area of active research in engineering design and applied mathematics communities.

In structural opimization, the parameters defining the performance of the structure need to be evaluated for desired output and these are termed as design parameters. The function characterizing the structural performance is called objective function. Typically there are few constraints to be satisfied in a design optimization problem, and thus defines the feasible domain in the design variable space. These constraints are generally referred to as design constraints. Also bound limits are imposed on the design variables and are referred to as side constaints.

In design optimization problems the objective function and the design constraints are described as implicit functions of the design variables. and are evaluated by numerical simulation techniques such as FEA/CFD.

The mathematical description of a structural optimization problem is expressed as,

$$\begin{aligned} \underset{x}{\text{Minimize}} \quad & f(x), \\ \text{Subject to} \quad & g_i(x) < 0 \quad (i = 1, 2, .., m), \\ & h_i(x) = 0 \quad (i = 1, 2, .., q), \\ & x_L \leq x \leq x_U, \end{aligned} \tag{2.12}$$

where $x \in \mathbb{R}^p$ is the vector of design variables, $f(x)$ is the objective function to be minimized and $g_i(x)$, $h_i(x)$ are the inequality and equality constraints respectively. x_L and x_U are vectors of lower and upper bounds of design variables, respectively. The objective and constraint functions can be expensive and since they are implicit functions of design variables, structural analysis is performed whenever the values are required. Structural cost, structural weight/ material volume, and performance metrics such as compliance, natural frequencies, buckling loads, nodal stresses & displacements are typical examples of objective and constraint functions. The design variables include geometrical dimensions, shape or topology of strucutre, material properties and other important parameters based on the definition of the underlying functions. In practical applications of design optimization, the number of design variables can be numerous and evaluating the function (i.e, objective and constraint functions) can lead to use of excessive computational power and there is a further increase in deducing the sensitivity analysis information. Hence it is effective to impose a relationship between coupled design variables so that the overall independent variables can be kept to minimum in design optimization studies. For further exposition of these aspects, please refer to Dolstinis et al. [36], Sigmund et al. [37] and Aurora [38].

Typically the optimal design of a structure is sought using conventional design optimization tools such as optimality criteria methods and numerical optimization techniques based on the deterministic analysis of the simulation model while considering nominal or deterministic values of the design parameters.

2.5 Overview of problem formulations

The design optimum attained using earlier formulation Eq. 2.12, signifies the best performance in theory, but in practical implementation such a design may not be feasible due to the uncertainties in the design parameters. Such variations about

the nominal values of design variables result in scatter of system performance and the ideal optimum of deterministic structure may perform far worse than an alternative design which is less sensitive to parameter variations [2-4].

The general procedure for structural optimisation taking into account the system uncertainties, is based on safety factors and there is always ambiguity involved in the choice of appropriate safety factor to be used for the design of novel structures. Some of the sophisticated formulations incorporating uncertainties into structural design optimization are given below.

2.5.1 Reliabity based design optimization

Reliability is the probabilistic study of a system performance over a given period of time under specified service conditions. Although originally developed in 19^{th} century for computing profitable rates to customer charges by maritime and financial companies, it found its importance in predicting the failure of structural sytems (i.e., aircrafts, automible, ships, bridges, etc.) under uncertainty factors inherent in these systems.

Here the structural response is considered satisfactory if the design requirements imposed on the structure are met within acceptable degree of certainty. These requirements are termed as limit-state or constraints. Thus the concept of structural reliability is associated with the calculation and prediction of the probability of occurence of limit-state violations and to choose alternative designs to improve the reliabilty of the strucuture further minimizing the risk of catastrophic failures.

In reliability based design optimization (RBDO), the failure of the system or a component under extreme events is taken into consideration. Lately this is the popular approach of taking account of uncertainty in design optimization studies. Here the objective function given in Eq. 2.12, is minimized satifying probabilistic constraints rather than deterministic constraints. In this formulation, the probability of structural failure defined using limit state functions is described in the constraint equations of the structural optimization problem.

From classical approach based on Apostalakis et al. [3], the reliability-based design optimization can be mathematically expressed as,

$$\begin{aligned} \underset{x}{\text{Minimize}} \quad & f(x), \\ \text{Subject to} \quad & P(g_i(x) \leq 0) - \Phi(-\beta_i) \leq 0 \quad (i = 1, 2, .., m), \\ & x_L \leq x \leq x_U, \end{aligned} \tag{2.13}$$

where $P(g_i(x) \leq 0)$ is the probability of failure, β_i is the safety index or reliability index and Φ is the integral for the standardised normal distribution i.e., over the range $(0,\ 1)$.

2.5.2 Non-probabilistic design optimization

It is very difficult during the early stages of structural design, the quantification of structural reliability or compliance to specific design requirements based upon insufficient data or information for design variables, parameters, operating conditions, boundary conditions etc. Design decisions are based upon fuzzy information that can be vague, imprecise and incomplete. The uncertain information can also be available as intervals with lower and upper limits.

As mentioned earlier in sec 2.2, the possibility, evidence, interval theory are used to account for representing uncertainty with incomplete information. Possibility based design optimization, evidence based design optimization are ways to handle a combination of probabilistic as well as non-probabilistic design variables. In non-deterministic optimization scenario, the structural optimization against failure is often performed based on worst case analysis [39].

2.5.3 Structual robust design optimization

The main aim in performing robust design is to reduce the variability and improve the mean performance of a structure in the presence of uncertainties. Hence mean value and standard deviations in performance functions are used to define the objective function and the constraints. The mathematical model of robust design problem is a multi-criteria optimization problem defined as,

$$\begin{aligned} \underset{x}{\text{Minimizing}} \quad & \{E(f(x)), \sigma(f(x))\}, \\ \text{Subject to} \quad & E(g_i(x)) + \beta_i \sigma(g_i(x)) \leq 0 \quad (i = 1, 2, .., m), \\ & \sigma(h_j(x)) \leq \sigma_j^* \quad (j = 1, 2, ..., l), \\ & x_L \leq x \leq x_U, \end{aligned} \tag{2.14}$$

where $h_j(x) \quad (j = 1, 2, ..., l)$ represent constraints on standard deviations of the response, $\beta_i \geq 0$ is a feasibility index for the respective constraint and σ_j^* is the upper limit for standard deviation of the response. For example if β is 3.0, in order for the constraint condition Eq. 2.14., to be satisfied, the probability of the original constraint being met should be higher than 0.9987. The feasibility index is considered as an appropriate measure of the robustness corresponding to design restrictions. The robust design problem is at least a two-design problem and often the interests may vary. But a Pareto optimal design is one way of achieving the trade-off between the two design objectives for robust design problems. The estimation of moments (mean, variance) of performance functions, is central to the robust design process.

This chapter presents formulation of stochastic systems and methods for estimation of randomness in input parameters for structural models. In later chapters, a conceptual framework for probabilsitic moment estimation in the context of robust design process for stochastic sytems is provided.

Chapter 3

Stochastic collocation approach

Uncertainty can be incorporated into stochastic structural systems by modeling the parametric uncertainties using probabilistic approach, where they are described as random variables. In this chapter, some important attributes about stochastic collocation methods and effective use of probabilistic moment estimation in high-dimensional spaces using a Smolyak formula is given, followed by solution to numerical examples with uncertain random variables.

The basic properties of random variables and the techniques for building the probabilistic collocation method are given in the following section.

3.1 Stochastic collocation method

From a general perspective, the probabilistic model for a stochastic system can be interpreted as a function $f(u, t : \xi)$, where ξ is the vector of random variables. The model f can be a simple mathematical function or "black box" function such as computer program (FEA, CFD). The useful information of a typical response $(f(u, t : \xi))$ is generally extracted through integration, i.e finding mean, variance and other higher order probabilistic moments, and further enables us the construction of trajectories for probability density functions. There are multiple approaches for numerically solving $f(u, t : \xi)$ as discussed in sec 2.1-2.3 and includes sampling based approaches, generalized polynomial chaos and collocation method, the latter of which is of interest here.

The important characteristics such as expectation (or mean μ), variance (σ^2) and other higher order moments of stochastic function $f(u, t : \xi)$ are expressed as integrals and given by,

$$E[f(u,t:\xi)] = \int_{\Gamma} f(u,t:\xi)p(\xi)\ \mathrm{d}\xi, \quad \xi \in \Gamma \subseteq \Omega. \tag{3.1}$$

$$\sigma^2[f(u,t:\xi)] = \int_{\Gamma} (f(u,t:\xi) - E[f(u,t:\xi)])^2 p(\xi)\ \mathrm{d}\xi. \tag{3.2}$$

where $p(\xi)$ is the joint PDF of the random variable ξ and Γ is the sample space. The moments (μ, σ^2) of a multi-variate function f with random variables ξ are difficult to estimate since the integrand is bounded in high-dimensional space. Numerical integration also popularly known as quadrature, is basically a problem of characterizing a function over a domain by sample points by sum of function values at n points, multiplied with respective weights w_i and defined as,

$$\int_{\Gamma} f(u,t:\xi_i)\ \mathrm{d}\xi, \simeq \sum_{i=0}^{n} w_i f(u,t:\xi_i) \tag{3.3}$$

For a large-sale structural system, rarely f may be calculated analytically and often simulation is required. To achieve high accuracy with minimal number of simulations it is desirable to use an efficient discretization scheme for Eq (3.3).

The classical integration rules such as trapezoidal and Simpson's rules are popular 1-D quadrature methods, collectively known as Newton-Cotes formulae. For concreteness let us consider the trapezoidal rule in dimension $\mathrm{d} = 1$ for unit interval $[0, 1]$. In trapezoidal rule, the integrand is evaluated at equally spaced discrete points in the integrable domain yielding an approximation,

$$\int_0^1 f(u)\ \mathrm{d}u \approx \sum_{n=0}^{m} w_n f(\frac{n}{m}) \tag{3.4}$$

where m is a positive integer and the weights w_n are given by $w_0 = w_m = 1/(2m)$ and $w_n = 1/m$ for $1 \leq n \leq m-1$. The error in the above approximation is in the order of $O(m^{-2})$, provided f is second order continuous on $[0, 1]$. For multi-dimensional case $d \geq 2$, the classical integration rules use Cartesian products of one-dimensional rules, where the node set is a Cartesian product of one-dimensional node sets, and corresponding weights are products of weights from

the one-dimensional rules. For integral domain $I^d = [0\ 1]^d$ the d-dimensional Cartesian product of the trpezoidal rules is illustrated as,

$$\int_{I^d} f(u)\ \mathrm{d}u \approx \sum_{n_1=0}^{m} ... \sum_{n_d=0}^{m} w_{n_1}....w_{n_d} f(\frac{n1}{m}, ..., \frac{n_d}{m}) \tag{3.5}$$

The total number of nodes in Eq (3.5), is $N = (m+1)^d$ and the error is of order $O(N^{-2/d})$. With increasing dimension d the usefullness of error bound declines rapidly. For example to attain a prescribed level of accuracy in absolute value $\leq 10^{-2}$ one must use approximately 10^d nodes and the number of nodes increases exponentially with d.

Hence as Newton-Cotes formulae extended to higher dimensions the accuracy tends to be quite poor in the order of $O(N^{2/d})$ and $O(N^{4/d})$ respectively, where N is the number of quadature points and d is the dimension. A detailed explanation of these quadrature rules and their limitations is given by Davis and Rabinowitz [40].

Gaussian Quadrature

Gaussian quadrature differs the Newton-cotes formulas in the selection of nodes and weights such that the approximation is exact for low order polynomial function F. The approximation to the weighted integral is expressed as,

$$\int_a^b F(u)w(u)\mathrm{d}u \simeq \sum_{i=1}^{n} \omega_i F(u_i) \tag{3.6}$$

Gaussian quadrature rules are based on data points that are not equally spaced but nodes of the orthogonal polynomials. Further, the selection of nodes and weights depends on the underlying weighting function according to theorem proposed by Davis and Rabinowitz [40].

Theorem 3.1

Assume $\varphi_l(x)_{l=0}^{\infty}$ is an orthonormal family of polynomials with respect to the weighting function $w(u)$ on the interval [a;b], and define α_l so that $\varphi_l(x) = \alpha_k x^k + ...$

Let $x_i, i = 1, ..., n$ be the roots of the polynomial $\varphi(x)$. If $a < x_1 < ... < x_n < b$ and if $F \in C^{2n}[a;b]$, then

$$\int_a^b F(x)w(x)\mathrm{d}x = \sum_{i=1}^{n} \omega_i F(x_i) + \frac{F^(2n)(\zeta)}{\alpha_n^2(2n)!} \tag{3.7}$$

for $\zeta \in [a;b]$ with

$$\omega_i = -\frac{\alpha_{n+1}/\alpha_n}{\varphi_n'(x)\varphi_{n+1}(x)} > 0 \tag{3.8}$$

The above theorem provides a means for estimating the nodes and weights for any weighting function and also there exist Gaussian quadrature formula for wide spectrum of weighting function with respective values of nodes and weights.

Gaussian quadrature rules which are polynomial based methods, use orthogonal polynomials such as Legendre, Hermite or Laguerre polynomials [41]. The classical orthogonal polynomials corresponding to special weight functions and the support space are given in the Table 3.1. A brief synopsis of orthogonal polynomials is provided in appendix [A].

Table 3.1: List of some important orthogonal polynomials :

Interval	Weight function	Symbol	Name
[-1 1]	1	$L_n(x)$	Legendre
(-∞ ∞)	e^{-x^2}	$H_n(x)$	Hermite
[0 ∞)	e^{-x}	$G_n(x)$	Laguerre
[-1 1]	$(1-x^2)^{-1/2}$	$T_n(x)$	Chebyschev

The choice of orthogonal polynomial basis is based upon the distribution of the random variable, since the PDF of the random variable differs the weight function of appropriate orthogonal polynomial by a constant. Typically Legendre polynomials are used for uniform random variables and Hermite polynomials for normal random variables. Gauss rules have polynomial exactness of $2n-1$ with n function evaluations. Thus an integrand with order $2n-1$ or less can be integrated exactly.

Gauss-Kronrod-Patterson quadratures was first developed by Kronrod [40] and an extension to Gaussian quadrature rules. Later Patterson [42] iterated the sequence developed by Kronrod to achieve nested quadratures. The n point Gaussian

quadrature rules have polynomial exactness of $2n-1$ and with p new points added in the successive levels the exactness of these rules can be increased to $2n-1+\sum p$.

Clenshaw-Curtis quadrature uses Chebyshev polynomials as a basis and they achieve polynomial exactness of n. The nested quadrature rules are preferred for high dimensional numerical integration, where lower order collocation points are a subset of the higher order collocation points. Further details regarding the economy and reliability of suitable 1-D quadrature rules is given in [42].

3.2 Sparse grid collocation approach

For high-dimensional integration, the number of collocation points where the integrand is to be evaluated, increases exponentially. Smolyak [43] introduced a formula to reduce such complexities mentioned above and is the principal constituent for sparse grid methods. The Smolyak formula uses a weighted linear combination of special tensor products to reduce the integration grid size. This proved to be an efficient discretization scheme and well suited for high dimensional problems [44-47]. Sparse grid collocation method was developed in the context of reducing computational cost for high dimensional problems.

3.2.1 Construction

Let k be the index of the grid and n be the number of points in the sparse grid. Let U_1^i and w_1^i denote the one-dimension quadrature points and weights which can be obtained by Gaussian quadrature, Clenshaw-Curtis rules, etc. For d-dimension sampling points $\overrightarrow{U}_d$, referred to as collocation points, with level k ($k \geq 0$), the tensor product rule specific to the sparse grid is represented as,

$$\overrightarrow{U}_d^k = \bigcup_{k-d+1 \leq |i| \leq k} U_1^{i_1} \otimes U_1^{i_2} \otimes ..... \otimes U_1^{i_d}, \tag{3.9}$$

$| \ i \ | = \sum_{i=1}^{d}$ denotes summation of multi-indices. The weight w_l corresponding to the l^{th} collocation point $\overrightarrow{\xi_l} = [\xi_{j_{i_1}}^{i_1}, ..., \xi_{j_{i_d}}^{i_d}]^T \ \epsilon \ \overrightarrow{U}_d^{\ k}$ is,

$$w_l = (-1)^{k+d-|i|} \binom{d-1}{k+d-\mid i \mid} (w_{j_{i_1}}^{i_1}, ..., w_{j_{i_d}}^{i_d}). \tag{3.10}$$

The integration of a multivariate function f, using the sparse grid approach is given by,

$$\int_{\overrightarrow{\xi} \epsilon \overrightarrow{U}_d{}^k} f(\overrightarrow{\xi}) p(\overrightarrow{\xi})\, \mathrm{d}\, \overrightarrow{\xi} \approx \sum_{l=1}^{P_s} w_l f(\overrightarrow{\xi_l}). \tag{3.11}$$

P_s is the number of all possible combinations of the multi-indices that satisfy $k-d+1 \leq |i| \leq k$. Here in the sparse grid construction, the one dimensional rules are considered to be nested. The relation between the level k and the order of sparse grid varies for different one dimensional rules. For example, for Clenshaw-Curtis rule, $n = 2^k + 1$, and for Gauss Hermite rule, $n = 2^{k+1} - 1$.

Fig 3.1 illustrates the construction of a sparse grid considering a one dimensional Clenshaw-Curtis rule for $(d = 2, k = 2)$. With 2-level $(k = 2)$ accuracy, the number of collocation points are 5 in a one dimensional scenario and if two dimensions are considered as equivalently important, there should be 5 points in each dimension. Therefore, 25 collocation points are obtained by the full grid method with the direct tensor product on the two sets of one-dimensional quadrature nodes. The total number of collocation points for sparse grids obtained by carrying out a tensor product on the possible combinations of $[i_1, i_2]$ is 13. Here the acceptable combinations are $[U_1^0\ U_1^1]$, $[U_1^1\ U_1^0]$, $[U_1^1\ U_1^1]$, $[U_1^0\ U_1^2]$, $[U_1^2\ U_1^0\ ]$ since $1 \leq i_1 + i_2 \leq 2$. The sparse grid approach enables one to exclude the combinations $[U_1^2\ U_1^2]$, $[U_1^2\ U_1^1]$ and $[U_1^1\ U_1^2]$. Sparse grid points in two and three dimensions using the Clenshaw-Curtis rule are shown in Figure 3.2.

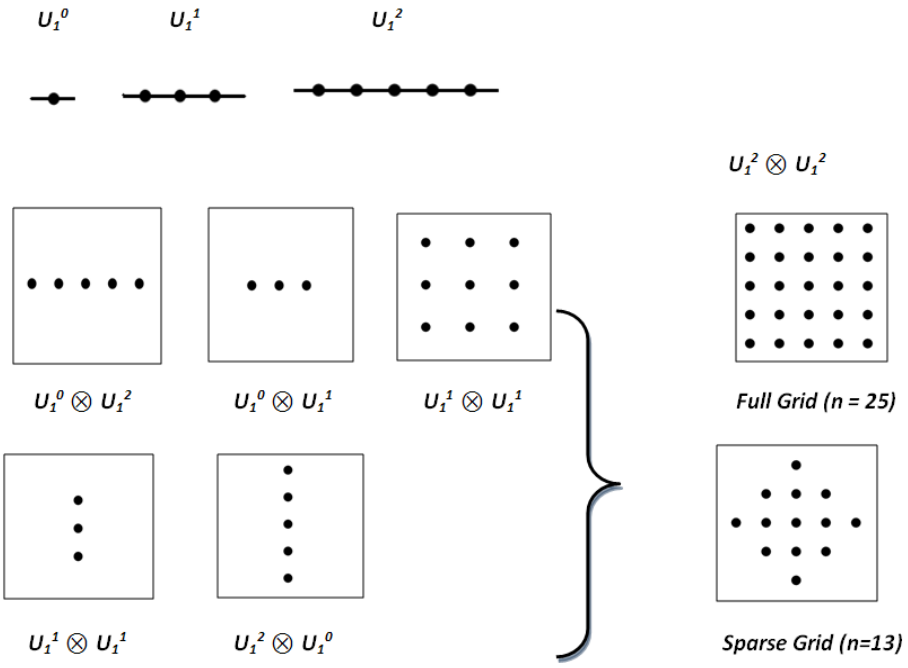

Figure 3.1: Construction of Sparse Grid Vs. Full Grid, d=2, k=2.

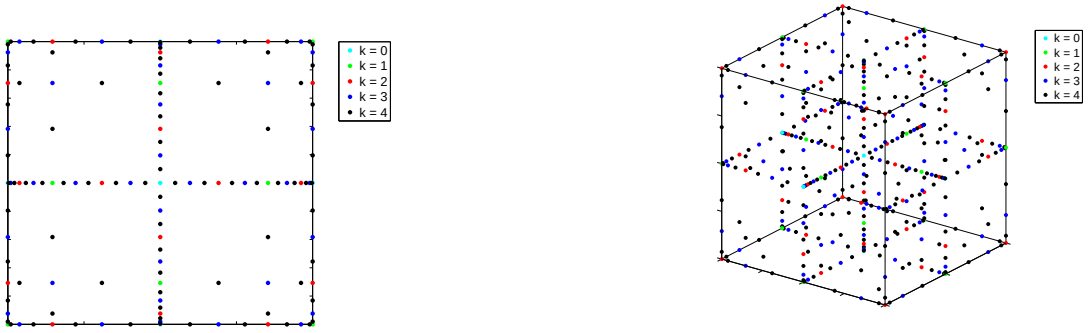

Figure 3.2: Sparse Grid in 2D, 3D with Clenshaw-Curtis rule ($k = 0, 1, 2, 3, 4$).

Table 3.2-3.3 lists the number of sparse grid collocation points required using Clenshaw-Curtis and Gauss Hermite rules for varying dimensionality (d = 2,6,10,12) and levels (k = 1,2..,5).

Table 3.2: Number of sparse grid points using Clenshaw-Curtis rule:

k	d =	2	6	10	12
1		5	13	21	25
2		13	85	221	313
3		29	389	1581	2649
4		65	1457	8801	17265
5		145	4865	41265	93489

Table 3.3: Number of sparse grid collocation points using Gauss-Hermite rule:

k	d =	2	6	10	12
1		5	13	21	25
2		21	109	261	361
3		73	713	2441	3873
4		225	3953	18881	340625
5		637	19397	126925	258681

In sparse grid quadrature methods, the points and weights are chosen from tensor products of low-order one dimensional quadrature rules and thus efficiently evaluate an integrand in high-dimensional space compared to the full quadrature rules where the number of collocation points grow exponentially. But similar to classical quadrature techniques, the sparse quadrature methods are sensitive to the smoothness of the integrand. Though sparse quadrature enable us to estimate the moments with less function evaluations for multivariate functions, it is difficult to accurately estimate the moments of complex non-linear functions. Higher order (level k) collocation points need to be used for such integral estimation. But with the increase of order of 1-D rule, the number of points further increases as shown in Table 3.2-3.3. In order to mitigate this problem, a dimension adaptive algorithm is proposed.

3.3 Adaptive sparse grid approach

A sparse grid interpolation method is developed using hierarchical rules by Klimke [48], based on piecewise polynomials which allows the inclusion of new points between two existing SG points. Similar to the sparse grid quadrature method, in sparse grid interpolation (SGI) the univariate interpolation basis is extended to multivariate case using tensor products. The main difference being, the sparse quadrature method uses 1-D quadrature points and weights, whereas SGI begins with univariate interpolation formulae such as piecewise Gauss polynomials, which are transformed to multi-dimensional basis functions. An interpolation method with few support nodes is obtained, compared with a conventional interpolation on a full grid.

3.3.1 Construction

Let x_j^i be 1-D interpolation nodes (with their locations $x_j^i(j = 1, ...m_i)$) and Φ_j^i 1-D basis functions, respectively; the univariate interpolate function is then given by,

$$U^i(f) = \sum_{j=1}^{m_i} f(x_j^i)\Phi_j^i. \tag{3.12}$$

For the multivariate case $d > 1$ by tensor product,

$$(U^{i_1} \otimes .... \otimes U^{i_d})(f) = \sum_{j_1=1}^{m_{i_1}} ... \sum_{j_d=1}^{m_{i_d}} f(x_{j_1}^{i_i}, ..., x_{j_d}^{i_d}).(\Phi_{j_1}^{i_1} \otimes ... \otimes \Phi_{j_d}^{i_d}). \tag{3.13}$$

The sparse grid interpolation of f with level k using Smolyak formula is given by,

$$A(q,d)(f) = (-1)^{q-|i|}\binom{d-1}{q-\mid i \mid}.(U^{i_1} \otimes .... \otimes U^{i_d}), \tag{3.14}$$

where $\mid i \mid = i_1 + ... + i_d$, $k = q - d$. In the computation of sparse grid interpolation $A(q,d)(f)$, only the function values at sparse grid points are to be known. The set of collocation points $H(q,d)$ are defined by,

$$H(q,d)(f) = \bigcup_{k+1 \leq |i| \leq q} (\chi^{i_1} \otimes ... \otimes \chi^{i_d}), \tag{3.15}$$

where $\chi^i = [x^i_1, ..., x^i_{m_i}]$ are the set of points used by U^i.

A dimension adaptive tensor product quadrature approach is proposed and implemented by Gerstner and Griebel [49,50], considering a optimal index set i from a more general index sets in the summation of Eq. (3.9). The self-adaptive algorithm is used to find the optimum index through an iterative procedure. The algorithm uses error estimate of the function and new nodal points are added locally to refine the sparse grid based on the function roughness. It is a generalisation to the sparse grid method and can improve the convergence rate and accuracy of the conventional sparse grid quadrature approach. Sethuraman et al. [51], used the adaptive technique using Lagrange polynomials in the analysis of cardiovascular simulations incorporating uncertainties. Liu et al. [52], implements the adaptive sparse grid algorithms for solving SPDE's with applications to electromagnetic scattering problems. The above studies suggest the effectiveness and substantial computational savings with the adaptive sparse grid approach.

3.4 Numerical Results & Discussion

In this section, the probabilistic moment estimation approaches are tested for a set of analytical functions, widely used as benchmark problems in optimization studies [53,54]. The eight functions are selected with increasing dimension/variables and are widely used as global optimisation functions with multiple minima respectively. The test functions are provided in the following subsection.

3.4.1 Test functions:

1. Forrester function (one variable):

$$y(\mathbf{x}) = (6x_1 - 2)^2 \sin(12x_1 - 4), \quad x1 \in [0, 1].$$

2. Branin function (two variables):

$$y(\mathbf{x}) = (x_2 - \frac{5}{4\pi^2}x_1^2 + \frac{5}{\pi}x_1 - 6)^2 + 10(1 - \frac{1}{8\pi}\cos(x_1)) + 10, \quad x1 \in [-5, 10], \ \ x2 \in [0, 15].$$

3. Six-hump Camelback function (two variables):

$$y(\mathbf{x}) = 4x_1^2 - 2.1x_1^4 + \frac{x_1^6}{3} + x_1x_2 - 4x_2^2 + 4x_2^4, \quad x1 \in [-2, 2], \quad x2 \in [-1, 1].$$

4. Mystery function (two variables):

$$y(\mathbf{x}) = 3 + 0.01(x_2 - x_1^2)^2 - x_1 + 2(2 - x_2)^2 + 7\sin(0.5x_1)\sin(0.7x_1x_2), \quad x1 \in [0, 5], \ \ x2 \in [0, 5].$$

5. Hartmann $H_{3,4}$ function (three variables):

$$y(\mathbf{x}) = -\sum_{i=1}^{4} \alpha_i \ \ exp[-\sum_{j=1}^{3} A_{ij}(x_j - P_{ij})^2], \quad x_j \in [0, 1].$$

where,

$$\alpha = \begin{bmatrix} 1 \\ 1.2 \\ 3 \\ 3.2 \end{bmatrix}, \quad A = \begin{bmatrix} 3.0 & 10 & 30 \\ 0.1 & 10 & 35 \\ 3.0 & 10 & 30 \\ 0.1 & 10 & 35 \end{bmatrix}, \quad P = \begin{bmatrix} 0.6890 & 0.1170 & 0.2673 \\ 0.4699 & 0.4387 & 0.7470 \\ 0.1091 & 0.8732 & 0.5547 \\ 0.0381 & 0.5743 & 0.8828 \end{bmatrix}.$$

6. Hartmann $H_{6,4}$ function (six variables):

$$y(\mathbf{x}) = -\sum_{i=1}^{4} \alpha_i \ \ exp[-\sum_{j=1}^{6} B_{ij}(x_j - Q_{ij})^2], \quad x_j \in [0,1].$$

where,

$$\alpha = \begin{bmatrix} 1 \\ 1.2 \\ 3 \\ 3.2 \end{bmatrix}, \ B = \begin{bmatrix} 10 & 0.05 & 3 & 17 \\ 3 & 10 & 3.5 & 8 \\ 17 & 17 & 1.7 & 0.05 \\ 3.05 & 0.1 & 10 & 10 \\ 1.7 & 8 & 17 & 0.1 \\ 8 & 14 & 8 & 14 \end{bmatrix}^T, \ Q = \begin{bmatrix} 0.1312 & 0.2329 & 0.2348 & 0.4047 \\ 0.1696 & 0.4135 & 0.1451 & 0.8828 \\ 0.5569 & 0.8307 & 0.3522 & 0.8732 \\ 0.0124 & 0.3736 & 0.2883 & 0.5743 \\ 0.8283 & 0.1004 & 0.3047 & 0.1091 \\ 0.5886 & 0.9991 & 0.6650 & 0.0381 \end{bmatrix}^T.$$

7. Trid function (ten variables):

$$y(\mathbf{x}) = -\sum_{i=1}^{10}(x_i - 1)^2 - \sum_{i=2}^{10} x_i x_{i-1}, \quad x_i \in [-3,3].$$

8. Dixon-Price function (twelve variables):

$$y(\mathbf{x}) = (x_1 - 1)^2 + \sum_{i=2}^{m} i[2x_i^2 - x_{i-1}]^2, \quad x_i \in [-10,10].$$

3.4.2 Comparative study

Section 3.4.1, summarises the eight test functions and the distribution of their inputs. The variables in the test functions are uniformly distributed. The first problem is a one-dimensional function, the second and fourth problems are two-dimensional quartic functions with cosine and sine functions respectively. The third problem is a two-dimensional sixth order polynomial function with interaction among the random variables. The fifth and sixth problems are three and six dimensional exponential functions. The seventh problem is a quadratic polynomial with ten random variables. The last problem is a quartic polynomial function with twelve design variables.

The first and second order moments of the first test function are calculated analytically and the analytical solution for moments of the test functions (2-8) can be found in the literature [53]. The analytical moments of the test functions are given in Table 3.4. The probability weighted integrals are calculated using the conventional sparse grid method (SGM), the adaptive sparse grid method (ASGM) and a comparison is provided with respect to MCS approach.

Table 3.4: Analytical moments of test functions:

Objective function	Moments μ	σ	Dimension
1. Forrester	0.453	4.457	1D
2. Branin-Hoo	54	51	2D
3. Camelback	20	26	2D
4. Mystery	6.80	5.98	2D
5. Hartmann $H_{3,4}$	-0.9	1.0	3D
6. Hartmann $H_{6,4}$	-0.3	0.4	6D
7. Trid	40	16.5	10D
8. Dixon-Price	619328	271959	12D

The results for estimation of moments are given in Table 3.5. The relative percentage error estimations (compared with analytical solutions) are given in Table 3.6. The errors (ϵ_μ, ϵ_σ) in the estimation of mean and standard deviation are calculated as,

$$\epsilon_\mu = |\frac{(\mu_{true} - \mu_{appr})}{\mu_{true}}| \times 100, \qquad \epsilon_\sigma = |\frac{(\sigma_{true} - \sigma_{appr})}{\sigma_{true}}| \times 100. \tag{3.16}$$

The moments are estimated using MCS with 10000 points and averaged for 100 different trials. The order of 1-D quadrature rule is critical in the moment estimation using SGM for the test functions. From Table 3.5, the mean and standard deviation converges for problem 1 and 2 with 17, 65 points respectively using SGM. The adaptive sparse grid method uses more points than SGM, to further discretize the grid in order to better approximate the integrand. For problem 3, the points required for the mean estimation is 29 and 145 points are required for calculating σ. This is due to the difference in the order of the integrand and similar trend exist for problems (7-8). For problem 4, 321 points are required to estimate the moments. For problem (5-6) the moments are calculated using 441, 4865 points respectively. The order of the integrand defines the order (or level) of SGM to be used for accurate estimation. The number of collocation points using adaptive

sparse grid method is high compared to SGM for problems (1-7). But for high dimensional ($> 10D$) non-linear problems, the number of points required to accurately estimate the moments can be too high using sparse grid method (SGM). The adaptive sparse grid method is preferred for such problems.

The objective functions (1-4) and their approximate representation using SGM for level ($k = 1, 2, ..6$) are shown in Figures 3.3-3.9. From the figures it can be concluded that for accurate estimation of σ the number of SG points required is relatively high (eg. Mystery function Fig. 3.7.) and depends on the smoothness of the integrable function.

In this chapter the application of the sparse grid method (SGM) and adaptive sparse grid method (ASGM) are demonstrated for eight mathematical test functions. The results presented in this chapter show that the methods are promising for problems with high dimensionality. The main goal is to attain a general understanding of sparse grid quadrature when applied to high dimensional problems with interactions among the random variable/inputs in the problems.

The use of sparse grid method (SGM) for uncertainty quantification approaches have significance in the context of engineering problems, because of considerable amount of variables involved in such problems.

However, for the moment estimation of complex systems, the number of uncertain variables can be quite high and there is a limitation in the number of simulation runs possible. SGM and ASGM methods enable us to estimate the moments of system output response with few collocation points but doesn't always address the required reduction in the number of function evaluations, which is the focus of further study.

Table 2.5.

Objective function	Moments	Analytical	MCS Averaged for 100 trials	SGM (k=1,..6) 1	2	3	4	5	6	ASGM
1. Forrester	μ	0.453	0.4485	3.7490	0.6245	0.4515	0.4532*	0.4532	0.4532	0.4535
	σ	4.457	4.4506	5.4577	2.9830	4.3496	4.4561*	4.4562	4.4562	4.4566
	N	NA	10000	3	5	9	17	33	65	129
2. Branin-Hoo	μ	54	54.860	56.577	50.287	54.856	54.865*	54.865	54.865	54.9765
	σ	51	51.659	52.483	58.316	50.076	51.696*	51.699	51.699	51.617
	N	NA	10000	5	13	29	65	145	321	705
3. Camelback	μ	20	20.161	52.30	17.846	20.160*	20.160	20.160	20.160	20.196
	σ	26	26.396	44.562	42.938	14.634	27.124	26.386*	26.386	26.2272
	N	NA	10000	5	13	29	65	145	321	1537
4. Mystery	μ	6.80	6.8096	5.1738	11.819	10.528	7.8789	6.5657	6.8081*	6.8098
	σ	5.98	5.9804	9.4483	7.3699	6.1372	2.8174	5.8721	5.9813*	5.9840
	N	NA	10000	5	13	29	65	145	321	5121
5. Hartmann $H_{3,4}$	μ	-0.9	-0.9432	-0.7864	-1.4089	-1.0675	-0.9567	-0.9451*	-0.9438	-0.9435
	σ	1.0	0.9559	0.7206	1.5333	1.1290	0.9691	0.9579*	0.9598	0.9561
	N	NA	10000	7	25	69	177	441	1073	4609
6. Hartmann $H_{6,4}$	μ	-0.3	-0.3230	-0.1673	-0.3144	-0.2958	-0.2981	-0.3252*	-0.3271	-0.3231
	σ	0.4	0.4336	0.0760	0.6523	0.3401	0.4633	0.4178*	0.4173	0.4336
	N	NA	10000	13	85	389	1457	4865	15121	10057

Table 2.5., Contd..

Objective function	Moments	Analytical	MCS Averaged for 100 trials	SGM (k=1,..6) 1	2	3	4	5	6	ASGM
7. Trid	μ	40	40.005	40.075*	40	40	40	40	40	40.01
	σ	16.5	16.517	18.6484	16.522*	16.522	16.522	16.522	16.522	16.831
	N	NA	10000	21	221	1581	8801	41265	171425	6913
8. Dixon-Price	μ	619328	618520	1029267	618601*	618601.2	618601	618600	618600	622813
	σ	271959	273720	1553828	816358	648012	273645*	273645	273645	272586
	N	NA	10000	25	313	2649	17265	93489	442001	201413

*converged

Table 2.6.
Errors in estimation (ϵ_μ,ϵ_σ).

Objective function	Moments	Analytical	MCS Averaged for 100 trials	SGM (k=1,..6) 1	2	3	4	5	6	ASGM
1. Forrester	ϵ_μ	0	0.9934	727.59	37.858	0.3311	0.0442*	0.0442	0.0442	0.1104
	ϵ_σ	0	0.1436	22.452	33.071	2.4097	0.0202*	0.0179	0.0179	0.0090
2. Branin-Hoo	ϵ_μ	0	1.5926	4.7722	6.8759	1.5852	1.6019*	1.6019	1.6019	1.8083
	ϵ_σ	0	1.2922	2.9078	14.3451	1.8118	1.3647*	1.3706	1.3706	1.2098
3. Camelback	ϵ_μ	0	0.8050	161.50	10.770	0.80*	0.80	0.80	0.80	0.98
	ϵ_σ	0	1.5231	71.3923	65.1462	43.7154	4.3231	1.4846*	1.4846	0.8738
4. Mystery	ϵ_μ	0	0.1412	23.9147	73.8088	54.8235	15.8662	3.4456	0.1191*	0.1441
	ϵ_σ	0	0.0067	57.9983	23.2425	2.6288	52.8863	1.8043	0.0217*	0.0669
5. $\text{Hartmann}_{3,4}$	ϵ_μ	0	4.8	12.6222	56.5444	18.6111	6.300	5.0111*	4.8667	4.8333
	ϵ_σ	0	4.4100	27.9400	53.3300	12.900	3.09	4.21*	4.02	4.39
6. $\text{Hartmann}_{6,4}$	ϵ_μ	0	7.6667	44.2333	4.8000*	1.4000	0.6333	8.4000	9.0333	7.700
	ϵ_σ	0	8.4	81	63.075	14.975	15.825	4.45*	4.325	8.4
7. Trid	ϵ_μ	0	0.0125	0.19*	0	0	0	0	0	0.0250
	ϵ_σ	0	0.103	13.02	0.1333*	0.1333	0.1333	0.1333	0.1333	2.0061
8. Dixon-Price	ϵ_μ	0	0.1305	66.1909	0.1174*	0.1174	0.1174	0.1175	0.1175	0.5627
	ϵ_σ	0	0.6475	471.35	200.1769	138.2756	0.6199*	0.6199	0.6199	0.2305

*converged

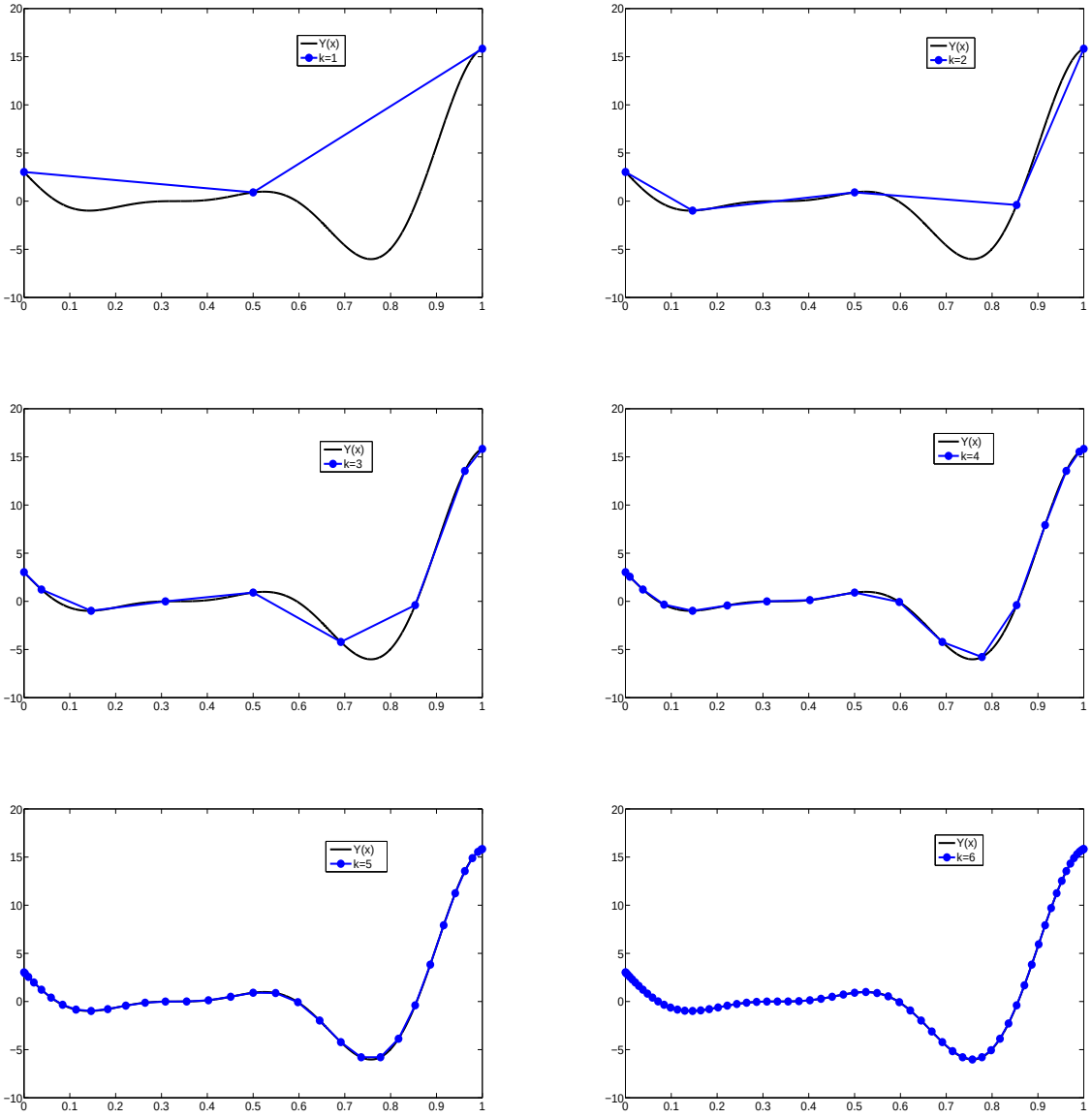

Figure 3.3: Approximate representation of Forrester function using SGM for k=1,..,6.

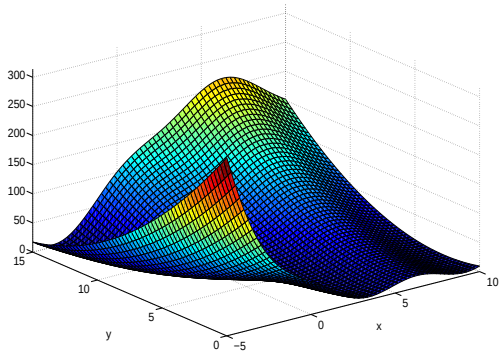

Figure 3.4: Branin-Hoo function.

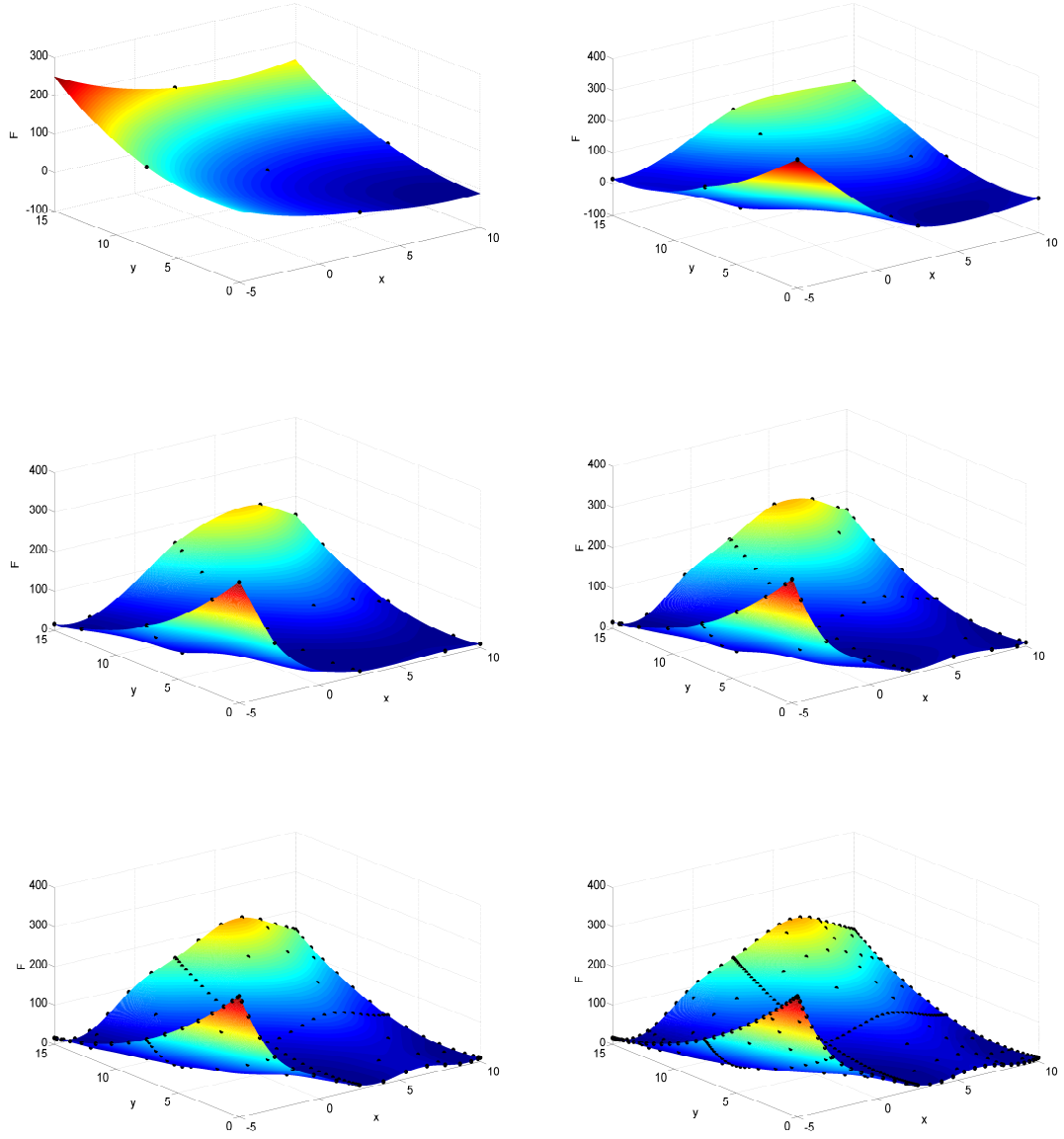

Figure 3.5: Approximate representation of Branin-Hoo function using SGM for k=1,..,6.

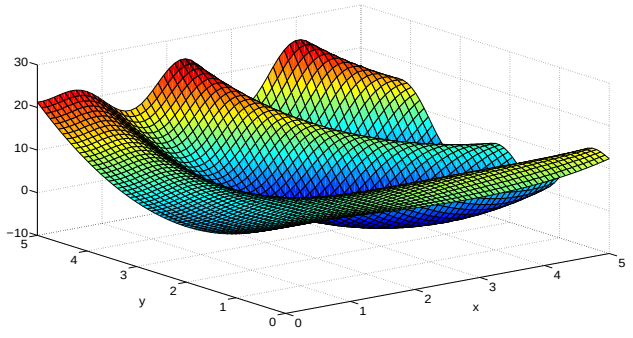

Figure 3.6: Mystery function.

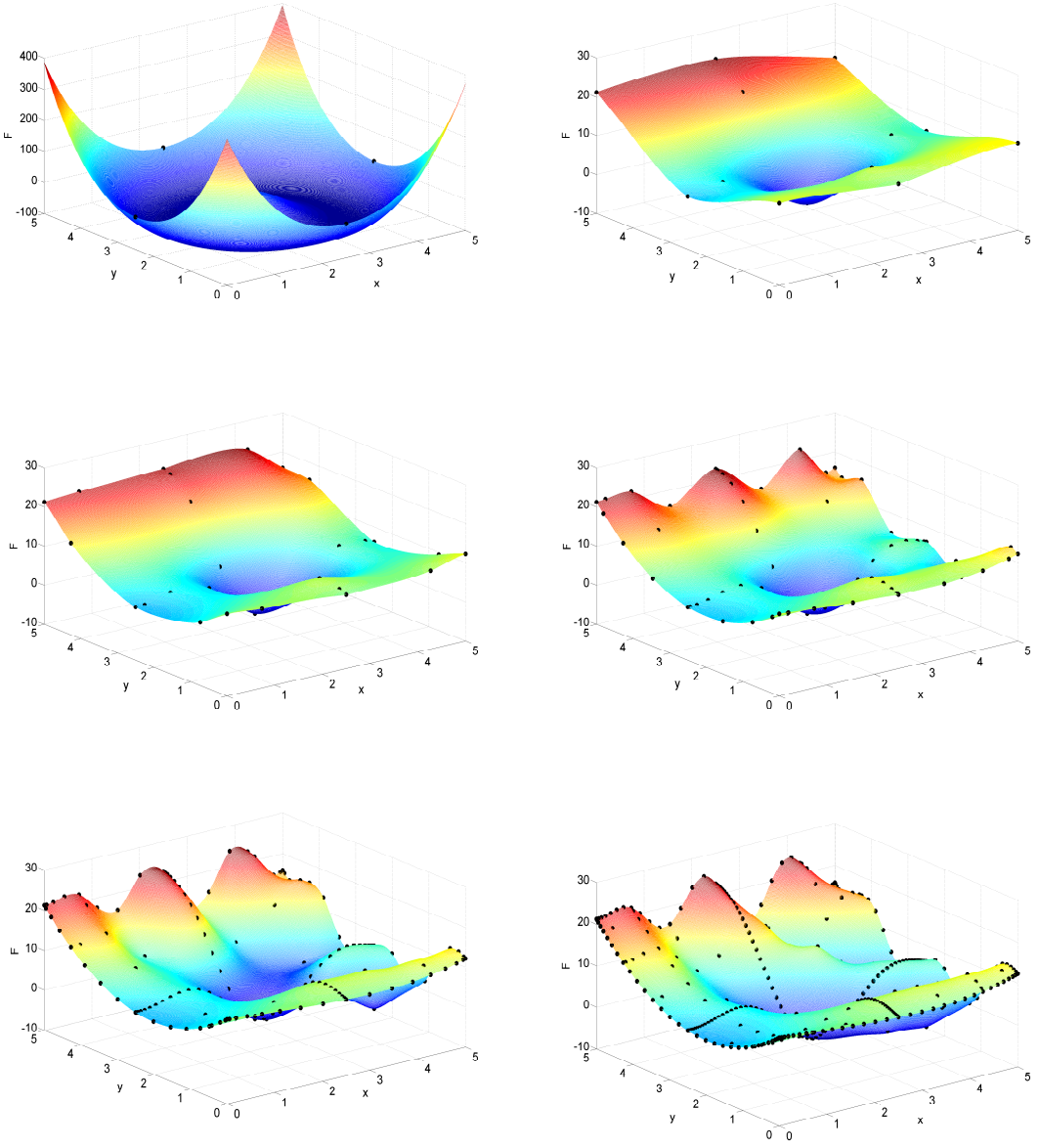

Figure 3.7: Approximate representation of Mystery function using SGM for k=1,..,6.

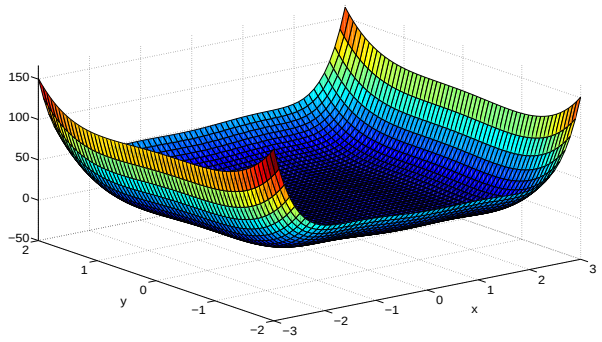

Figure 3.8: Camelback function.

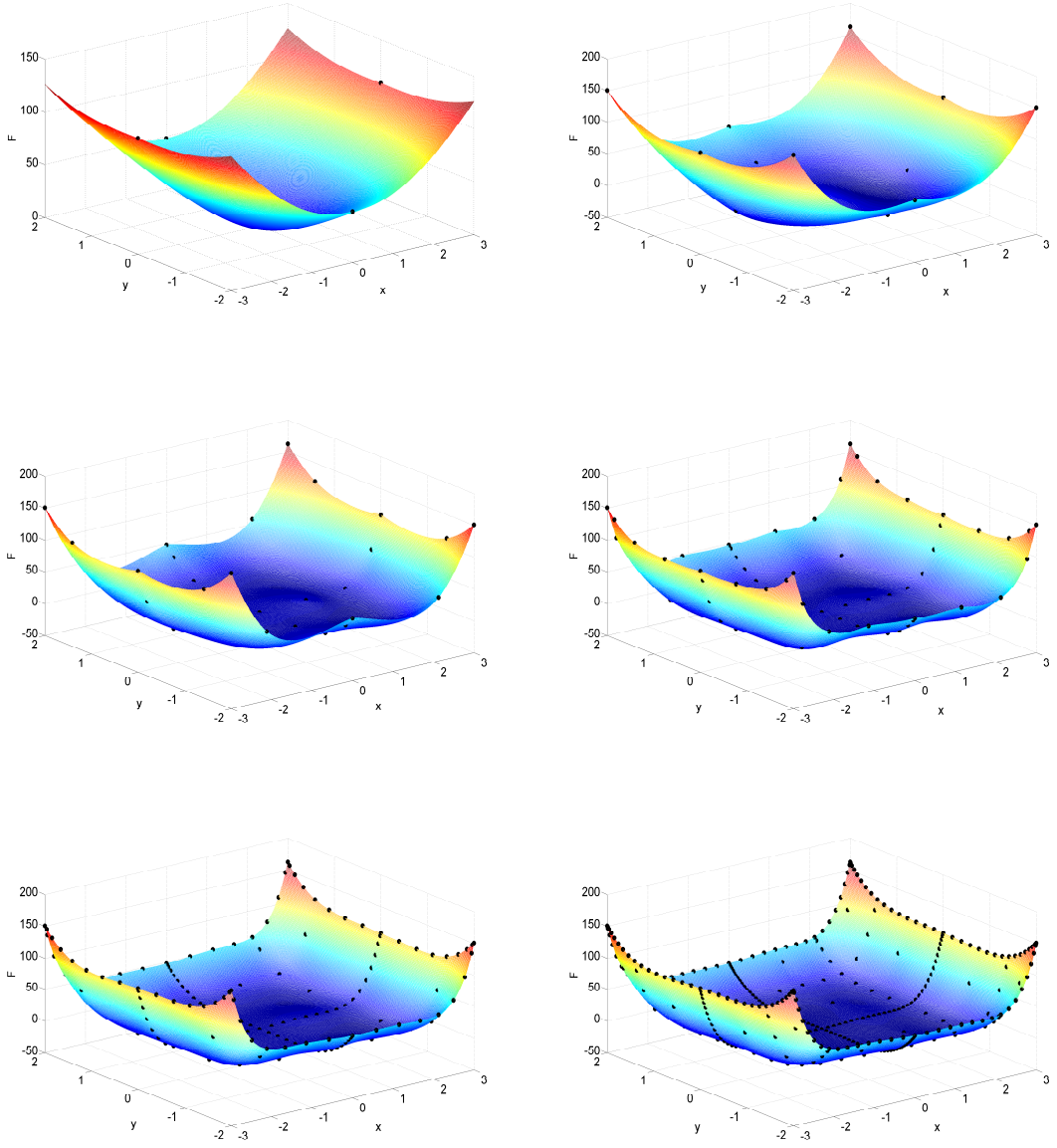

Figure 3.9: Approximate representation of Camelback function using SGM for k=1,..,6.

Chapter 4

Surrogate modeling for probabilistic moment estimation

In this chapter, we discuss an important problem that is often encountered in wide variety of engineering problems: *function approximation*. Usually such a problem arises when computational effort needed in evaluating the objective function is costly and complex in nature.

The uncertainty quantification techniques developed for stochastic systems should be efficient in their implementation and execution. The simulation run time for complex systems can be quite expensive. Response surface methods are commonly used to characterize the system response, using an approximate mathematical model. UQ methods can be applied on the response surface, rather than performing deterministic simulations on the actual system. Such strategies further help in reducing the computational time involved in UQ studies.

Response surface methodology uses mathematical and statistical tools in the construction of empirical model. The objective is to build a surrogate model[1] that can optimally represent the system response by conducting a series of experiments or runs of the simulation model at selected sample points in the design space as shown in Fig 4.1.

After performing a series of runs of the simulation model, a set of outputs for respective input data are obtained, on which regression or curve fitting is done. The response surface seeks to find the functional relationship between the output variable and a set of input variables using first order, second order or other higher

[1] In this thesis the terms "surrogate model" and "response surface" are used interchangeably.

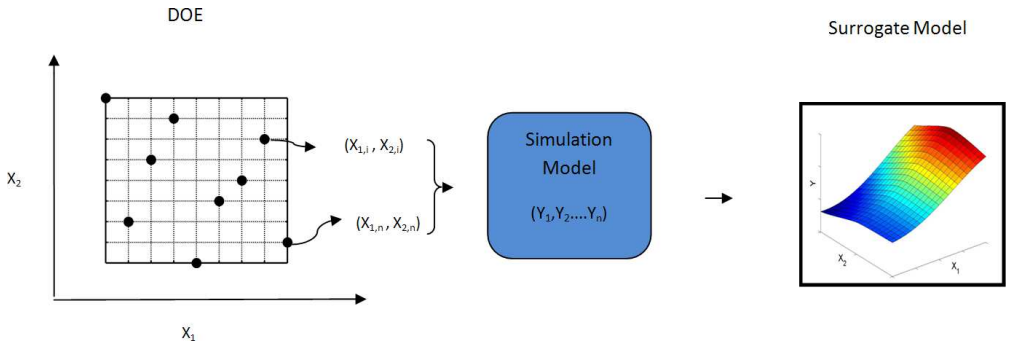

Figure 4.1: Surrogate modelling of simulation based problems.

order polynomials. An important objective in response surface approximations is to build a globally accurate surrogate model while attempting to minimise the computational effort i.e the number of function evaluations.

The choice of design of experiments (DOE) used to sample the system, influences the accuracy of the surrogate model. Several different strategies exist in performing such experiments or runs, eg., full factorial design (FFD), central composite design (CCD), Taguchi methods, etc [54].

In standard curve fitting by polynomial regression techniques, the true function y sampled at n points, is approximated with regression functions f_h and respective coefficients β_h,

$$y(\mathbf{x}^{(i)}) = \sum_h \beta_h f_h(\mathbf{x}^{(i)}) + \epsilon^{(i)}, \qquad (i = 1, ..., n). \tag{4.1}$$

here ϵ is the error in approximation. The above equation can be written as,

$$y = \mathbf{X}\beta + \epsilon. \tag{4.2}$$

where y is $(n \times 1)$ vector of responses and $\mathbf{X}$ is a $(n \times q)$ matrix of sample data points, β is $(q \times 1)$ vector of regression parameters, ϵ is a $(q \times 1)$ vector of error terms and q is the number of design points. The parameters β are determined through least-squares regression, which minimizes the sum of the squares of the deviations of predicted values, $y(\hat{\mathbf{X}})$, from the function evaluations $y(\mathbf{X})$. Let L is the square of the error given by,

$$\begin{aligned} L = \sum_{i=1}^{n} \epsilon_i^2 = \epsilon^T \epsilon = (y - \mathbf{X}\beta)^T (y - \mathbf{X}\beta), \\ = y^T y - 2\beta^T \mathbf{X}^T y + \beta^T \mathbf{X}^T \mathbf{X} \beta. \end{aligned} \tag{4.3}$$

To minimise L, Eq. (4.3), is differentiated with respect to β and equated to zero,

$$\frac{\partial L}{\partial \beta} = -2\mathbf{X}^T y + 2\mathbf{X}^T \mathbf{X}\beta = 0. \tag{4.4}$$

The fitted regression model is given by,

$$\hat{y} = \mathbf{X}\hat{\beta}, \qquad \hat{\beta} = (\mathbf{X}^T \mathbf{X})^{-1} \mathbf{X}^T y. \tag{4.5}$$

In the above polynomial regression model, higher order polynomials are required to model the response of highly nonlinear functions. It may take a considerable amount of sample data to estimate all the coefficients in the Eq. (4.5). There are other alternative surrogate modelling techniques to represent the output response, such as radial basis functions, neural networks, smoothing spline models, Kriging, etc. A brief review of radial basis functions and Kriging is explained in the following sections.

4.1 Radial basis functions

Radial basis functions developed by Broomhead and Lowe [55], use a weighted sum of simple basis functions in order to represent the complex nonlinear response. Let the approximated function denoted by $\hat{f}(x)$, be used as a surrogate model for true function $f(x)$. The surrogate model is obtained for input sampling data $X = \{x_1, x_2, .., x_m\}^T$ and the observed responses $y = \{y_1, y_2, .., y_m\}^T$. The surrogate model $\hat{f}(x)$ obtained using radial basis functions interploates the sampling data and is given by,

$$\hat{f} = \sum_{j=1}^{m} \lambda_j \psi(||x - x_j||) = y_j \ , \quad j = 1, 2, , ...m. \tag{4.6}$$

here x_j are the centres of basis functions considered to be the sample data points. The term $\psi(||x-x_j||)$ represents a set of m basis functions evaluated as Euclidean distance between prediction x and centres x_j of the basis functions. A list of basis functions is given in Table 4.1, here $\mathbf{z}$ is the Euclidean norm. Using the

Table 4.1: Possible choices for basis functions $\psi(\mathbf{z})$:

1. Linear	$\psi(\mathbf{z}) = \|\|\mathbf{z}\|\|$
2. Cubic	$\psi(\mathbf{z}) = \|\|\mathbf{z}\|\|^3$
3. Thin plate spline	$\psi(\mathbf{z}) = \|\|\mathbf{z}\|\|^2 \log(\|\|\mathbf{z}\|\|)$
4. Gaussian	$\psi(\mathbf{z}) = \exp(-\frac{\|\|\mathbf{z}\|\|^2}{2\sigma^2})$
5. Multiquadraic	$\psi(\mathbf{z}) = \sqrt{\|\|\mathbf{z}\|\|^2 + \sigma^2}$
6. Inverse multiquadric	$\psi(\mathbf{z}) = \frac{1}{\sqrt{\|\|\mathbf{z}\|\|^2+\sigma^2}}$
7. Kriging	$\psi(\mathbf{z}) = \exp(-\sum_{l=1}^{d} \theta_l \|\|\mathbf{z}\|\|^{p_l})$

interpolation condition from Eq. (4.6), the coefficients λ_j can be deduced from the set of linear equations,

$$\begin{pmatrix} y_1 \\ \vdots \\ y_m \end{pmatrix} = \begin{pmatrix} A_{11} & \cdots & A_{1m} \\ \vdots & \ddots & \vdots \\ A_{m1} & \cdots & A_{mm} \end{pmatrix} \begin{pmatrix} \lambda_1 \\ \vdots \\ \lambda_m \end{pmatrix}.$$

where $A_{ij} \triangleq \psi(||\ x - x_j\ ||\ , \quad i,j = 1,2,...m.$

The coefficients $\lambda_\mathbf{j}$ are calculated as $\lambda \equiv \mathbf{A}^{-1}\mathbf{y}$, if the inverse to matrix $\mathbf{A}$ exists. Apart from λ, additional parameters are estimated for certain class of basis functions (eg. Kriging basis function).

4.2 Kriging

Kriging is a popular surrogate modeling technique and has been applied to a variety of engineering design problems such as aerodynamic, structural and multi-objective design problems [56]-[59]. Th origins of Kriging lies in the field of geo-statistics [60] and was later developed for the field of engineering by Sacks et al [61]. Kriging is rooted in the statistical framework thereby fits well in the uncertainty quantification studies. A brief overview of Kriging is presented here.

For an approximated function $\hat{f}(x)$ using Kriging, the observed responses $\mathbf{y}$ are considered from a stochastic process and denoted by $\mathbf{Y} = \{\mathrm{Y}_1, \mathrm{Y}_2, ..., \mathrm{Y}_\mathrm{n}\}^T$. The output of the function $f(x)$ at x, is characterized by random variable $\mathbf{Y}(x)$, normally distributed with mean μ and variance σ^2. Let x_i and x_j are two sample points and assuming the function modeled is smooth and continuous, the output responses $y(x_i)$ and $y(x_j)$ are close if the distance $||x_i - x_j||$ is small. This is statistically represented by assuming that the random variables $\mathrm{Y}(x_i)$ and $\mathrm{Y}(x_j)$ are likely to be correlated if $||x_i - x_j||$ is small. The correlation between the random variables is given by,

$$\mathrm{Corr}[\mathbf{Y}(x_i), \mathbf{Y}(x_j)] = \exp(-\sum_{h=1}^{d} \theta_h \parallel x_{ih} - x_{jh} \parallel^{p_h}) \ , \quad (\theta_h \geq 0, \ p_h \in [0, 2]). \tag{4.7}$$

From Eq. (4.7), a $n \times n$ correlation matrix can be constructed for all the observed data. The correlation matrix $\mathbf{\Psi}$ is given by,

$$\mathbf{\Psi} = \begin{pmatrix} \mathrm{Corr}[\mathbf{Y}(x_1), \mathbf{Y}(x_1)] & \cdots & \mathrm{Corr}[\mathbf{Y}(x_1), \mathbf{Y}(x_n)] \\ \vdots & \ddots & \vdots \\ \mathrm{Corr}[\mathbf{Y}(x_n), \mathbf{Y}(x_1)] & \cdots & \mathrm{Corr}[\mathbf{Y}(x_n), \mathbf{Y}(x_n)] \end{pmatrix}.$$

The covariance matrix equals to,

$$\mathrm{Cov}(\mathbf{Y}, \mathbf{Y}) = \sigma^2 \mathbf{\Psi}. \tag{4.8}$$

The correlation is 1 if $x_i = x_j$, and zero as $\parallel x_i - x_j \parallel \rightarrow \infty$. In Eq. 4.7, ($\theta_h$,

p_h) are the two hyperparameters, θ_h accounts for different levels of correlation in each dimension and p_h governs the degree of smoothness of correlation ($p_h = 2$ results in Gaussian correlation).

The hyperparameters θ_h and p_h are fitted to maximize the likelihood on observed data. Maximizing the likelihood identifies the parameters that model the function approximation consistently with the observed data. The likelihood function proposed by Donald Jones [62] is given by,

$$L(\theta, \mu, \sigma^2) = \frac{1}{(2\pi\sigma^2)^{n/2} \mid \mathbf{\Psi} \mid^{1/2}} \exp[\frac{-(y - \mathbf{1}\mu)^T \mathbf{\Psi}^{-1}(y - \mathbf{1}\mu)}{2\sigma^2}], \tag{4.9}$$

or, after natural logarithms of the function,

$$-\frac{n}{2} ln(\sigma^2) - \frac{1}{2}\, ln(|\mathbf{\Psi}|) - [\frac{(y - \mathbf{1}\mu)^T \mathbf{\Psi}^{-1}(y - \mathbf{1}\mu)}{2\sigma^2}], \tag{4.10}$$

where 1 is vector of ones of dimension n. The optimal values of mean and variance maximizing Eq. (4.10) are obtained by taking derivatives of the above equation and setting to zero, giving

$$\hat{\mu} = \frac{\mathbf{1}^T \mathbf{\Psi}^{-1} y}{\mathbf{1}^T \mathbf{\Psi}^{-1} \mathbf{1}}\,, \qquad \hat{\sigma}^2 = \frac{(y - \mathbf{1}\hat{\mu})^T \mathbf{\Psi}^{-1}(y - \mathbf{1}\hat{\mu})}{n}. \tag{4.11}$$

A concentrated log-likelihood function can be derived by substituting the above mean and variance into the log-likelihood function Eq. (4.10),

$$ln(L) = -\frac{n}{2} ln(\hat{\sigma}^2) - \frac{1}{2} ln(|\mathbf{\Psi}|). \tag{4.12}$$

The concentrated likelihood function depends on correlation matrix $\mathbf{\Psi}$ and hence on the hyper parameters (θ_h, p_h). The calculation of log-likelihood function is computationally intensive in Kriging process. The inversion of the positive definite correlation matrix ($\mathbf{\Psi}^{-1}$), is performed with Cholesky factorization.

The hyperparameters are optimally choosen in order to maximise the likelihood function and is an optimization problem. Tuning the hyperparameters can be computationally expensive with cost depending on the dimensionality of the problem

and the number of sample points required to build the Kriging response surface which in turn defines the size of correlation matrix $\mathbf{\Psi}$. In this report, the hyperparameters are selected using a hybrid particle swarm based optimization algorithm, to reduce the cost involved in the optimization of log-likelihood function. The hybrid strategy developed by Toal et al. [63], performs well compared to genetic algorithm and traditional particle swarm optimization with respect to likelihood optimization.

4.3 Prediction using a Kriging model

Once an appropriate set of hyperparameters are obtained, the surrogate model can be used to make new prediction $\hat{y}$ at point x which is consistent with the observed data $\mathbf{y}$. The quality of the estimate is evaluated by adding $\hat{y}$ to the observed data, $\tilde{\mathbf{y}} = \{\mathbf{y}, \hat{y}\}^T$, and computing the augmented likelihood function.

The augmented correlation matrix is given by,

$$\tilde{\mathbf{\Psi}} = \begin{pmatrix} \mathbf{\Psi} & \psi \\ \psi^T & 1 \end{pmatrix}, \tag{4.13}$$

where ψ is the vector of correlations between observed data and the prediction,

$$\psi = \begin{pmatrix} \mathrm{Corr}[\mathbf{Y}(x_i), \mathbf{Y}(x)] \\ \vdots \\ \mathrm{Corr}[\mathbf{Y}(x_n), \mathbf{Y}(x)] \end{pmatrix}. \tag{4.14}$$

By substituting the augmented correlation matrix Eq. (4.13) into the log-likelihood equation (4.10), the augmented likelihood function which is a function of $y(x)$ is derived,

$$-\frac{n}{2} ln(\hat{\sigma}^2) - \frac{1}{2}\, ln(|\tilde{\mathbf{\Psi}}|) - \frac{(\tilde{\mathbf{y}} - \mathbf{1}\hat{\mu})^T \tilde{\mathbf{\Psi}}^{-1} (\tilde{\mathbf{y}} - \mathbf{1}\hat{\mu})}{2\hat{\sigma}^2}. \tag{4.15}$$

where $\hat{\mu}$ and $\hat{\sigma}^2$ are known from Eq. (4.11).

The augmented likelihood calculated using optimum parameters, reflects how consistent the prediction is with the observed data. The best estimate for this prediction is the value of $\hat{y}$ that maximises the augmented likelihood function.

By substituting a partitioned inverse formulation [64] of $\tilde{\mathbf{\Psi}}^{-1}$ into Eq. (4.13), and by differentiating with respect to $\hat{y}$ we obtain,

$$\left[\frac{-1}{\hat{\sigma}^2(1-\psi^T\mathbf{\Psi}^{-1}\psi)}\right](\hat{y}-\hat{\mu})+\left[\frac{\psi^T\mathbf{\Psi}^{-1}(\mathbf{y}-1\hat{\mu})}{\hat{\sigma}^2(1-\psi^T\mathbf{\Psi}^{-1}\psi)}\right]. \tag{4.16}$$

By equating the above equation to zero the Kriging predictor is obtained, and is given by,

$$\hat{y}(x)=\hat{\mu}+\psi^T\mathbf{\Psi}^{-1}(\mathbf{y}-1\hat{\mu}). \tag{4.17}$$

The Kriging predictor is deduced for interpolating model. In the presence of noise in the observed data, the above Kriging formulation may yield a model that overfits the observed data. This can be filtered by using a regression constant λ. The regression constant is added to the leading diagonal of $\mathbf{\Psi}$ producing $\mathbf{\Psi}+\lambda\mathbf{I}$, where $\mathbf{I}$ is the identity matrix. Using the similar derivation for interpolating model, the Kriging prediction for regression model can be deduced. The regression based predicted model is given by,

$$\hat{y_r}(x)=\hat{\mu_r}+\psi^T(\mathbf{\Psi}+\lambda\mathbf{I})^{-1}(\mathbf{y}-1\hat{\mu_r}), \tag{4.18}$$

where,

$$\hat{\mu_r}=\frac{1^T(\mathbf{\Psi}+\lambda\mathbf{I})^{-1}\mathbf{y}}{1^T(\mathbf{\Psi}+\lambda\mathbf{I})^{-1}1}. \tag{4.19}$$

Using maximum likelihood estimation, a suitable regression constant λ is found in the similar way as other model parameters.

4.3.1 Sample test case

Probabilistic moment estimation of a two-dimensional Branin-Hoo function is performed considering radial basis functions and Kriging based surrogate model.

Sparse grid moment estimation approach is performed on the surrogate model built using a linear, cubic and thin plate spline radial basis functions and a Kriging response surface, for Branin-Hoo function provided in the section 3.4.1.

The analytical solution for the moments of Branin-Hoo function are 54 and 51 respectively and the number of collocation points required to accurately estimate the mean and variance using sparse grid method is 65. To enable a direct comparison for probabilistic moment estimation with respect to analytical solution, the models are built using 65 sample space design points. Latin hypercube based sampling points are used to build the surrogate models. The probabilistic moments estimated using the surrogate models are averaged for 20 different trials of LHS points. The approximate representation of Branin-Hoo function using the surrogate models built with 65 LHS design points are shown in Fig 4.2-4.3. The estimated moments and the relative percentage errors in the moment estimation with respect to analytical moments are provided in Table 4.2.

Table 4.2: Probabilistic moments for Branin-Hoo test function.

Objective function	Moments		Error %	
	μ	σ	ϵ_μ	ϵ_σ
1. Linear basis function	55.194	47.849	2.21	6.18
2. Cubic basis function	54.834	48.937	1.54	4.05
3. Thin plate spline basis function	54.626	49.730	1.16	2.49
4. Kriging	54.8657	51.6999	1.60	1.37

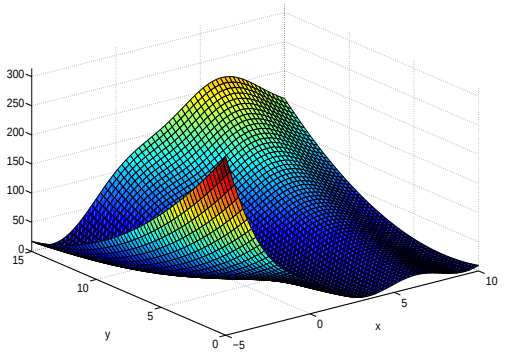

Figure 4.2: Branin-Hoo function.

The moments are estimated within (ϵ_μ, $\epsilon_\sigma < 2\%$) accuracy using the Kriging model. The error in estimation of standard deviation ($\epsilon_\sigma > 2\%$) is relatively high using linear, cubic and thin plate spline basis functions.

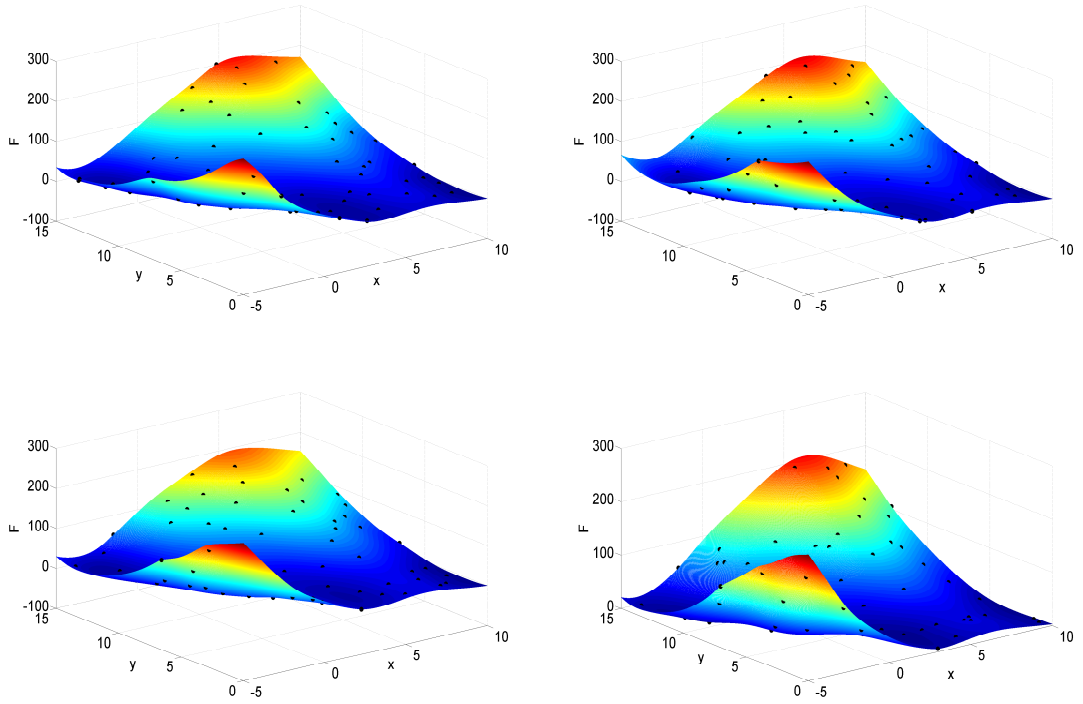

Figure 4.3: Surrogate models using linear, cubic, thin plate spline and Kriging basis functions.

UQ approaches require a large number of function evaluations and the problem is computationally intensive if the evaluating function is an expensive simulation model. Surrogate modeling techniques can be useful in performing such studies. The modeling cost involved in constructing a surrogate model depends on the number of sample points and the type of surrogate model used.

Although the moments are estimated within 2% accuracy using a Kriging model for two dimensional Branin-Hoo function built with a sampling plan comprising of 65 points. Similar studies cannot be performed for moment estimation of multi-variable objective functions in a high-dimensional space. Since the number of function evaluations required to built the surrogate model is too high. A Kriging based adaptive approach is presented in the next section to address such problems.

4.4 Kriging based adaptive approach

In stochastic engineering simulations, the non-intrusive UQ methods directly solve the deterministic problem rather than using a suitable approximation concept to interface the analysis software and surrogate modeling techniques. As mentioned

earlier surrogate modeling techniques can be used in UQ studies where the objective function f with random variables is represented by a surrogate model $\hat{f}$. In the current study, Kriging based surrogate models are used to characterize the objective function over the stochastic space Γ. The modeling cost involved in constructing a Kriging model depends on the selected sampling plan. Some of these aspects are discussed in the following sections.

4.4.1 Basic Strategy & Sampling Plan Criteria

A Kriging model is an approximation of a true function and may not be a globally accurate model unless the initial sampling plan comprises of all the observed data points in the design space. A basic strategy commonly used in Kriging based approaches is presented as a flow chart in Fig. 4.4. Initially, without prior knowledge of the design space, a initial sample based on sampling plan (DOE) is used. In the first stage, the Kriging model is built based on true simulations using the initial sample. The second stage searches the surrogate via infill sampling criteria to find a new update point. The update point is evaluated by model evaluation and added to the other sample points. The Kriging model is tuned and the process is repeated for maximum number of affordable simulations, or until sufficient accuracy of model is reached. The Kriging based approach provides an estimate of the error in the model prediction. The mean squared error (MSE) in a Kriging model based prediction proposed by Jones [62] is given by,

$$\hat{s}^2(x) = \sigma^2 \left[1 - \boldsymbol{\psi}^T \boldsymbol{\Psi}^{-1} \boldsymbol{\psi} + \frac{1 - \mathbf{1}^T \boldsymbol{\Psi}^{-1} \boldsymbol{\psi}}{\mathbf{1}^T \boldsymbol{\Psi}^{-1} \mathbf{1}} \right]. \tag{4.20}$$

In the current work for the process of model refinement, the update points can be chosen based on the above criteria.

The Kriging model built using the initial sampling plan can be based on psuedo-random points, Latin hypercube points or sparse grid collocation points, etc. The sample points should be chosen optimally to yield a response surface that represents the underlying function.

Sparse grid collocation points are fixed and deterministic in the multi-dimensional stochastic space. For moment estimation of complex non-linear functions in high dimensional space, a very high number of sparse grid points may be required. Building a surrogate model considering of all the points is often unrealistic. Few

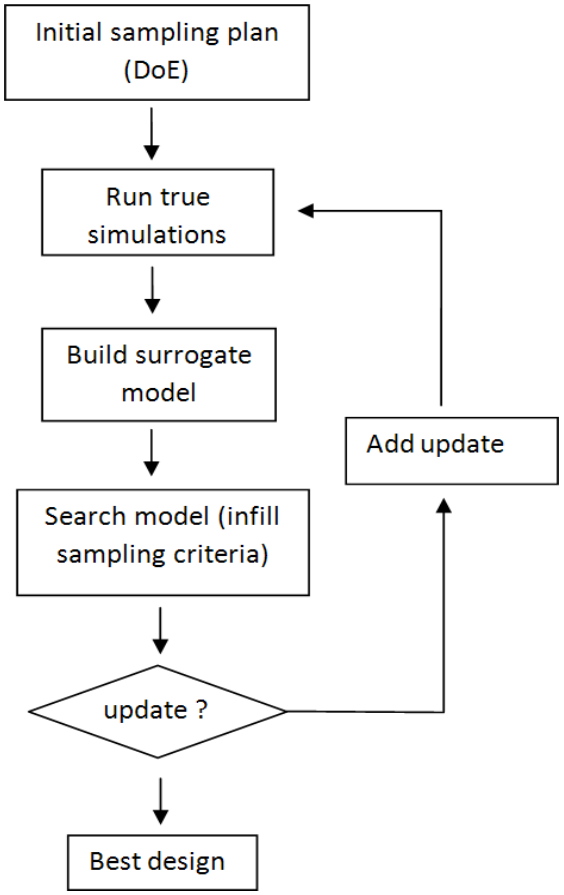

Figure 4.4: Basic strategy for surrogate modeling.

studies have been conducted considering surrogate modelling in UQ studies by Park and Grandhi et al. [65]. Dwight et al. [66], proposed a flexible non-intrusive approach to parametric uncertainty quantification problems. They employ a Kriging based response surface in the parameter space. The test cases considered are low to moderate dimension problems (d=2,4). The models were built using LHS points and moment estimation was done on the surrogate model using various moment estimation approaches. The advantage of using surrogate model with respect to other approaches (MCS, SGM) is presented. Further studies are needed to extend the method to solve high-dimensional problems.

Here a new approach is proposed to build the Kriging model using collocation points, where the subsequent function evaluations will be carried out for moment estimation. The main objective is to improve the quality of Kriging response surface for moment estimation, considering only few collocation points in the support space for which,

i) the moments estimated using the Kriging model are within sufficient accuracy

(±5%),

ii) the built-in Kriging surface represents the true objective function with few collocation points (a subset of the full sample space design points[1]).

Two different approaches can be used to select the update points to the initial sampling plan,

i) based on the Euclidean distance between the successive infill points,

ii) or minimising the variance (or mean squared error (MSE)) between predictions from successive surrogate models that is built from additional sampling points.

The second approach is considered in this work, since the first one considers the distance metric (eg. Morris-Mitchell criteria [67]) between the collocation points. It can be quite deceptive in high-dimensional stochastic space with large numbers of sparse grid points. The proposed adaptive approach considering the above criteria is shown in Fig 4.5. The following steps are performed in the adaptive approach,

Step 1: First a surrogate model is built with a few initial samples taken from the sparse grid sampling plan, the Kriging hyperparameters are estimated using a hybrid particle swarm optimization alogrithm proposed by David et al.[63].

Step 2: In the next step, the screening of sample space design comprising of sparse grid design points using the Kriging model is done.

Step 3: A few additional points (5-10) from the sparse grid sample space design, with maximum predicted error (MSE) are added to the initial sampling plan to improve the surrogate model. Probabilistic moments are estimated on the updated surrogate model.

Step 4: The procedure is repeated till the estimated moments on the Kriging model are obtained within desired accuracy with respect to reference solution. A sparse grid method with higher order, is used both to choose the sample points and to estimate the moments on the Kriging model. The error predicted by the Kriging model in the sample space design reduces as additional points are added to the initial sampling plan.

[1] Sample space design comprises of higher order collocation points (k=6) and first order collocation points (k=1) are chosen as initial sampling plan.

For engineering problems requiring high fidelity computer simulations, the stopping criterion for the proposed algorithm is governed by the maximum number of function evaluations feasible for performing the adaptive approach. The choice of ε /(MSE) error criteria for Kriging model update, depends on the range of objective function, typically a value of 0.001 is assigned [54]. It is necessary to have a limitation on the total number of points to be used in the sampling plan, obtained after each update, since it is computationally expensive to build a Kriging surface using a large sampling plan for high dimensional problems. But this approach is very much preferred over conventional SGM approach where function evaluations needed to accurately estimate the probabilistic moments is very high and the order of error convergence is $O(2^k k^{d-1})$ [44].

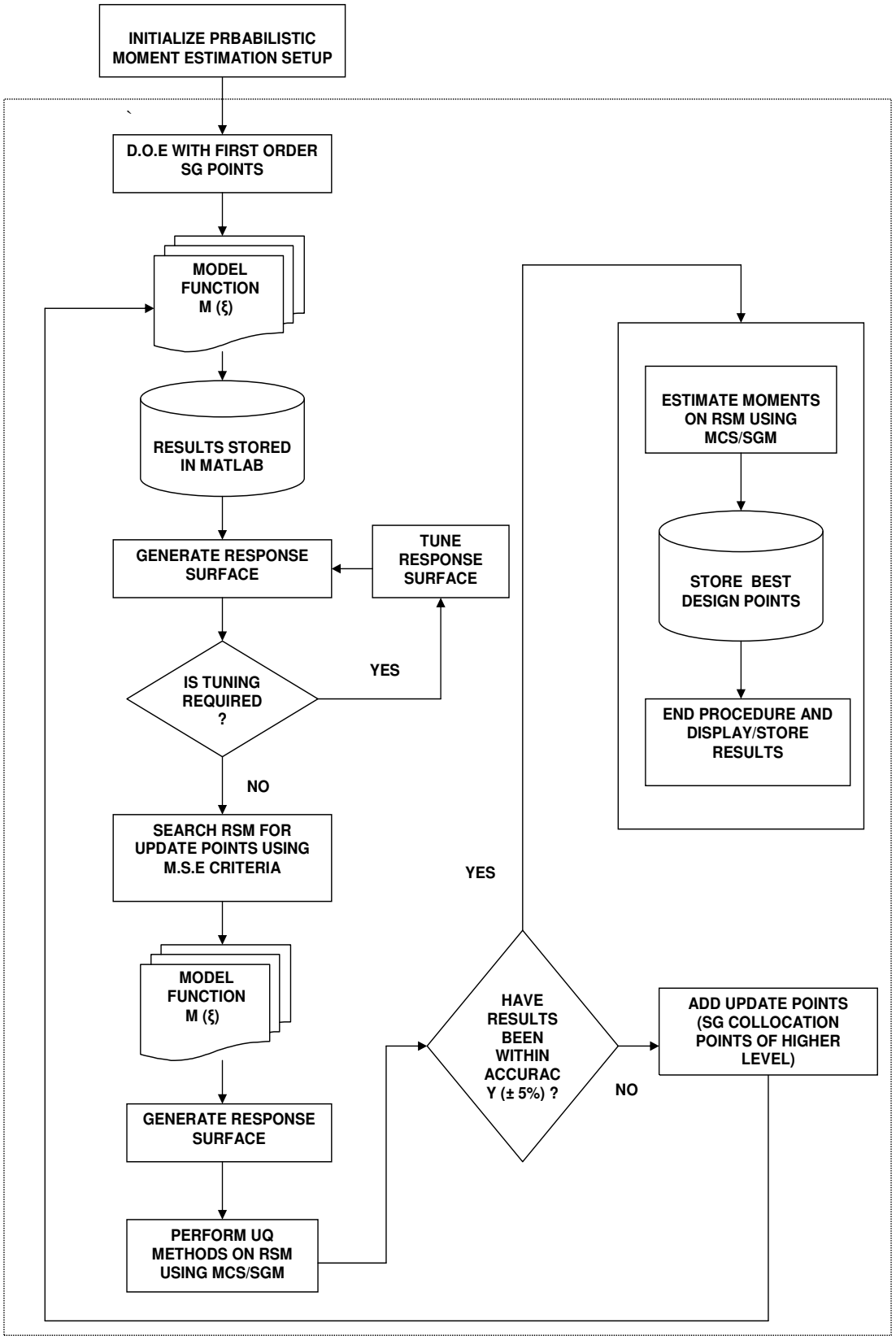

Figure 4.5: Overview of Kriging based adaptive procedure

4.5 Numerical Results & Discussion

In this section the application of MCS, the sparse grid method, adaptive sparse grid method, a simple Kriging based surrogate model and the Kriging based adaptive approach are demonstrated for eight mathematical test functions with varying dimensionality and strong interaction among the random variables. The test functions are presented in section 3.4.1.

The results for estimation of moments are given in Table 4.1. The relative percentage error estimations are given in Table 4.2. The errors (ϵ_μ, ϵ_σ) in the estimation of mean and standard deviation are calculated as,

$$\epsilon_\mu = |\frac{(\mu_{analytical} - \mu_{appr})}{\mu_{analytical}}| \times 100, \qquad \epsilon_\sigma = |\frac{(\sigma_{analytical} - \sigma_{appr})}{\sigma_{analytical}}| \times 100. \quad (4.21)$$

To begin with, MCS is used to estimate the moments of the eight test problems. The number of points used for MCS is 10000, as shown in Table 4.1.

Sparse grid method (SGM) is used in probabilistic moment estimation of the analytic functions. The estimated moments of the test functions and the points/nodes required to accurately estimate the moments using SGM are presented in Table 4.1.

For Kriging based adaptive approach, the initial sample points (DOE) used for building the Kriging model are first order sparse grid points. The full sample space design comprises of sixth order SG points. The mean square error is predicted using Kriging model on the sample space design and $5-10$ points with maximum error (MSE) are updated to the initial sampling plan. Moments are estimated using SGM on the updated Kriging response surface attained. The process is continued till sufficient accuracy is reached in estimating the moments.

Finally, the Kriging model is built using Latin Hypercube sample (LHS) points and moment estimation is done using SGM on the resulting Kriging model. The number of optimal sampling points obtained using adaptive approach are used to build the Kriging model. Here the aim is to compare probabilistic moment estimation by the conventional Kriging approach and Kriging based adaptive approach for same number of sampling points.

The number of function evaluations required to accurately estimate the moments is very high using MCS, and ASGM methods. The error in the moment estimation is particularly high for problems 5 and 6, which are exponential functions.

The number of model evaluations needed for moment estimation (within $< \pm 5\% accuracy$) of problems 1-8, is much less using the adaptive approach compared to MCS, SGM and ASGM methods. A small fraction of sample space design points are used to build the Kriging response surface. The function evaluations needed in building a Kriging model for ten dimensional Trid function is less compared to $Hartmann_{6,4}$ function (428 points), because of the exponential nature of the later function. Similar trend is observed for two dimesional test functions 2, 3 & 4. The number of points required in the model construction differs for each problem using the adaptive approach due to the variation in those nonlinear functions.

If same number of LHS points are used with conventional Kriging based approach, the errors in estimation are quite high for problems 4-6, & 8 as shown in Table 4.2. But the moments are estimated with an accuracy of ($< \pm 3\%$) for problems 1-3, & 7 respectively. The Kriging model built using LHS points performs better than other approaches in estimating the moments of functions (1-3). The Kriging based adaptive approach performs well for problems 1-4, & 7, but there is small amount of variation in the estimated moments for problems 5, 6, & 8. For a reasonably accurate moment estimation ($\pm 5\%$), the proposed approach best estimates the moments of high-dimensional non-linear functions.

Table 4.1.
Estimation of moments.

Objective function	Moments	Analytical	MCS Averaged for 100 trials	SGM*	ASGM	Adaptive Approach	Simple Kriging Averaged for 20 trials
1. Forrester	μ	0.453	0.4485	0.4532	0.4535	0.4533	0.4533
	σ	4.457	4.4506	4.4561	4.4566	4.4564	4.4565
	N	NA	10000	17	129	15	15
2. Branin-Hoo	μ	54	54.860	54.865	54.976	54.932	54.530
	σ	51	51.659	51.696	51.617	51.899	51.469
	N	NA	10000	65	705	30	30
3. Camelback	μ	20	20.161	20.160	20.196	20.2529	20.1946
	σ	26	26.396	26.386	26.2272	26.4730	26.4051
	N	NA	10000	145	1537	65	65
4. Mystery	μ	6.80	6.8096	6.8081	6.8098	6.7750	6.5687
	σ	5.98	5.9804	5.9813	5.9840	5.8669	6.1151
	N	NA	10000	321	5121	64	64
5. $\text{Hartmann}_{3,4}$	μ	-0.9	-0.9432	-0.9451	-0.9435	-0.9437	-0.9475
	σ	1.0	0.9559	0.9579	0.9561	0.9592	0.9625
	N	NA	10000	441	4609	122	122
6. $\text{Hartmann}_{6,4}$	μ	-0.3	-0.3230	-0.3252	-0.3231	-0.2857	-0.3367
	σ	0.4	0.4336	0.4178	0.4336	0.3814	0.4243
	N	NA	10000	4865	10057	428	428

*converged

Table 4.1. Contd..
Estimation of moments.

Objective function	Moments	Analytical	MCS Averaged for 100 trials	SGM*	ASGM	Adaptive Approach	Simple Kriging Averaged for 20 trials
7. Trid	μ	40	40.005	40	40.01	39.9214	39.8787
	σ	16.5	16.517	16.522	16.831	16.5549	16.1394
	N	NA	10000	221	6913	161	161
8. Dixon-Price	μ	619328	618520	618601	622813	638779	655411
	σ	271959	273720	273645	272586	284881	249709
	N	NA	10000	17265	201413	614	614

*converged

Table 4.2.
Errors in moment estimation.

Objective function	Moments	Analytical	MCS Averaged for 100 trials	SGM*	ASGM	Adaptive Approach	Simple Kriging Averaged for 20 trials
1. Forrester	ϵ_μ	0	0.9934	0.0442	0.1104	0.0662	0.0662
	ϵ_σ	0	0.1436	0.0202	0.0090	0.0135	0.0112
	N	NA	10000	17	129	15	15
2. Branin-Hoo	ϵ_μ	0	1.5926	1.6019	1.8083	1.7272	0.9831
	ϵ_σ	0	1.2922	1.3647	1.2098	1.7645	0.9206
	N	NA	10000	65	705	30	30
3. Camelback	ϵ_μ	0	0.8050	0.80	0.98	1.2645	0.9730
	ϵ_σ	0	1.5231	1.4846	0.8738	1.8192	1.5581
	N	NA	10000	145	1537	65	65
4. Mystery	ϵ_μ	0	0.1412	0.1191	0.1441	0.3676	3.4015
	ϵ_σ	0	0.0067	0.0217	0.0669	1.8913	2.2592
	N	NA	10000	321	5121	64	64
5. Hartmann$_{3,4}$	ϵ_μ	0	4.8	5.0111	4.833	4.8556	5.2778
	ϵ_σ	0	4.41	4.21	4.39	4.0800	3.7500
	N	NA	10000	441	4609	122	122
6. Hartmann$_{6,4}$	ϵ_μ	0	7.6667	4.8000	8.4000	4.7667	12.2333
	ϵ_σ	0	8.4	4.45	8.4	4.6500	6.0750
	N	NA	10000	4865	10057	428	428

*converged

Table 4.2. Contd..
Errors in moment estimation.

Objective function	Moments	Analytical	MCS Averaged for 100 trials	SGM*	ASGM	Adaptive Approach	Simple Kriging Averaged for 20 trials
7. Trid	ϵ_μ	0	0.0125	0	0.0250	0.1965	0.3032
	ϵ_σ	0	0.103	0.1333	2.0061	0.3327	2.1855
	N	NA	10000	221	6913	161	161
8. Dixon-Price	ϵ_μ	0	0.1305	0.1174	0.5627	3.1407	5.8262
	ϵ_σ	0	0.6475	0.6199	0.2305	4.7515	8.1814
	N	NA	10000	17265	201413	614	614

*converged

Objective functions (1-4) and their approximate representation using the SGM, the adaptive approach, and random Latin hypercube points are shown in Figures 4.6-4.13. From the figures it can be concluded that the LHS based Kriging approach approximates the functions reasonably well for problems (1-3) but fails to represent the Mystery function due to the multi-modal nature of the Mystery function, as shown in Fig 4.10. The adaptive approach well represents the objective functions (1-4) with fewer SG collocation design points.

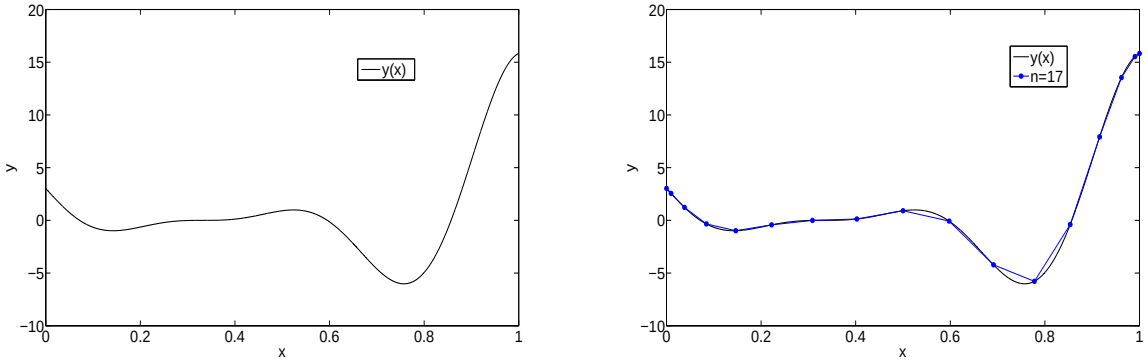

Figure 4.6: Forrester function and approximate representation of true function using SGM (k=4).

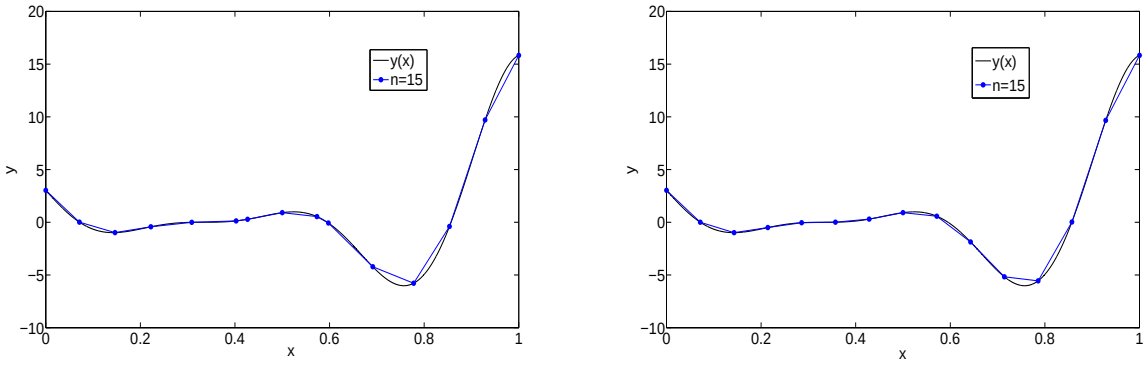

Figure 4.7: Approximate representation of true function using adaptive and simple Kriging approaches.

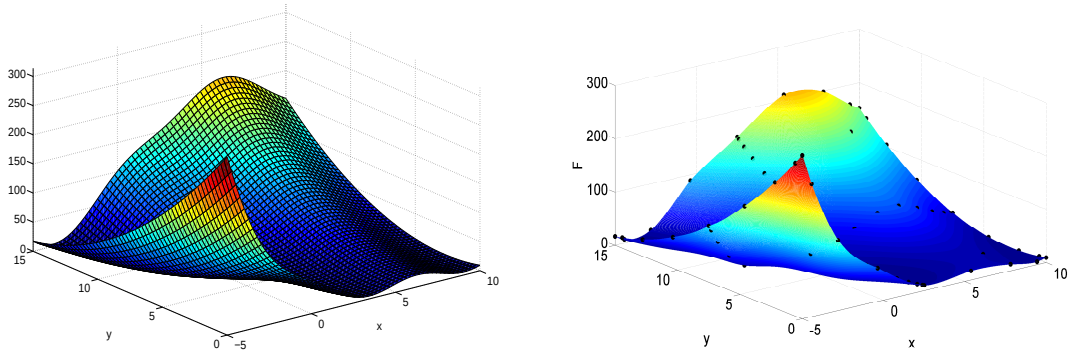

Figure 4.8: Branin-Hoo function and approximate representation of true function using SGM (n=65).

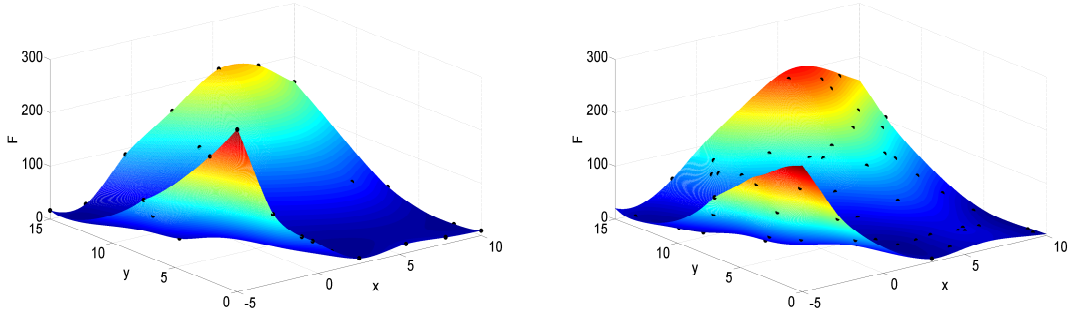

Figure 4.9: Approximate representation of true function using adaptive and simple Kriging approaches (n=30).

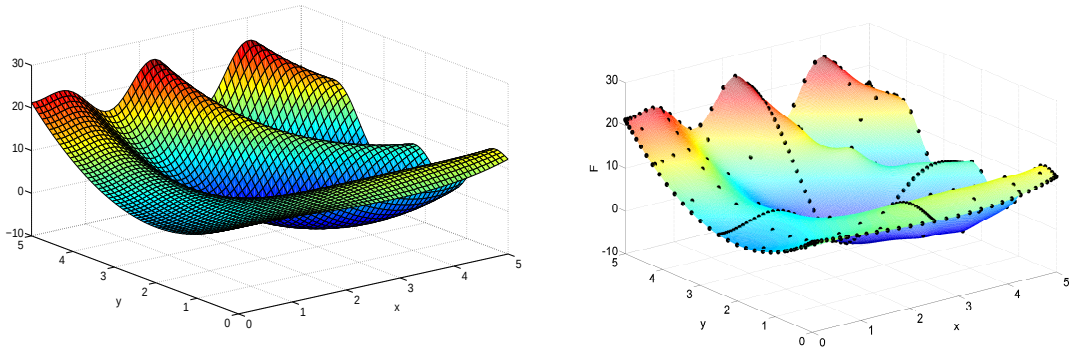

Figure 4.10: Mystery function and approximate representation of true function using SGM (n=321).

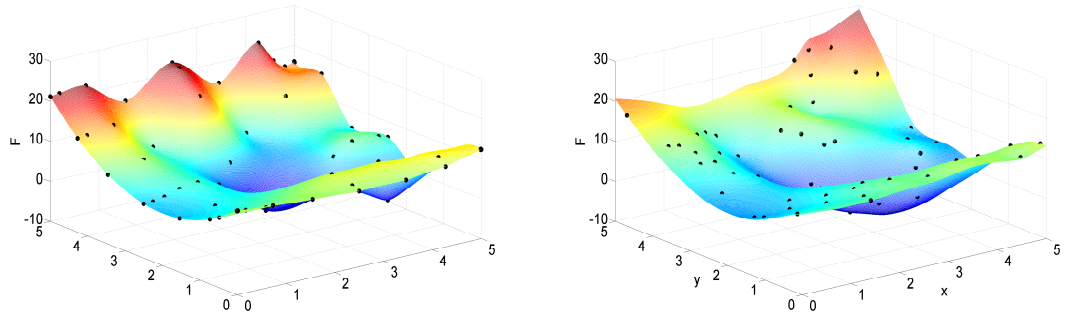

Figure 4.11: Approximate representation of true function using adaptive and simple Kriging approaches (n=64).

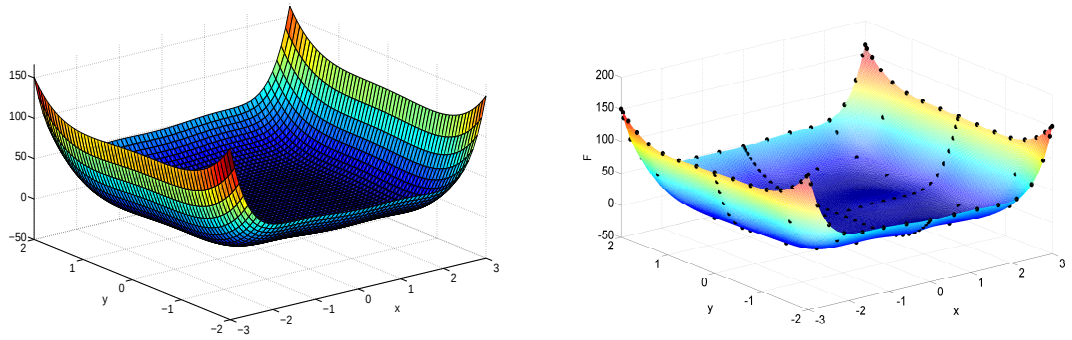

Figure 4.12: Camelback function and approximate representation of true function using SGM (n=145).

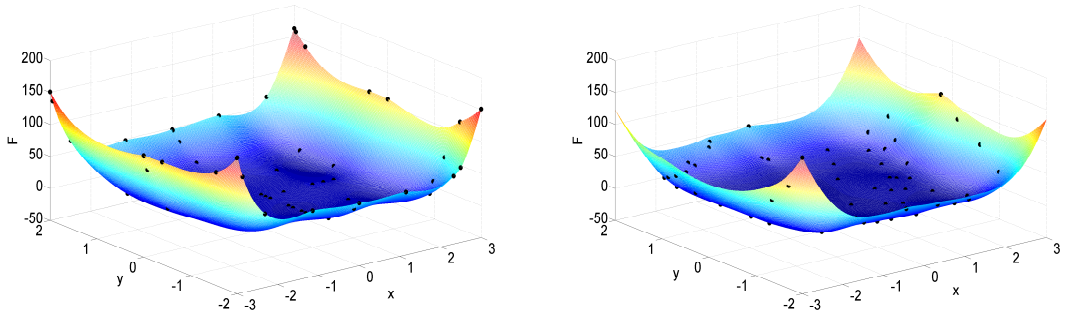

Figure 4.13: Approximate representation of true function using adaptive and simple Kriging approaches (n=65).

Chapter 5

Application of uncertainty quantification methods for structural systems

In the previous chapters, a wide variety of methods are studied and applied to improve the performance and also to reduce the computational cost in the estimation of probabilistic moments for high dimensional numerical test functions. From a heuristic point of view, it can be concluded that the probabilistic content of the output response quantity is characterized in its probabilistic density function. Two engineering application oriented problems are presented in this chapter in order to illustrate the performance of the various probabilistic moment estimation approaches described in the previous chapters.

The first example deals with a comparison of the approaches for uncertainty quantification of maximum von Mises stresses in a plate with holes. The discontinuity in the stress field along with the complexities in approximation of the output response makes the test model of particular interest and poses specific difficulties for UQ methods.

The second example deals with an elastic truss structure, with the exception that the random variables are described using non-Gaussian random variables. This example allows to illustrate the capabilities and limitations of the proposed approach and further illustrating the flexibility of the adaptive approach over conventional techniques in probabilistic moment estimation.

A schematic view of the typical working procedure for probabilistic moment estimation is shown in Fig. 5.1. The following steps are performed in estimating the probabilistic moments :

Step 1 : Identifying the input parameters (ξ_i) of the simulation model and prescribing them in a probabilistic context using appropriate definition of random variable. Since the variables can be uniform, Gaussian, or exponentially distributed as given in appendix [A]. Next generate a script file for the description of random variable.

Step 2: The random variables are perturbed based on the given uncertainty and incorporated into the nominal input file of the simulation model. Simulations are carried out to estimate the response of the structural model, for varied degrees of uncertainty in the random variables.

Step 3: After performing a number of deterministic simulations on the model, considering all the realizations of the random variables (ξ_i), one collects an ensemble of solutions, i.e., realizations of the random solutions $M(\xi_i)$ where M refers to the simulation model.

Step 4: Various probabilistic moment estimation approaches proposed in the earlier chapters were performed to estimate the response statistics such as mean, variance, and other higher order moments of the output respose of a given stochastic simulation model.

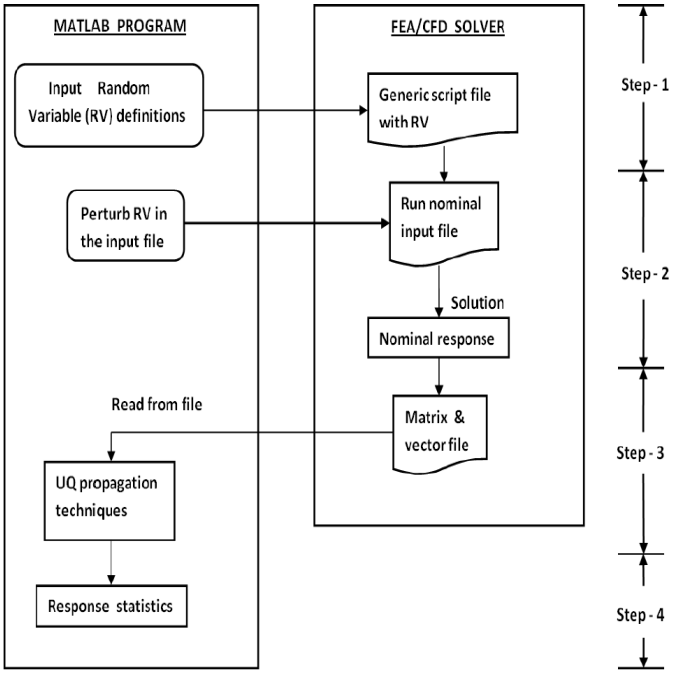

Figure 5.1: Flowchart for implementation probabilistic moment estimation approaches.

5.1 Elasticity problem - a plate with holes

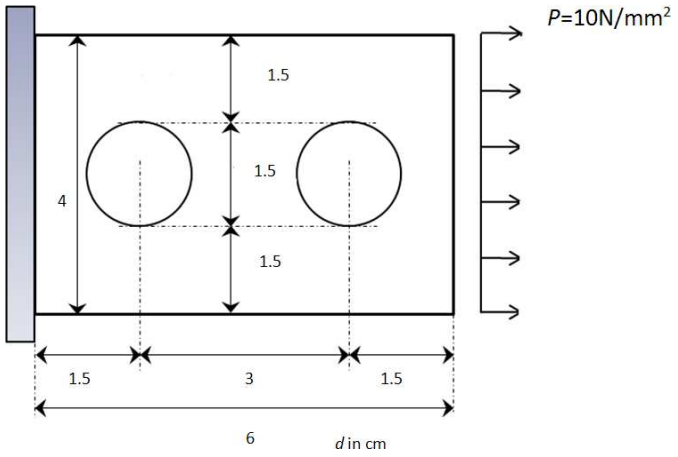

Figure 5.2: Plate with two holes.

The moment estimation approaches presented in this thesis are next used to estimate the moments in a two-dimensional plate with two holes as shown in Fig 5.2. The positions $(X_1,\ Y_1)$, $(X_2,\ Y_2)$ of the two holes are constrained to move randomly in x and y directions. The four random variables are uniformly distributed as shown in Table 5.1. The output quantity of interest are the maximum von Mises stresses in the plate. The plate is clamped at the left edge and a pressure of p= 10 N/mm^2 is applied on the other end. The Young's modulus of the plate is E= 209 GPa, and Poisson ratio, $(\upsilon) = 0.3$. The in-plane stresses in the deformed plate are shown in Fig 5.3.

Table 5.1

Variable	Min. Value	Max. Value
X_1(mm)	-14.5	-15.5
Y_1(mm)	-0.5	0.5
X_2(mm)	14.5	15.5
Y_2(mm)	-0.5	0.5

Four different probabilistic moment estimation methods are applied to the test problem and results are shown in Table 5.2. In the first case, Monte-Carlo simulations are carried out to estimate the probabilistic moments. The number of stochastic simulations performed using MCS are 5000.

In the second case, the sparse grid method (SGM) is used for probabilistic moment estimation. A Clenshaw-Curtis one-dimensional rule is used in the sparse grid

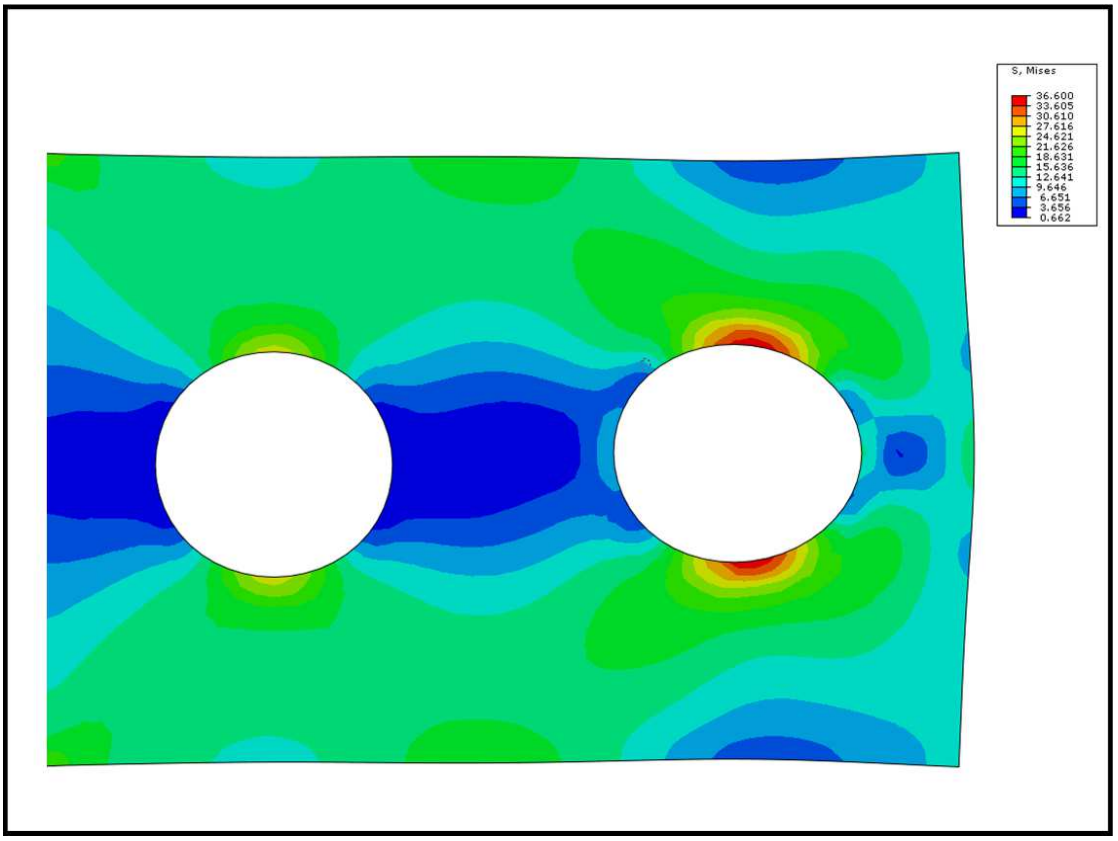

Figure 5.3: von Mises stresses in plate with deformed geometry.

construction. The order or level of 1-D rule used in the sparse grid construction is varied from lower to higher level to accurately estimate the moments.

In the third case, Kriging based adaptive approach is used for probabilistic moment estimation. The initial sample points (or DOE) used to build the Kriging model are the first order sparse grid (SG) points. Here we consider a full sample space design comprising of fifth order SG points. The mean square error (MSE) criteria is used to screen the design points from the full sample space design and the points with maximum error are updated to the initial DOE. Moments are estimated using SGM on the improved Kriging response surface attained using the updated sampling plan.

In the final case, the Kriging model is built using Latin-hypercube sample points and moment estimation is performed using sparse grid method on the bult-in Kriging surrogate model. The number of LHS points used to build the Kriging model are considered to be the same number as attained using the adaptive approach. The intent is to provide a comparision using a simple bulit-in Kriging model and the one obtained iteratively using adaptive approach. The estimated moments

Table 5.2: Probabilistic moment estimation of maximum von Mises stresses in the plate :

Method		μ	σ	time(t)	Fcalls	ϵ_μ	ϵ_σ
MCS		36.2176	0.8633	17hr. 19 min	5000	0	0
SGM	level(k)						
	1	36.0812	0.6079	2 min	9	0.38	29.58
	2	36.0822	0.6185	8 min	41	0.37	28.36
	3	36.4146	0.7054	27 min	137	0.54	18.29
	4	36.4575	0.7385	1hr. 18 min	401	0.66	14.46
	5	36.340	0.8735	3hr. 41 min	1105	0.34	1.18
	6	36.340	0.8691	9hr. 52 min	2929	0.34	0.67
Adaptive approach		**36.4348**	**0.8463**	**2hr.18 min (47 min)**	**229**	0.60	1.97
Kriging (Averaged for 20 trials)		36.4544	0.7195	47 min (15hr. 39 min for 20 trials)	229	0.65	16.65

are averaged for 20 different trials of Kriging models built successively using LHS points.

Similar to earlier studies the relative percentage errors (ϵ_μ, ϵ_σ) in the estimation of mean and standard deviation of the stresses are calculated as,

$$\epsilon_\mu = |\frac{(\mu_{MCS} - \mu_{appr})}{\mu_{MCS}}| \times 100, \qquad \epsilon_\sigma = |\frac{(\sigma_{MCS} - \sigma_{appr})}{\sigma_{MCS}}| \times 100. \tag{5.1}$$

Here the reference solution for the estimated moments of the plate is calculated using MCS. The convergence criteria considered for the estimated moments is $\pm 2\%$ with respect to reference solution.

In the current problem, a single model evaluation takes $\approx (11-13)$ seconds. Figure 5.4., shows the convergence for MCS, SGM (k=5) and adaptive approaches in estimating the probabilistic moments. Figures 5.5 and 5.6, shows the positions of the centres of two holes (X_1, Y_1), (X_2,Y_2) perturbed according to random variable

definition and where model simulations are carried out using adaptive and SGM (k=5) approaches.

The four methods estimate the mean reasonably well ($\epsilon_\mu < 1\%$), but there is a distinctive variation in the estimation of standard deviation of the stresses. The number of FEA simulation runs required to accurately estimate σ is very high using MCS and SGM methods. The error in the estimation of σ reduces as the order of SGM is increased. The sparse grid method uses 1105 simulation runs to estimate mean and standard deviation within $\pm 1\%$ and $\pm 2\%$ accuracy respectively. The adaptive approach estimates σ accurately with 229 simulation runs with relative error $\epsilon_\sigma < 2\%$. The time taken to perform the simulation runs is 47 *minutes* but there is an additional amount of time (91 *minutes*) spent in tuning the hyperparameters and overall update process of the Kriging model.

The number of model evaluations required for probabilistic moment estimation, is much less using the adaptive approach compared with MCS and SGM approaches as shown in Table 5.2. A fraction of sample space design points are needed in building the Kriging model. But if LHS points of same number are used to build the Kriging model, the errors in estimation of σ is high (16.65%). Hence the adaptive approach performs best compared to other approaches although there is an extra time involved in tuning the hyperparameters and overall update process of the Kriging model.

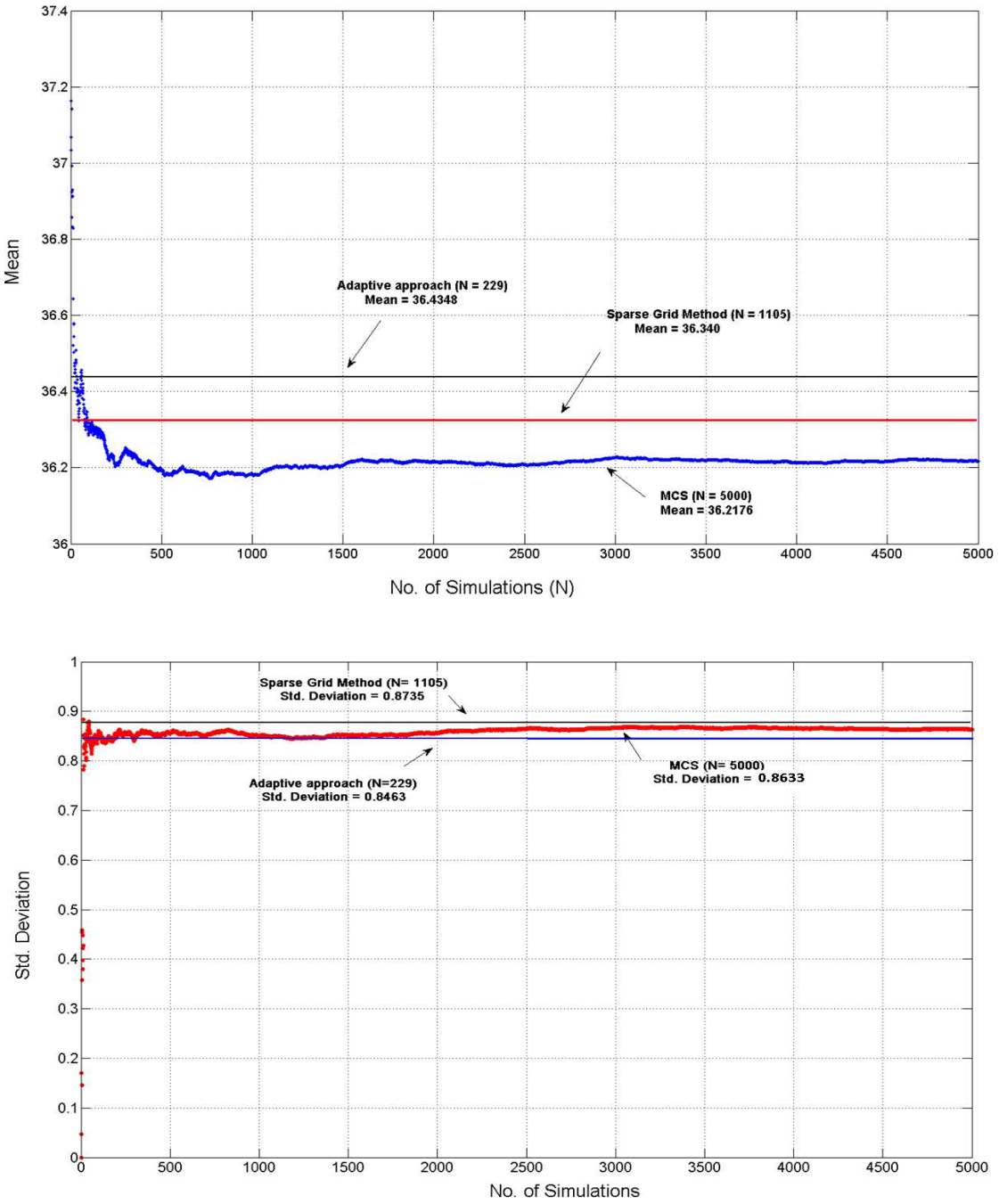

Figure 5.4: Moment estimation using MCS, SGM (k=5) and adaptive approaches.

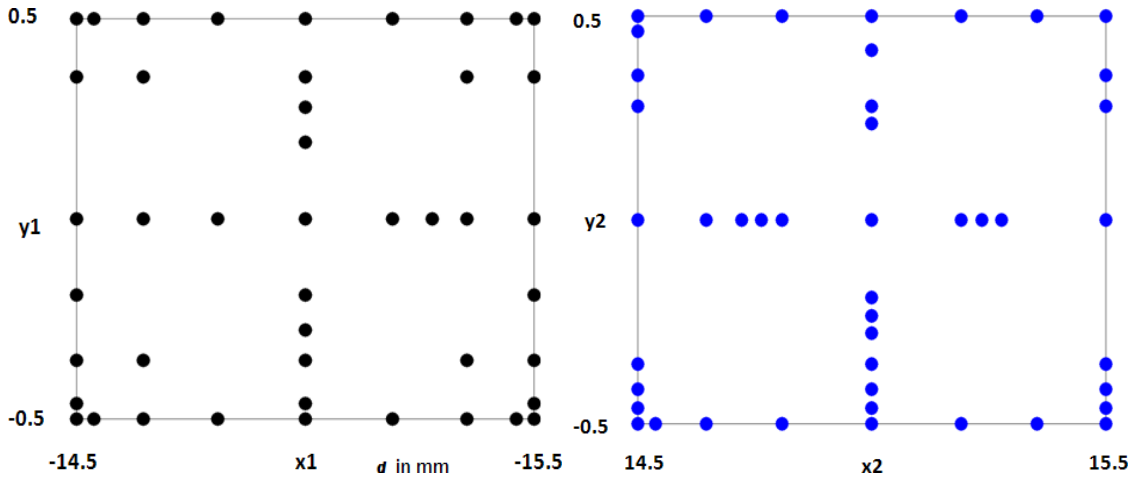

Figure 5.5: Positions of centres of two holes obtained and analysed using Kriging based adaptive approach (n=229).

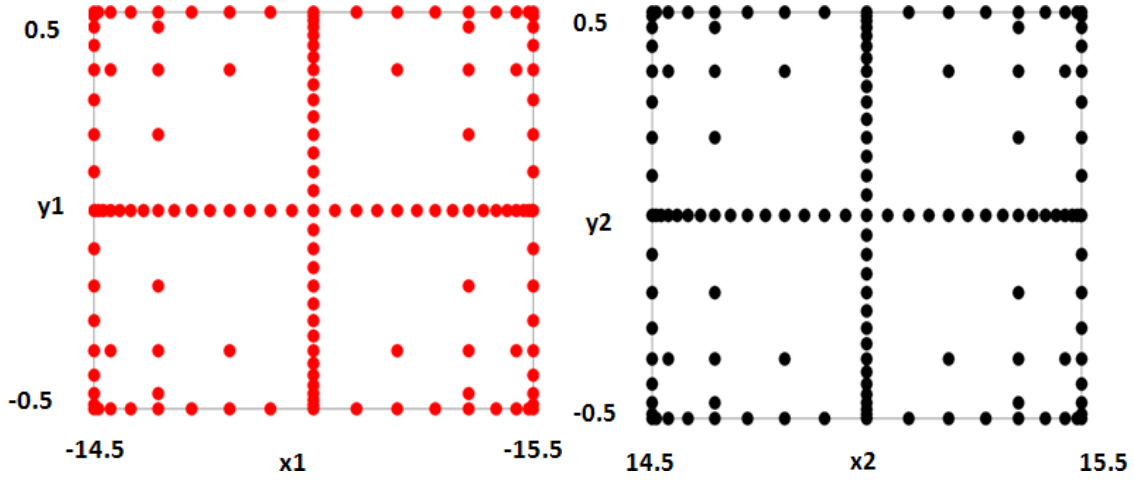

Figure 5.6: Positions of centres of two holes obtained using SG (n=1105) design.

5.2 Elastic truss structure

The geometry for a simply supported truss structure presented in Figure 5.7, is considered for the application of UQ approaches. The test problem is used as a benchmark test case in order to solve a reliability problem involving non Gaussian random variables. Further a regression method was performed on this problem for estimating the PC coefficients by regression [19]. A comprehensive representation of intrusive computational schemes for the truss structure in the context of reliability based studies can be found in [68]. The truss structure is made of 23 member elastic bars, whose Young's modulus and cross sections are uncertain. The truss structure is loaded by six vertical loads P1-P6. The ten independent random variables with respective distribution, mean, standard deviation are given in Table 5.3.

Here the simple elastic structure is used to estimate the probabilistic moments by various approaches described in the previous sections. The response statistics such as probability density function and moments of the mid-span vertical displacement of the truss structure are considered with respect to a maximal admissible displacement.

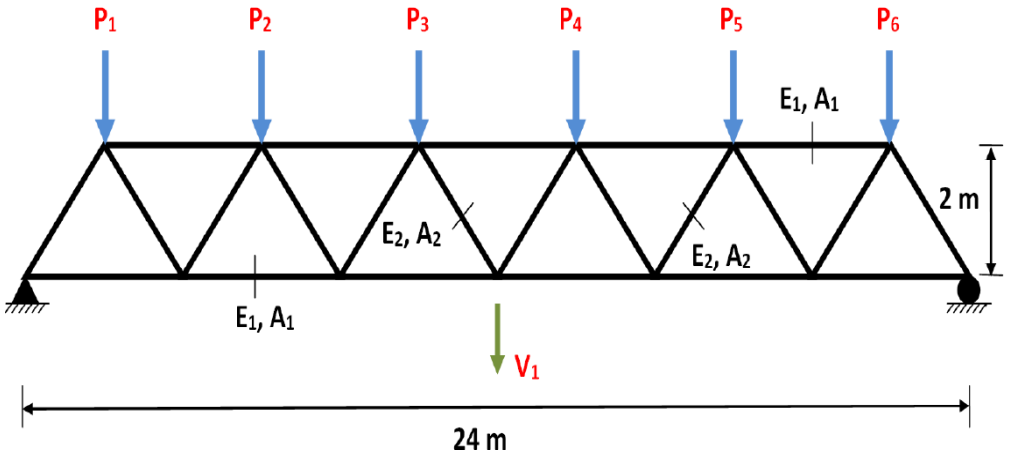

Figure 5.7: Elastic truss structure with 23 members.

The typical output response, in this case the mid-span deflection v can be modeled as a function of input random variables ξ and is given by,

$$v = M(E_1, E_2, A_1, A_2, P_1....P_6). \tag{5.2}$$

where M is the finite element based model function. By transforming the input random vector $X = \{E_1, E_2, A_1, A_2, P_1....P_6\}^T$ into a standardized Gaussian vector,

$$\xi_i = F_{X_i}^{-1}(\phi(X_i)), \quad i = 1, ...10. \tag{5.3}$$

where F_{X_i} is the CDF of the i^{th} component of X and ϕ is the standard normal CDF.

Table 5.3: Truss structure - Input random variables :

Description	Name	Distribution	Mean	Standard deviation
Young's modulus	E1, E2 (Pa)	Lognormal	2.10×10^{11}	2.10×10^{10}
Cross section of the horizontal bars	A1(m^2)	Lognormal	2.0×10^{-3}	2.0×10^{-4}
Cross section of the vertical bars	A2(m^2)	Lognormal	1.0×10^{-3}	1.0×10^{-4}
Loads	P1-P6 (N)	Gumbel	5.0×10^{4}	7.5×10^{3}

The non intrusive UQ methods applied for probabilistic moment estimation and comparison in this problem includes:

- Monte Carlo simulation (MCS); 100000 samples are used .
- LHS sampling; 10000 samples are used.
- collocation scheme, i.e, sparse grid quadrature constructed using Gauss patterson 1-D rules,
- multi-point adaptive strategy, using sparse grid collocation design points.

In the first case, the reference solution is obtained by crude Monte Carlo simulation using 100,000 runs of the finite element model. In second case, LHS sampling points are used to perturb the random variables and the moments are estimated from the ensemble of random solutions for the output response.

In the third case, sparse grid collocation method is used, where the random variables are defined using appropriate definitions and Gauss-patterson 1-D rules are used in the sparse grid construction. The first, second, third and fourth order moments are estimated relatively accurate with 221 finite element simulations.

In fourth case, the Kriging based adaptive approach is used where similar to SGM, Gauss patterson based sparse grid points are selected as sampling plan. Initally 5 points are used to built the Kriging model and additional sampling points are selected based on MSE criteria. The moments are estimated on the Kriging model using sparse grid method, the estimated moments are relatively accurate with 98 model simulations.

The probability density function (PDF) of the maximal deflection (as shown in Fig .5.8) can be estimated by post processing the results obtained using the four methods mentioned above. It is observed that the sparse grid expansion and adaptive approaches converge more rapidly and closer to reference solution than LHS based simulation technique.

The multi-point Kriging based adaptive approach performs noticeably faster with computational gain in terms of number of simulations to be carried out. It allows adaptive approach to estimate moments closer to reference solution using 98 sparse grid nodes and with less function calls to FEA program, than the one associated with a conventional sparse grid approach performed using 221 nodes.

Here we used a structural test case problem with considerable number of random variables with strong interaction. But similar scenario do not exist for other complex problems, where each simulation may last for hours and also the random parameters can be quite high (10-20). Hence there is a limitation on the maximum number of simulations to be carried out for estimating the moments. The Kriging based adaptive approach is affordable and preferred over other approaches for such high-dimensional problems.

Table 5.4: Truss structure - Estimates of the first four statistical moments of the mid-span displacement:

Moment	Ref. Solution	Simulation LHS	Sparse grid SGM (K=2)	Adaptive approach SG Points
Mean Value	0.0847	0.0858	0.0847	0.0848
Std. deviation	0.0117	0.0181	0.0117	0.0118
Skewness	-0.4691	-0.6550	-0.4843	-0.4779
Kurtosis	3.3502	3.6917	3.3816	3.2568
Number of FE runs	100,000	10,000	221	98

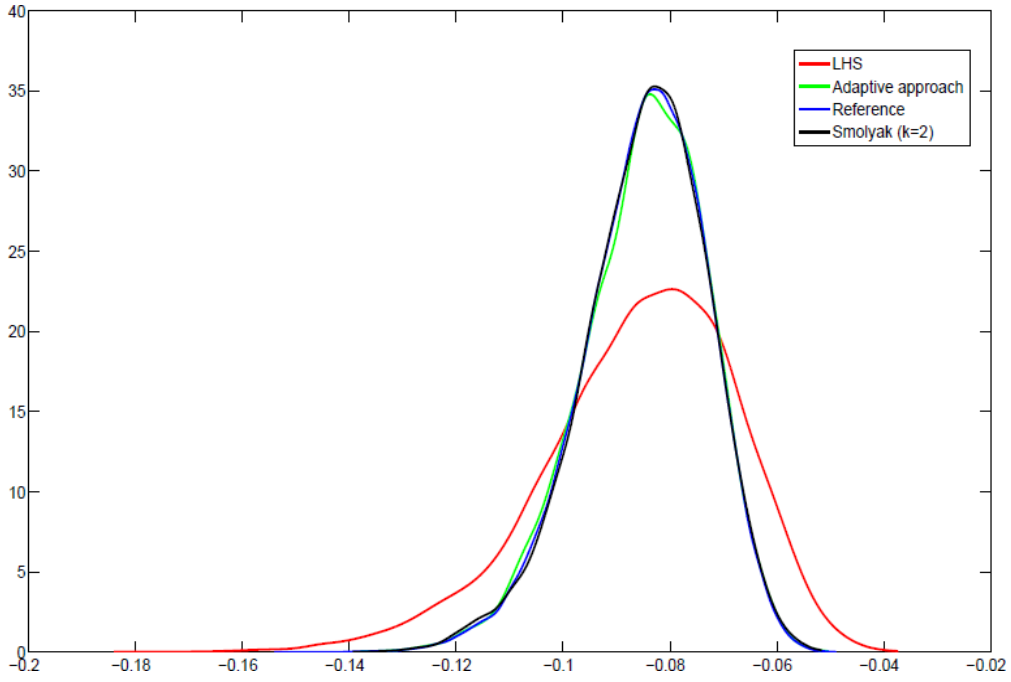

Figure 5.8: Truss - probability density function of the maximal deflection.

Chapter 6

Conclusions & Recommendations for Further Work

The final chapter of the thesis is divided into two parts: conclusions and recommendations. Section 6.1 gives a summary of the finding in the present study. Section 6.2 illustrates the scope for improvement.

6.1 Conclusions

In search for efficient probabilistic moment estimation method, stochastic collocation approach was developed. Sparse grid collocation approach shows spectral convergence with respect to the order of approximation for many numerical test cases. However the method varies in performance according to the parmeters involved in the numerical test cases and becomes too computationally intensive for high dimensional problems. Due to the response of the underlying objective function being highly nonlinear and the number of nodes required to estimate the probabilistic moments increases exponentially with the number of uncertain parameters.

Surrogate model approximation techniques offer a way to solve some of the issues. In order to reduce the number of simulations required for uncertainty quantification, two approaches have been followed. First a surrogate model is built using a sample design comprising of lower order sparse grid collocation points and Kriging based function approximation were used to approximate the high dimensional surface. The second approach was the screening approach, where additional points

are selected from sample space design comprising of higher order sparse grid points using maximum square error criteria (MSE) and the surrogate model is re-built. The procedure is continued till an acceptable convergence in the estimated probabilistic moments is attained. The test cases show that for 1 to 12 uncertain parameters, the proposed adaptive approach is a good alternative to sparse grid collocation approach.

Current work has focused on probabilistic moment estimation when multiple uncertain parameters are present in the stochastic system. The intent was to provide a sytematic background in the field of robust design and use of statistical approaches in the design of stochastic structural systems. The development and adoption of new adaptive approach to represent stochastic systems in the presence of uncertainty enables the reduction in simulations henceforth required for high dimensional problems.

In Chapter 2, we presented various aspects pertaining to stochastic systems. Specifically the concept of modeling uncertainty was discussed with graphical interpretations. Various approches used in defining the uncertainty such as probabilistic approach, interval analysis, possibility theory, evidence theory and fuzzy based approach for modeling uncertainties are presented. Turning to uncertain propagation, simulation based approaches such as MCS, Quasi MCS, Lattice rules are presented. The intent is to greatly reduce the learning time to comprehend the basic idea of simulation based approaches for interested readers. Lastly, various design formulations developed over the period of time for design optimisation in the presence of uncertainties is provided.

Chapter 3, describes stochastic collocation method for multi-variate numerical integration in high dimensions. A short discussion of Newton-Cotes formulas and Gaussian formulas their strengths and weakness are provided. Sparse grid collocation method using one dimensional Clenshaw-Curtis rule is developed. The importance of adaptiveness for sparse grid is stressed out and the development of adaptive sparse grid using dimension adaptive algorithm is described. The application of SGM, ASGM are demonstrated with illustration of numerical problems comprising of random variables. The main aim is to understand the importance and limitations of SGM and ASGM when applied to high dimensional numerical problems.

Chapter 4, describes the importance of surrogate modeling in UQ studies. A detailed view of surrogate modeling approaches such as radial basis functions and

Kriging approach is provided along with application of surrogate modeling approach for simple two dimensional test function. The results present the limitations of radial basis functions for UQ studies but suggests the need for the use of Kriging based adaptive approach. From the results presented in the chapter, Kriging based adaptive method performs better than other approaches using fewer function evaluations in moment estimation of high-dimensional nonlinear functions in terms of accuracy and computational efficiency.

In Chapter 5, we demonstrated the stochastic simulation procedure for structural problems involving Gaussian and non-Gaussian random variables. In order to understand the efficiency and applicability of the proposed Kriging based adaptive approach it is necessary to consider large-scale structural problems. Thus we applied the procedure to a nonlinear structural model (ten bar truss structure) using UG-NX6/ABAQUS and Matlab software. At this point, we showed how the method can be used for 1) probabilistic description of randomness with different distributions of random variables in a simulation model whilst performing stochastic simulations, 2) estimate the probabilistic moments using few nodes or very few simulations compared to conventional approaches such as MCS, sparse grid method and conventional surrogate modeling approaches.

6.2 Recommendations for Further Work

The thesis discusses the application of SGM, ASGM, the implementation of a novel Kriging based adaptive approach for moment estimation of a few mathematical test problems and structual problems. The new adaptive approach for uncertainty quantification studies has significance in the context of engineering problems with strong interaction of the variables involved, where otherwise a high number of function evaluations are needed to accurately estimate the probabilistic moments.

The main aim of this research is to improve the design that is less sensitive to input variations or uncertainties. As mentioned earlier the estimation of probabilistic moments is central in robust design framework. Future work will focus on improving the probabilistic moment estimation approach proposed i.e., Kriging based adaptive approach and explore its potential for high dimensional problems with considerable number of random variables 50-100, where the objective function/simulation model can be complex and nonlinear. The following are the broad directions to further research :

6.2.1 Strategies for stochastic simulations

In the current adaptive approach, the surrogate model was built using SG points in the high dimensional stochastic space. Further work can be carried out by considering different sampling plans comprising of low-discrepancy sequences, lattice points etc. Using lattice rules the probabilistic moments can be calculated when apriori probabilistic moment estimates of simulation model are not attainable using conventional approaches such as MCS. A comprehensive code can be developed encompassing sampling plan techniques, moment estimation approaches with appropriate definitions for randomness using probability, possibility, evidence based theory and fuzzy techniques.

6.2.2 Non-intrusive generalized polynomial chaos (gPC) expansion

To study the potential of non-intrusive generalized polynomial chaos (gPC) expansions for high dimensional problems. This is a good technique for uncertainty propagation due to its strong mathematical basis and its ability to produce functional representation of stochastic processes [19]. A comparative study using simple Kriging and PC expansion was provided by Keane et al. [69] in the estimation of moments of a two-dimensional mathematical problem with normally distributed random variables. The coefficients of PC expansion are estimated using regression and sparse grid interpolation techniques. There are many obstacles for the implementation of PC expansion for high-dimensional problems since the approximation is a higher order PC expansion with many coefficients. Hence effective algorithms need to be developed to truncate such expansions. Further studies include a comparison of adaptive approach to PC expansion for moment estimation of high-dimensional problems with non-Gaussian random variables. The advantage of using adaptive approach for estimating the coefficients of PC expansion in the evaluation of higher order moments should be studied.

Appendix A

Orthogonal polynomials and quadrature schemes

A.1 Orthogonal polynomials

Definition:

Sets of orthogonal polynomials play central role in numerical integration, here we discuss some of the important aspects pertaining to them.

Let F is a real linear space of square integrable functions with simple rectifiable boundary C i.e $F = C[a\ b]$. Let w is the weight function, $w(x) \geq 0$ and $\int_C w(x)dx > 0$. The inner product $< f, g >$ defined on F is a bilinear functional of f, $g \in F$ given by

$$< f, g >_C = \int_a^b w(x)f(x)g(x)\mathrm{dx}. \tag{A.1}$$

If $f_0, f_1, f_1, ..$ is a finite set of elements of F such that

$$< f_i, f_j >= 0, \quad i \neq j \tag{A.2}$$

the set is called orthogonal. In addition,

$$< f_i, f_j > = 1, \quad i = 0, 1, ..., \tag{A.3}$$

the set is called orthonormal. A set of polynomials ploynomials f_i satisfying Eq. (B.2), are called orthogonal polynomials with respect to inner product $(f,\ g)$

The unique set of orthogonal polynomials $f_n^*(x)$, $f_m^*(x)$ with respect to w on finite or infinite interval [a, b] can be attained using Gram-Schmidt orthogonalization of the monomials (1,x,..x^n, $n \in$ N) where

$$< f_n^*, f_m^* >= \int_a^b w(x) f_n^*(x) f_m^*(x) \mathrm{dx} = \delta_{\mathrm{mn}} = \begin{cases} 0, & \mathrm{m} \neq \mathrm{n}, \\ 1, & \mathrm{m=n.} \end{cases} \tag{A.4}$$

and leads to recurrence relationship:

$$P_{n+1}(x) = (x - a_n) P_n(x) - b_n P_{n-1}(x), \qquad \forall n \in \mathrm{N} \tag{A.5}$$

$$P_{-1}(x) \equiv P_0(x) = 1. \tag{A.6}$$

where the coefficients (a_n, b_n) :

$$a_n = \frac{< xP_n, P_n >}{< P_n, P_n >} \tag{A.7}$$

$$b_n = \frac{< P_n, P_n >}{< P_{n-1}, P_{n-1} >} \tag{A.8}$$

The classical orthogonal polynomials corresponding to special weight functions and the support space are given in the Table B.1. Other hyper geometric functions and related groups of polynomials exist and termed as Askey polynomials.

Table A.1: List of some important orthogonal polynomials :

Interval	Weight function	Symbol	Name
[-1 1]	1	$L_n(x)$	Legendre
(-∞ ∞)	e^{-x^2}	$H_n(x)$	Hermite
[0 ∞)	e^{-x}	$G_n(x)$	Laguerre
[-1 1]	$(1-x^2)^{-1/2}$	$T_n(x)$	Tschebyscheff

The properties of orthogonal Hermite polynomials which are used in this thesis, is discussed here.

A.2 Hermite polynomials

The Hermite polynomials are solution to differential equation:

$$y^{''} - 2xy^{'} + 2ny = 0, \quad y = H_n(x). \tag{A.9}$$

The recurrence relationship is given by

$$H_{n+1}(x) = 2xH_n(x) - 2xH_{n-1}(x); \quad H_0 = 1, \quad H_1 = 2x. \tag{A.10}$$

They are orthogonal with respect to the Gaussian probability measure φ,

$$\int_{-\infty}^{\infty} H_n^*(x)H_m^*(x)\varphi(x)\mathrm{dx} = \mathrm{n!}\delta_{\mathrm{mn}}, \qquad \delta_{\mathrm{mn}} = \begin{cases} 0, & \mathrm{m}\neq\mathrm{n}, \\ 1, & \mathrm{m}=\mathrm{n}. \end{cases} \tag{A.11}$$

The first four Hermite polynomials(one-dimensional) are:

$$H_1 = x, \quad H_2 = x^2 - 1, \quad H_3 = x^3 - 3x, \quad H_4 = x^4 - 6x^2 + 3. \tag{A.12}$$

A.3 Gaussian quadature rule:

Let us consider a one dimensional integral

$$I = \int_C f(x)w(x)\mathrm{dx}. \tag{A.13}$$

The integral is expressed as weighted sum of function evaluations of the integrand,

$$I = Q^i(f) = \sum_{i=1}^{n} w_i f(x_i) \tag{A.14}$$

x_i are the collocation points or roots of orthogonal polynomials(Legendre, Hermite, etc.) The associated weights are,

$$w_n = \frac{< P_{n-1}(x), P_{n-1}(x) >}{P'_n(x_n)P_{n-1}(x_n)} \tag{A.15}$$

In Gaussian quadrature scheme the number of points n (or order) is significant and determines the accuracy of the quadrature rule. As mentioned earlier with n points they can integrate polynomial function of order $2n-1$ exactly.

A.4 Clenshaw-Curtis rule:

It is useful to have interpolatory rules rather than abscissas (or roots) which are equidistant (for Newton-Cotes), clustered (Gauss rules) at the bounds of the integral domain. Clenshaw-Curtis used the change of variables x to cosine functions and finding the zeroes of the polynomials T_n that have trigonometric expressions and explicit formulae. The rule is fast convergent for even, periodic integrable polynomial functions.

The abscissas of the Clenshaw-Curtis rule are given by,

$$x_k = cos(\frac{k-1}{n-1}\pi), \quad k = 1, ...n. \tag{A.16}$$

The abscissas are the extreme points of Tschebycheff polynomials (T_n) on [-1 1] and the associated weights w_k are,

$$w_1 = w_n = \left\{ \begin{array}{cc} 1/(n-1)^2, & n \ even, \\ 1/n(n-2) & n \ odd. \end{array} \right\} \tag{A.17}$$

$$w_k = \left\{ 1 - \sum_{j=1}^{[(n-1)/2]} \frac{1}{4j^2-1} cos\frac{2j(k-1)}{n-1}\pi, \quad k = 2, ..., n-1. \right\} \tag{A.18}$$

References

[1] Helton, J.C., and Oberkampf, W., "*Alternative representations of epistemic uncertainties,*" Reliability Engineering and System Safety, 85 (Special Issue), 2004.

[2] Elishakoff, I., "*Safety Factors and Reliability: Friends or Foes?,*" Kluwer Academic Publishers, Boston, 2004.

[3] Taguchi, G., "*Robust technology development: Bringing quality engineering upstream,*" ASME Press, Newyork, 1993.

[4] Apostolakis, G.E., "*The concept of probability in safety assessment of technological systems,*" Science, Vol. 250, 1990 , pp. 1359.

[5] Oberkampf, W. L., DeLand, S.M., Rutherford, B.M., Diegart Helton, K.V., and Alvin, K. F., "*Error and uncertainity in modeling and simulation,*" Reliability Engineering and system safety, Vol. 75, 2002, pp. 333-357.

[6] Matthies, H.G., Brenner, C.E., Bucher, C.G., and Soares, C.G., "*Uncertainties in Probabilistic Numerical Analysis of Structures and Solids-Stochastic Finite Elements,*" Structural Safety, Vol. 19, 1991, pp. 283-336.

[7] Bendat, J.S., Piersol, A.G., "*Measurement and analysis of random data,*" John Wiley, Newyork, 1971.

[8] Sobol, I., and Kucherenko, S., "*Global sensitivity indices for nonlinear mathematical models,*". Mathematica and Computers in Simulation, Vol. 55, 2001, pp. 271-280.

[9] Niederreter, H., "*Random Number Generation and Quasi-Monte Carlo Methods,*" SIAM, Philadelphia, Pennsylvania, 1992.

[10] Morokoff, W.J., and Caflisch, R.E., "*Quasi-random sequences and their discrepancies,*" SIAM, Journal of Scientific Computation, Vol. 15, 1994, pp. 1251-1279.

[11] Stein, M., "*Large sample properties of simulations using Latin hypercube sampling,*" Technometrics, Vol.29, 1987, pp. 143-151.

[12] Tatang, M.A., Pan, W.W., Prinn, R.G., and GMcRae, J., "*An efficient method for parametric uncertain analysis of numerical geophysical model,*" Journal of Geophysical Research, Vol. 102, 1997, pp. 1925-1932.

[13] Xiu, D., Hesthaven, J., "*High-order collocation method for differential equations with random inputs,*" SIAM Journal of Scientific Computing, Vol. 27, 2005, pp. 1118-1139.

[14] Acharjee, S., and Zabaras, N., "*A non-intrusive stochastic Galerkin approach for modeling uncertainty propagation in deformation processes,*" Journal Computers and Structures, Vol. 85, 2007, pp. 242-272.

[15] Klieber, M., and Hein, T.D., "*The stochastic Finite Element Method,*" John Wiley, Newyork, 1992.

[16] Liu, W.K., Belytchko, T., and Mani, A., "*Probabilistic finite elements for non-linear structural dynamics,*" Computer Methods in Applied Mechanics and Engineering, Vol. 56, 1986, pp. 61-81.

[17] Yamazaki, F., Shinozuka, M., and Dasgupta, G., "*Nuemann expansion for stochastic finite element analysis,*" Journal of Engineering Mechanics, Vol. 114, 1988, pp. 1335-1354.

[18] Deodatis, G., and Shinozuka, M., "*Weighted integral method.II. Response variability and reliability,*" Journal of Engineering Mechanics, Vol. 117, 1991, pp. 1865-1877.

[19] Weiner, N., "*The Homogeneous Chaos,*" American Journal of Mathematics, Vol. 60, 1938, pp. 897-936.

[20] Ghanem , R.G., and Spanos, P.D., "*Stochastic Finite Elements: A spectral Approach,*" Springer-Verlag, New York, 1991.

[21] Debusschere, B.J., Najim, H.N., Pebay, P.P., Knio, O.M., Ghanem, R.G., and Maitre, O.P.L., "*Numerical challenges in the use of polynomial chaos representations for stochastic processes,*" SIAM Journal of Scientific Computing, Vol. 26, 2004, pp. 698-719.

[22] Eldred, M.S., and Webster, C.G., "*Evaluation of non-intrusive approaches for Weiner-Askey generalized Polynomial chaos,*" AIAA., Vol. 1892, 2008, pp. 698-719.

[23] Myers, R.H., Khuri, A.I., and Carter, W.H., "*Response surface methodology,*" Technometrics, Vol. 31, 1988. pp. 137-153.

[24] Helton, J.C., and Jhonson, D.J., "*Quantification of margins and uncertainties: Alternative representations of epistemic uncertainty,*" Reliability Engineering and System Safety, Vol. 96, 2011. pp. 1034-1052.

[25] Apley, D.W., Liu, J., and Chen, W., "*Understanding the effects of model uncertainty in robust design with computer experiments,*" Journal of Mechanical Design, Vol. 128, 2005. pp. 945-958.

[26] Moore, R.E., "*Methods and applications of interval analysis,*" Society of Industrial Mathematics, Philadelphia, 1979.

[27] Khodaparast, H.H., Mottershead, J.E., and Badcock, K.J., "*Interval model updating with irreducible uncertainty using the Kriging predictor,*" Mechanical Systems and Signal Processing, Vol. 25, 2011, pp. 1204-1226.

[28] Jaulin, L., Kieffer, M., Didrit, O., and Walter, E., "*Applied interval analysis,*" Springer-Verlag, Newyork, NY, 2001.

[29] deCooman, G., "*Possibility theory part I: measure- and integral-theoretic ground-work; Part II: conditional possibility; Part III: possibilisitc inde- pendence,*" International Journal of General Systems, Vol. 25, 1997, pp.291-371.

[30] Halpern, J.Y., and Fagin, R., "*Two views of belief: belief as generalized probability and belief as evidence,*" Artificial Intelligence, Vol. 54, 1992, pp. 275-317.

[31] Shafer, G.A., "*Mathematical theory of evidence,*" Princeton University Press, Princeton,NJ, 1976.

[32] Dempster, A.P., "*A generalization of Bayesian inference,*" Journal of the Royal Statistical Society, Vol. 30, 1968, pp. 205-247.

[33] Dubois, D., and Prade, H., "*Fuzzy sets, probability and measurement,*" European Journal of Operational Research, Vol. 40, 1989, pp.135-154.

[34] Sloan, I.H., and Joe, S., "*Lattice Methods for Multiple Integration,*" Oxford University Press, Oxford, 1994.

[35] Kuo, F.Y., and Sloan, I.H., "*Lifting the curse of dimensionality analysis of output from a computer code,*" American mathematical society, Vol. 52, 2001, pp. 1320-1328.

[36] Dolstinis, I., Kang, Z., and Cheng, G.D., "*Robust design of non-linear structures using optimization methods,*" Computer Methods in Applied Mechanics and Engineering, Vol.194, 2005, pp.1779-1795.

[37] Buhl., T., Pederson, C.B.W., and Sigmund, O., "*Stiffness design of geometrically nonlinear structures using topology optimisation,*" Structural and Multidisciplinary Optimization, Vol.19, 2000, pp. 93-104.

[38] Aurora., J.S., "*Computational design optimization:A review and future directions,*" Structural Safety, Vol.7, 1990, pp. 131-148.

[39] Nikitha, T., Keane, A.J., and Nair, P.B., "*Robust design of turbine blades against manufacturing variability,*" International Journal of Reliability and Safety, Vol. 5, 2011 pp. 420-436.

[40] Rabinowitz, P., and Davis, P.J., "*Methods of numerical integration,*" Academic Press, Orlando, 1984.

[41] Gabor Szegó, "*Orthogonal polynomials,*" American mathematical society, Colloquium publications, Vol. 23, 1939.

[42] Clenshaw C.W., and Curtis, A.R., "*A method for numerical integration on an automatic computer,*" Numerische Mathematik., Vol. 2, 1960, pp. 197.

[43] Smolyak, S.A., "*Quadrature and interpolation formulas for tensor products of certain classes of functions,*" Sov Math, Dokl Vol. 4, 1963, pp. 240-243.

[44] Gerstner, T., Griebel, M., "*Numerical integration using sparse grids,*" Number Algorithms, Vol. 18, 1998. pp. 209-232.

[45] Novak, E., Ritter, K., "*High dimensional integration of smooth functions over cubes,*" *Numerische Mathematik*, Vol. 75, 1996, pp. 79-97.

[46] Xiu, D., and Karniadakis, G.E., "*Supersensitivity due to uncertain boundary conditions,*" International Journal of Numerical Methods Engg., Vol. 61, 2004, pp. 2114-2138.

[47] Xiu, D., "*Numerical Methods for Stocahstic Computations: A Spectral Method Approach,*" Princeton University Press, 2010.

[48] Klimke, A., and Wohlmuth, M., "*Algorithm 847: spinterp: Piecewise multilinear hierarchial sparse grid interpolation in MATLAB,*" Journal of ACM Transactions on Mathematical Software (TOMS)., Vol. 31, 2005, pp. 561-579.

[49] Gerstner, T., Griebel, M., "*Dimension- Adaptive tensor product quadrature,*" Journal of Computing, Vol. 71, 2003, pp. 65-87.

[50] Hegland, M., "*Adaptive sparse grids,*" In *Proceedings of CTAC, July 16-18, 2001*.

[51] Sethuraman, S., Marsden, A.L., "*A stochastic collocation method for uncertainity quantification and propagation in cardiovascular simulations,*" Journal of Biomechanical Engineering, Vol. 133, 2011, 031001.

[52] Liu, M., Gao, Z., Hesthavan, J.S., "*Adaptive sparse grid algorithms with applications to electromagnetic scattering under uncertainty,*" Applied Numerical Mathematics, Vol. 61, 2011, pp. 24-37.

[53] Viana, F.A.C., Haftka R.T., and Steffen V., "*Multiple surrogates: how cross-validation errors can help us to obtain the best predictor,*" Structural and Multidisciplinary optimization, Vol. 39, 2009, pp. 439-457.

[54] Forrester, A.I.J., Sóbester, A., and Keane, A.J., "*Engineering Design via Surrogate Modelling,*" Wiley Sons, 2008.

[55] Broomhead, D.S., and Lowe D., "*Multivariable functional interpolation and adaptive networks,*" Complex systems, Vol. 2, 1988, pp. 321-355.

[56] Keane, A.J., Nair, P., "*Computational Approaches for Aerospace Design,*" John-Wiley Sons, Newyork, 2005.

[57] Yoneta, R., Sasaki, D., and Nakahashi, K., "*Aerodynamic optimization of an over the wing nacelle mount configuration,*" In 48^{th} *AIAA Sciences Meeting Including the New Horizons Forum and Aerospace Exposition, 2010.*

[58] Sakata, S., Ashida, F., and Zako, M., "*Structural optimization using kriging approximation,*" Computer Methods in Applied Mechanics and Engineering, Vol. 192, 2003, pp. 923-939.

[59] Keane, A.J., "*Statistical improvement criteria for use in multiobjective design optimization,*" AIAA Journal, Vol. 4, 2006, pp. 879-891.

[60] Krige, D.G., "*A statistical approach to some basic mine valuation problems on the witwatersrand,*" Journal of the Chemical, Metallurgical and Mining Engineering Society of South Africa, Vol. 52, 1951, pp. 119-139.

[61] Sacks, J., "*Design and analysis of computer experiments,*" Statistical Science, Vol. 4, 1989, pp. 409-435.

[62] Jones, D.R., Schonlau, M., and Welch, W.J., "*Efficient global optimization of expensive black-box functions,*" Journal of Global Optimization, Vol. 13, 1998, pp. 455-492.

[63] Toal, D.J.J., Bressloff, N.W., Keane, A. J., and Holden, C.M.E., "*The development of a hybridized particle swarm for kriging hyper parameter tuning,*" Engineering Optimization, Vol. 43, 2011, pp. 675-699.

[64] Theil, H., "*Principles of Econometrics,*" John Wiley & Sons, Newyork, 1971.

[65] Park, I., and Grandhi, R.V., "*Quantifying multiple types of uncertainty in physics based simulation using Bayesian model averaging,*" AIAA Journal, Vol. 49, 2011, pp. 1038-1044.

[66] Dwight, R.P., and Han, Z.H., "*Efficient uncertainty quantification using gradient enhanced Kriging,*" In *AIAA, non-deterministic approaches, 4-7 May, California, 2009,* pp. 1-23.

[67] Morris, M.D., and Mitchell, T.J., "*Exploratory designs for computational experiments,*" Journal of Statistical Planning and Inference, Vol. 43, 1995, pp. 381-402.

[68] Blatman, G. and Sudret, B., "*Adaptive sparse polynomial chaos expansions - Apllication to structural reliability,*" Technical Report H-T26-2008-00668-EN, EDF.

[69] Keane, A.J., "*Moment estimation of a black box function using various approaches,*" Report, 2010, pp. 1-20.

[70] Chandra Sekhar, D., Keane, A.J. and Forrester, A.I.J., "*Adaptive strategies for moment estimation using Stochastic Collocation and Kriging based approaches,*" Presented at European Congress on Computational Methods in Applied Sciences and Engineering (ECCOMAS 2012) J. Eberhardsteiner et.al. (eds.) Vienna, Austria, September 10-14, 2012.